

# **Analysing changes in assimilate transport and grapevine ripening metabolism induced by the ripening disorder Berry Shivel**

Doctoral Dissertation Submitted by

**Sara Crespo Martínez**

in partial fulfilment of the requirements for the degree

Doctorrerum naturalium technicarum

Supervised by

**Prof. Dr. Astrid Forneck**

Division of Viticulture and Pomology

Department of Crop Sciences

University of Natural Resources and Life Sciences, Vienna

Vienna, 2017

# Acknowledgements

I would like to express my gratitude to Prof. Dr. Forneck for giving me the opportunity to join her working group and funding my position during 3 years at the viticulture group. Particularly thanks for the experienced advice and for her clarifying vision of the manuscript.

Special thanks to Dr. Griesser for introducing me into the berry shrivel topic and the physiology of grapevine. Thanks to the close support during the project, the respect to new ideas and the work together during these years.

Thanks to Dr. Sobczak from Warsaw University for his collaboration in the TEM experiments, for sharing his expertise with my initial scarce histological knowledge and his great disposition to help.

The acknowledgments would not be complete without mentioning the other members of the viticulture group at BOKU during this time. In special to Ulrike Anhalt, Verena Dockner, Markus Eitle, Brigitte Hasenauer, Sigrid Hensler, Vanessa Loiacono, Roswitha Prinz-Mammerler, Katharina Schödl-Hummel...for the great teamwork and everyday living. 'None of us is as smart as all of us.'

Finally thanks to my beloved people.

## Abstract

Berry Shivel (BS) is a physiological disorder that alters cv. Zweigelt grape berry ripening. The illness affects single grapevine clusters with an irregular incidence between years, fields and plants. BS grapes are mainly characterized by high acidity, low sugar,  $K^+$  and anthocyanin content and loss of turgor. Different studies investigated BS berry nutrient profile, transport capacity and cell viability but the reasons of its causes are still unknown. In this work we aim to shed light over the mechanisms associated with BS initiation to clarify its induction process. Based on previous studies our hypothesis is that nutrient allocation to BS berries is disturbed, we proposed two main reasons: an irregular sink activity and/or degradation of vascular tissues. To examine sink activity and sugar unloading we successfully analysed the transcriptional and enzymatic activity of sugar transporters and invertases. Results show irregular activity of tonoplast transporters from pre-ripening until full-ripe. Furthermore, we hypothesize a relation among irregular sugar content and irregular anthocyanin content, which may not be related with anthocyanin gene activity, in addition, sugar metabolism is disturbed but its role in BS induction is not clear. To examine vascular tissues different microscopic techniques were applied in rachis and pedicel sections at first symptoms appearance (*véraison*) and late symptoms (full-ripe). Anatomic studies indicated morphologic differences at cambium with reduced cell layers in BS clusters. Further, phloem alterations were quantified as secondary tissue development and reduced phloem conductivity, what may indicate limited assimilate transport capacity in BS clusters. Collapsed sieve plates due to callose and reduced density of sieve plates may exacerbate restricted assimilate conductance. According to our results both physiology and metabolism are disturbed in BS development what enhance the complexity of BS disorder.

# Zusammenfassung

Traubenwelke (TW) ist eine physiologische Störung, die den Reifeverlauf von Trauben der Sorte Zweigelt verändert. Die Krankheit befällt einzelne Weintrauben mit einer unregelmäßigen Häufigkeit zwischen den Jahren, Felder und Pflanzen auf. TW befallene Beeren werden vor allem durch hohe Säure, wenig Zucker, K<sup>+</sup> und Anthocyangehalt und Verlust von Turgor geprägt. Verschiedene Studien haben das Nährstoffprofil von TW befallene Beeren, die Transportkapazitäten und die Lebensfähigkeit der Zellen untersucht, aber die Gründe für das Auftreten von TW sind noch unbekannt. In dieser Arbeit wollen wir uns mit dem Mechanismen mit TW Iniziation beschäftigen und den Induktionsprozess zu klären. Basierend auf früheren Studien unsere Hypothese ist, dass Nährstoffzufuhr zu mit TW befallene Beeren gestört ist und wir dafür zwei wesentliche Gründe anführen: Ein gestörte ‚sink/source‘ Aktivität und/oder Abbau von vaskulären Gewebe. Um die ‚sink/source‘ Aktivität und Zuckerentladung zu untersuchen, haben wir erfolgreich die transkriptionelle und enzymatische Aktivität von Zucker Transporter und Invertasen analysiert. Unsere Ergebnisse zeigen unregelmäßige Aktivität von Tonoplasttransporter aus unreifeneifen bis reifen Beeren. Weiterhin nehmen wir eine Beziehung zwischen dem unregelmäßigen Zucker und Anthocyanin-Gehalt an, der nicht mit der Anthocyanin-Gen-Aktivität in Zusammenhang stehen kann. Unsere Ergebnissen zeigen einen gestörten Zuckerstoffwechsel, aber seine Rolle in TW Induktion ist nicht klar. Um vaskuläres Gewebe, von Rachis und Abschnitten des Fruchtsiels auf die ersten Symptome (bei *Véraison*) und späten Symptome (bei der Reife) zu untersuchen, wurden verschiedene mikroskopische Techniken angewendet. Anatomische Studien zeigten morphologische Unterschiede im Kambium mit reduzierten Zellschichten in TW-Trauben. Weitere Änderungen im Phloem wurden als sekundäre Gewebeentwicklung und reduzierter Phloemleitfähigkeit quantifiziert, was möglicherweise zu begrenztem Nährstofftransport in TW Trauben führt. Zusammengebrochen Siebböden Aufgrund von Kallose und eine geringe Dichte an Siebböden verschärfen den eingeschränkter Nährstofftransportfähigkeit. TW zeigte eine hohe Komplexität und nach unseren Ergebnissen hauptsächlich physiologische, aber auch der Zuckerstoffwechsel könnte an der Entwicklung beteiligt sein.

# Table of contents

|       |   |    |
|-------|---|----|
| 1     | Objectives.....   | 7  |
| 2     | Introduction.....   | 9  |
| 2.1   | Introduction to grape berry development and ripening.....   | 9  |
| 2.1.1 | Grape berry development and ripening .....  | 9  |
| 2.1.2 | Grape berry sugar metabolism .....  | 13 |
| 2.1.3 | Grape flavonoid biosynthesis .....  | 18 |
| 2.1.4 | Vascular system and assimilate transport in grapevine .....                                       | 21 |
| 2.2   | Berry shrivel .....   | 25 |
| 2.2.1 | BS berries nutrient profile .....   | 27 |
| 2.2.2 | BS berries carbohydrate metabolism.....   | 29 |
| 2.2.3 | BS berries polyphenol profile.....  | 30 |
| 2.2.4 | BS physiological modifications .....  | 31 |
| 3     | Materials and methods .....   | 34 |
| 3.1   | Collection of plant material .....  | 34 |
| 3.2   | Metabolite analysis.....  | 35 |
| 3.2.1 | Measurement of total anthocyanin content.....   | 35 |
| 3.2.2 | Sugar analysis.....   | 35 |
| 3.2.3 | Polyphenol analysis using LC-MS/MS.....   | 36 |
| 3.3   | RNA extraction and qPCR analysis .....  | 37 |
| 3.4   | Enzyme activity assay of the carbohydrate metabolism.....   | 39 |
| 3.5   | Microscopic procedures .....  | 40 |
| 3.5.1 | Light microscopy .....  | 40 |
| 3.5.2 | Scanning Electron Microscopy .....  | 41 |
| 3.5.3 | Transmission Electron Microscopy .....  | 42 |
| 3.6   | Statistical analysis .....  | 43 |
| 4     | Results .....   | 44 |
| 4.1   | Molecular biology: sugar and anthocyanin metabolism.....  | 44 |
| 4.1.1 | Comparative accumulation of sugar and anthocyanin in healthy and BS berries on a time scale ..... | 44 |
| 4.1.2 | Comparative analysis of glucose, fructose and sucrose on a time scale.....                        | 45 |
| 4.1.3 | Comparative analyses of single polyphenols.....   | 47 |
| 4.1.4 | Gene expression profiles.....   | 49 |
| 4.1.5 | Invertase enzyme activity .....   | 59 |
| 4.2   | Tissue anatomy analysis .....   | 60 |
| 4.2.1 | Microscopic observation of pedicel and rachis tissues: xylem, cambium and phloem                  | 61 |

|       |   |     |
|-------|---|-----|
| 4.2.2 | Measurement of xylem and phloem dimension.....                            | 66  |
| 4.2.3 | Sieve plate observation, characterization and conductance .....           | 69  |
| 4.2.4 | Chemical tissue composition .....   | 75  |
| 4.2.5 | Microorganisms in BS affected samples.....                                | 77  |
| 5     | Discussion .....  | 80  |
| 5.1   | Sugar metabolism at BS berries .....                                      | 80  |
| 5.1.1 | Pre-ripening stage: apoplastic sink establishment .....                   | 80  |
| 5.1.2 | Sink establishment from symplast to apoplast.....                         | 83  |
| 5.1.3 | Ripening: apoplastic sink strength .....                                  | 83  |
| 5.2   | Polyphenol metabolism .....   | 85  |
| 5.3   | Anatomic analysis .....   | 86  |
| 5.3.1 | Anatomic abnormalities of phloem, cambium and xylem tissues .....         | 86  |
| 5.3.2 | Reduced phloem conductivity and callosed sieve plates in BS berries ..... | 88  |
| 5.4   | Outlook.....  | 89  |
| 6     | Summary.....  | 94  |
| 7     | Appendix .....  | 96  |
| 8     | References .....  | 100 |
| 9     | Abbreviations.....  | 111 |
| 10    | Declaration .....   | 113 |
| 11    | Curriculum vitae.....   | 114 |

# 1 Objectives

Berry shrivel (BS) is a physiological ripening disorder of grapevine, and its causes are unknown. The grapevine variety (*Vitis vinifera* L.) Zweigelt cv. among others develops the ripening disorder BS that affects irregularly the ripening of clusters within fields, plants and years. BS grapes do not reach ripeness and fail the standards for quality wine, leading to high economic losses in Austria and worldwide. Research to elucidate the cause of BS and describe the symptoms in detail has been intensified during the last 10 years. As BS appears frequently in only some clusters of a vine it is suggested that disturbance may not be due to external causes and rather causes of induction seem to originate within the cluster (Keller et al. 2016). Nowadays its symptoms are well described as low sugar content, low pH, low anthocyanin content, low nutrient content (in special  $K^+$ ) and loose of turgor between others (Krasnow et al. 2009; Knoll et al. 2010; Hall et al. 2011; Griesser et al. 2012; Bondada and Keller 2012; Bachteler et al. 2015; Keller et al. 2016). Reduced sugar and  $K^+$  content are the most repeatable symptoms in different studies, locations and cultivars. The transport of sugars and  $K^+$  towards ripening grapes occurs through the phloem suggesting a possible role of phloem transport capacity and phloem unloading mechanisms in BS symptom development or even induction of the ripening disorder (Bondada 2016; Griesser et al. 2017). Therefore, we hypothesize that BS is induced by a not functional phloem transport towards ripening grapes/berries. Specifically we aimed to analyse and evaluate: 1) the process of apoplastic phloem unloading by its apoplastic enzymes and transporters. Reduced activity of transporters and changes in sugar metabolism could influence the sink strength leading to reduced sugar and assimilate content in BS grapes/berries. 2) phloem morphology and the phloem conductivity. Low or decreased phloem conductivity may reduce the transport of assimilates and nutrients towards BS grapes/berries.

Analytical methods, expression analyses and different microscopic techniques were applied in order to characterise the sink activity and strength of BS berries as well as the phloem morphology and transport capacity in symptomatic and pre-symptomatic BS grape clusters. The first symptoms of BS can be observed after *véraison*, when high amounts of sugars are accumulated in grape berry vacuoles. The phloem unloading during this ripening phase is based on apoplastic transport mechanisms and

berries become strong sinks within the vine. To quantify the sink activity, expression of sugar metabolism key genes, such as invertases and sugar transporters (CWINV, VINV, NINV, HT and TMT) were evaluated on transcriptional level, moreover invertases enzymatic activity level was also assessed. In parallel histological studies of the rachis and pedicels of healthy and BS grapes were conducted. Thereby several microscopic techniques (LM, SEM and TEM) were used to have a deep insight in the xylem, cambium and in especial phloem tissues. These were evaluated according to their development, size and transportation capacity.

The causes of BS symptoms in grapes are unknown as well as the induction time of the processes related to BS induction. By applying different methods to elucidate on the one hand sink activity and sugar metabolism of BS affected grapes and on the other hand the morphology of the vascular system, we aim to evaluate BS induction and provide concise data of related processes.

## **2 Introduction**

### **2.1 Introduction to grape berry development and ripening**

#### **2.1.1 Grape berry development and ripening**

Grape berries are formed after flowering, also called anthesis, in spring. Grapevine flowers of the most important cultivars are hermaphrodite so they are able to self-pollinate (Dokoozlian 2000). Pollination and fertilization depend on external conditions, mainly temperature, but also availability of nutrients and competition with other organs of the plant is defining the process. Flowers are not strong competitors for assimilates which can lead to low support and reduced pollination (Keller 2010). Only around a quarter of the successfully pollinated flowers will develop into berries. Extreme temperatures and excessive rainfall also negatively influence berry set. When the flower is successfully fertilized the seeds are able to grow in a phase known as fruit set. During the lag phase seeds grow fast and reach their maturity. After fruit set grape berry growth is ongoing during 11 to 15 weeks until grapes reach maturation.

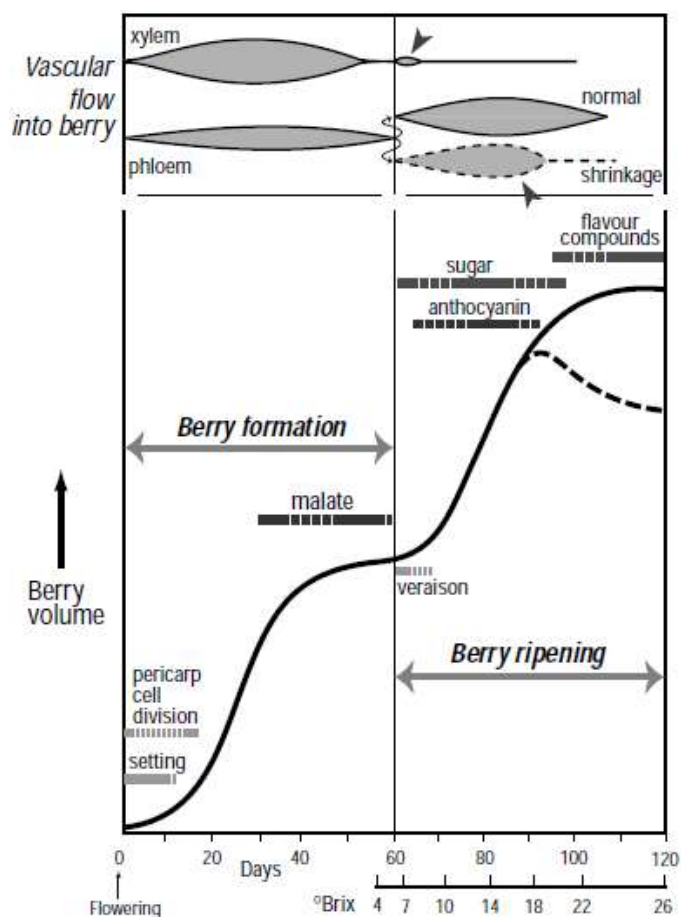


**Figure 1:** Diagram of the berry development from flowering till full-ripen. In the diagram is described in the time scale (days from flowering) the income pathways of assimilates (phloem and xylem), berry volume and the different compound synthesis (flavour, sugar, anthocyanin). Extracted from (Coombe and McCarthy 2000).

Grape berry development and ripening follows a double sigmoid curve with three distinct phases (Fig. 1): a first stage of rapid berry growth with cell division, a second phase known as lag phase with no growth and a third stage, which is a second growing phase of rapid sugar accumulation and ripening.

The first growing phase takes around 60 days from anthesis. In the first growing phase water enters via xylem and solutes enter via phloem in a symplastic manner (Greenspan et al. 1994). Grape berries grow especially in cell number through cell division. Similarly to other fruits as tomato, early cell division and growth in grape berry is mainly governed by phytohormones: auxin and gibberellin (Coombe 1960; De Jong et al. 2009). Auxin induces cell division as well as cell enlargement (Coombe 1960). Gibberellin act as a accelerator of cell division by the induction of DNA replication but it does not induce cell growth (Francis 2001). Auxin is naturally delivered by seeds and

furthermore it promotes genetically the synthesis of gibberellin: auxin enhance the expression of GA3ox biosynthesis pathway gene (Ozga et al. 2003). Higher number of seeds will turn into a higher amount of auxin in the berry inducing the production of gibberellins, which promote cell division and elongation. This fact has been proven in mutant fleshless grapevine and in fact auxin and gibberellin treatments are used in seedless table grapes to stimulate growth (Fernandez et al. 2006; Harrell and Williams 1987). Cell division is of special importance, as it will determine the final fruit size at ripening. From the metabolic point of view, organic acids are synthesized at this phase being tartaric and malic acid the most abundant ones. Acids have a great importance for wine production providing stability for winemaking as well as for tasting issues. Tartaric acid is synthesized before *véraison* and its content is then stable through ripening. The main reservoir of tartaric acid is located in the skin. A synthesis pathway related to ascorbic acid as precursor has been proposed but still its synthesis mechanisms remain partly obscure (Loewus 1999; Conde et al. 2007). Similarly, malic acid is synthesized before *véraison* and is accumulated in the mesocarp. This acid is synthesized through the PEP pathway and the rate of synthesis is very variable, the content is decreased through the ripening process as it is consumed as substrate for further glucose synthesis as well as for respiration through the TCA cycle. Malate it's imported via phloem and becomes the predominant acid at fruit set; it can also be synthesized *in situ* by degradation of sugar through glycolytic respiration (Ruffner and Hawker 1977; Sweetman et al. 2009). Temperature has a strong influence on malic acid biosynthesis and degradation, as it controls the activity of malic synthesis enzyme (PEP carboxylase and malic dehydrogenase) and malic acid-degrading enzyme (malic enzyme). In general lower temperatures lead to higher amounts of acids in grapes (Lakso and Kliewer 1975). Other important metabolites produced in the first growing phase are e.g.: proanthocyanins and methoxypyrazines. Proanthocyanins are important secondary metabolites for wine conservation, provide astringency and a bitter taste. Methoxypyrazines are aromatic compounds with a very high abundance in skin and seeds of grape berries and provide vegetable-like aromas to wine. It is still not determined if the main methoxypyrazines are synthesized within the grape or imported from leaves (Darriet et al. 2012).

The lag phase separates the two growing phases and takes around two weeks. In the lag phase, the grape berry does not increase its size but important metabolic changes are induced preparing the berry for apoplastic transport and strong growth. The end of

the phase is called *véraison*, which is the time point when berries start to soften and red wine varieties start their colouring. This process is driven by the reduction of auxin content and dramatically rise of ABA content (Robinson and Davies 2000).

After *véraison* the second growing phase or ripening phase starts which lasts approximately 8 weeks. The ripening phase is characterized by cell expansion of grape berry cells and a massive accumulation of sugars as well as the synthesis of many phenolic compounds (Harris et al. 1968; Coombe 1992). During the growth phase a massive accumulation of hexoses downloaded from the phloem in an apoplastic manner takes place (Coombe and McCarthy 2000). Phloem transport becomes dominant while the transport through the xylem towards ripening grape berries is ceased (Zhang et al. 2006). Different phytohormones regulate the ripening process, being of special importance ABA, which content in berries shows a pick at *véraison* (Coombe and Hale 1973; Davies et al. 1997; Zhang et al. 2006; Dai et al. 2014) and it is related to anthocyanin biosynthesis at *véraison* (Pirie and Mullins 1976; Mori et al. 2007; Wheeler et al. 2009). Apart from the well-known role activating stress response system, ABA accelerates ripening while its absence can delay this process (Davies and Robinson 2000). So far, it is not clear if ABA is stored in an inactive form in seeds and transformed to an active form at *véraison* or if it is synthesized on demand in grape berries or in leaves. (Wheeler et al. 2009). Ethylene, brassinosteroids and gibberellins have also been described to regulate grape berry ripening, although their role is still not completely understood. Ethylene has been directly related to sugar accumulation: the absence of ethylene inhibits the activity of important sucrose transporters (SUC11, SUC12) (Giovannoni 2001; Chervin et al. 2006). Brassinosteroids biosynthesis enzymes (*VviDWARF* and *VviDWF1*) and the BR receptor (*VviBR1*) have been described in grapevine and further brassinosteroid application promotes ripening while inhibition of brassinosteroids synthesis delays ripening (Symons 2006). Gibberellins are also involved in the active transcription of sugar transporters and enzymes in berries (*VviHT3,4,5,6*, *VviSUC12-27* and *VviCWINV*) (Xu et al. 2015). The massive cell growth that grape berries undergo it is possible due to cell wall modifications. After *véraison* mesocarp cell walls become more elastic in a process called softening. Cell wall loosening is mainly performed by the enzymes polygalacturonase and  $\beta$ -galactosidase which expression levels increase sharply at *véraison* leading to the cleavage of pectin groups and so increase pectin solubility (Aryan et al. 1987; Nunan et al. 1998). Accumulation of hexoses in vacuoles increases the osmotic pressure,

which drives additional water into the cells leading to a controlled cell expansion, which is facilitated by the loosening of the cell walls during softening. During the grape berry ripening phase important quality traits as colour, size and sugar content are determined. Further other important molecules, as the volatiles such as terpenes, are synthesized contributing to wine aroma. Terpenes introduce the floral and fruity aromas to wine (Darriet et al. 2012). In Muscat type varieties terpenes are mainly synthesized during the ripening phase while in non-Muscat varieties, like Cabernet Sauvignon, their synthesis may happen earlier at the developmental phase (Kalua and Boss 2009; Wen et al. 2015). The synthesis pathway has been described and, as many other processes at ripening, gene expression of related genes is promoted by ABA and ethylene (Conde et al. 2007; Wen et al. 2015). Furthermore environmental conditions as high sun exposure and limited rainfall may accelerate berry maturation and limit terpene synthesis (Wen et al. 2015).

In some grape varieties an additional phase takes place, in which grape lose weight, sugar content increases and cell death in the mesocarp is recorded. In this third phase winemaking grape maturity is reached and this natural process is also called berry shrivel or late season dehydration which shares the name but differs from the disorder at study here (Rogiers et al. 2004).

### **2.1.2 Grape berry sugar metabolism**

Plant metabolism involves a great amount of mechanisms, reactions and cycles that are able to produce a very diverse range of molecules: from simple carbohydrate necessary for basic cell metabolism up to very complex molecules with specialized targets e.g. phytohormones. To simplify the study of this complex machinery, plant metabolism is generally divided into primary and secondary metabolism. Primary metabolism implies all the molecules and reactions involved in the essential processes for plant development and growth. Fundamental pathways, as energy fixing Calvin cycle (photosynthesis) or energy realising Krebs cycle and glycolysis (cellular respiration), are part of the primary metabolism. During Calvin cycle plants are able to transform light, CO<sub>2</sub> and water into organic compounds as ATP, NADPH and CH molecules (triose phosphates) through photosynthesis. Triose phosphate is further metabolized into starch for storage or into sucrose for export to other plant tissues.

During berry growth and ripening the fruit is the strongest sink in the grapevine plant. This means that competition for assimilates is between berries and not between other organs of the plant. Sink strength is the capacity of a sink organ to import solutes and is partly determined by fruit size and content (Ho 1988). Sink strength results from the combination of - the sink size, which is a physical component defined by berry number per cluster and number and size of cells per berry (Dokoozlian 2000). Sink activity, is physiologically determined by the mechanisms that enable assimilate import: phloem unloading, uptake through the cell wall into the cell cytoplasm and further usage or storage (Ho 1988). Sink activity is rather dynamic as covers many factors that control apoplastic sugar phloem unloading and the sink-source gradient as transporters (SUCT, HT, TMT) and enzymes such as invertases (Ho 1988). Transporters are of special importance in sink establishment as they will determine compartmentation of sugars.

Sugars arrive to berries in form of sucrose, which has to be split into its unit hexose molecules, fructose and glucose, before further usage. This reaction is performed by two enzyme families, invertases (INV) and sucrose synthases (SUS) which are key factors in fruit ripening (Roitsch et al. 2003; Koch 2004). Invertases are divided in three groups, cell wall invertases (CWINV), vacuolar invertases (VINV) and cytosolic invertases (CINV), all the aforementioned divide sucrose molecules into two simple hexoses, fructose and glucose. Invertase gene expression is enhanced in the presence of sugars (sucrose and hexoses). It is suggested that that the activity of acid invertases (VINV and CWINV) might be regulated by ABA, pH and its substrate sucrose (Roitsch and González 2004; Pan et al. 2005); others authors suggest that ABA regulates only VINV (Giribaldi et al. 2010; Dai et al. 2011).

Sucrose synthases divide sucrose into fructose and UDP-glucose and the reaction is reversible, enabling also sucrose synthesis (Fig. 2). Sucrose is transported via the phloem from mature grapevine leaves to berries during grape berry formation and ripening (Swanson and El-Shishiny 1958; Lebon et al. 2008).

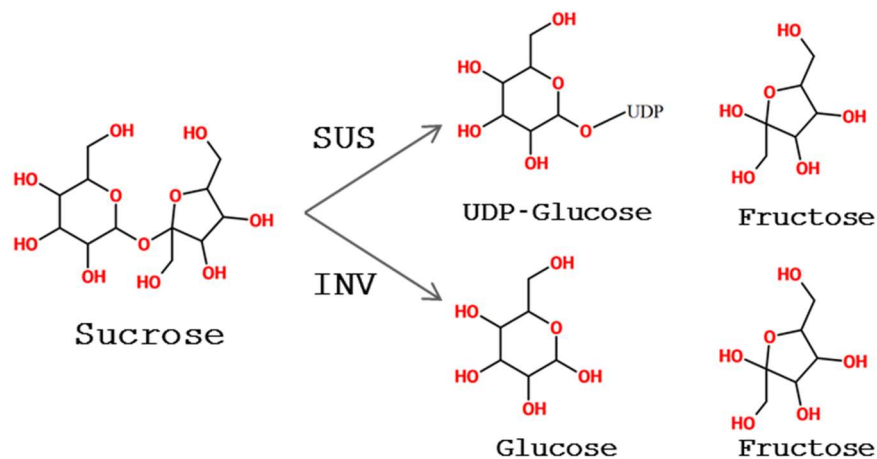


**Figure 2:** Reaction of sucrose synthase (SUS) and invertase (INV). Sucrose as substrate of both reactions and fructose as one of its product is shared. The second product of the reactions is different: while SUS produces UDP-glucose, INV produces glucose (Cabello Campos 2013).

During the first growing period, the vascular system of the vine and the berries is connected through plasmodesmata so sucrose follows the solute gradients towards growing berries via the symplast. The amount of assimilates delivered to grape berries at the cell division phase will depend mainly on sink size (cell number) which may have a higher influence than sink strength at this time (Ho 1988). When sucrose arrives to the vacuoles, it is cleaved into glucose and fructose throughout VINV activity, the resulting hexoses can be further processed in the PEP cycle and stored as malic acid, consumed in respiration or stored to increase turgor pressure in the vacuoles for cell expansion (Sturm 1999). Genetically VINV is coded by the grape genes *VviGIN1* and *VviGIN2*. Both produce vacuolar isoforms of invertase but have different patterns of expression: *VviGIN1* is highly expressed in grape skin and mesocarp cells during the first 8 weeks after flowering while expression of *VviGIN2* is lower but has appreciable activity in the first 4 weeks after flowering (Davies and Robinson 1996). The regulation of this enzyme has been largely studied due to the pivotal role in pre-ripening grapes.

Metabolic changes during the lag phase lead to a predominantly apoplastic phloem unloading during the second growth phase of grape berry ripening. Plasmodesmata become blocked or their conductivity is reduced (Zhang et al. 2006). Therefore, sucrose has to be cleaved into glucose and fructose before entering the cell. Just after *véraison* when BS symptoms become visible, the most important factor for sink establishment is sink activity due to the high activity of CWINV for sugar unloading and

the importance of active sugar transporters for sugar compartmentation. Afterwards, during the ripening phase, sink strength will be increasingly more determined by sink size and less determined by sink activity (Coombe 1988). CWINV responsible gene *VviCWINV* is strongly induced just prior *véraison* preceding the fast accumulation of sugars (Zhang et al. 2006). After being split hexoses are actively transported into the cell by plasma membrane transporters (Roitsch and Ehneß 2000; Koch 2004; Robinson and Davies 2000; Coombe 1992). A group of grapevine hexose transporters from *VviHT* gene family, *VviHT1*, *VviHT2*, *VviHT3*, *VviHT4*, *VviHT5*, *VviHT6*, *VviHT7*, *VviHT11*, *VviHT12*, *VviHT13*, have been described (Fillion et al. 1999; Vignault et al. 2005; Conde et al. 2006; Hayes et al. 2007; Afoufa-Bastien et al. 2010).

Hexose transporter gene *VviHT1*, *VviHT2* and *VviHT3* are expressed in grape berries, having the highest expression *VviHT1*. The peak expression of *VviHT1* is reached after *véraison*, but there is a smaller expression induction during the first growing phase that indicates it may be involved in cell division and enlargement. Similarly to invertases *VviHT1* expression is modulated by acid pH (around 4.5), sugar concentration and ABA (Çakir and Giachino 2012). In grapes *VviHT1* has been observed in the plasma membrane of the complex sieve element/companion cell what confirms its role in apoplastic phloem unloading (Vignault et al. 2005). *VviHT2* and *VviHT3* are expressed at a lower extent in *véraison* and post-*véraison* grapes (Fillion et al. 1999). Furthermore *VviHT1*, *VviHT3* and *VviHT5* genes are highly expressed in leaves associated with phloem cells and their expression was related to the activity of CWINV, suggesting a role in phloem loading of mature leaves (Hayes et al. 2007; Afoufa-Bastien et al. 2010). Once hexoses are introduced in the cytoplasm they have to be transported into the vacuoles.

Most of the hexoses are transported by tonoplast monosaccharide transporters (TMT) (Wormit et al. 2006; Lecourieux et al. 2013). Three grapevine TMT genes are known, *VviTMT1*, *VviTMT2* and *VviTMT3*. All of them are expressed in berries during *véraison* and at a lower extent during the ripening phase (Wormit et al. 2006; Afoufa-Bastien et al. 2010). But also some hexoses are reassembled into sucrose and then transported into the vacuoles by sucrose transporters (Terrier et al. 2005). Four different sucrose transporter genes named *VviSUC11/VviSUT1*, *VviSUC12*, *VviSUC27* and *VviSUT2* are known in *Vitis vinifera* L.. *VviSUC11/VviSUT1* and *VviSUC12* are located in the plasma membrane and their induction correlates with increasing hexose accumulation

in the vacuole and increased ethylene levels underlining their importance for grape berry ripening (Davies et al. 1999). The role of *VviSUC27* and *VviSUT2* during berry ripening is limited. *VviSUC27* is involved in seed development and *VviSUT2* is mainly expressed in roots (Afoufa-Bastien et al. 2010). *VviSUC11*, *VviSUC12* and *VviSUC27* transporters can also work in a reverse mode. In Figure 3 the mechanisms described in this section are summarized.

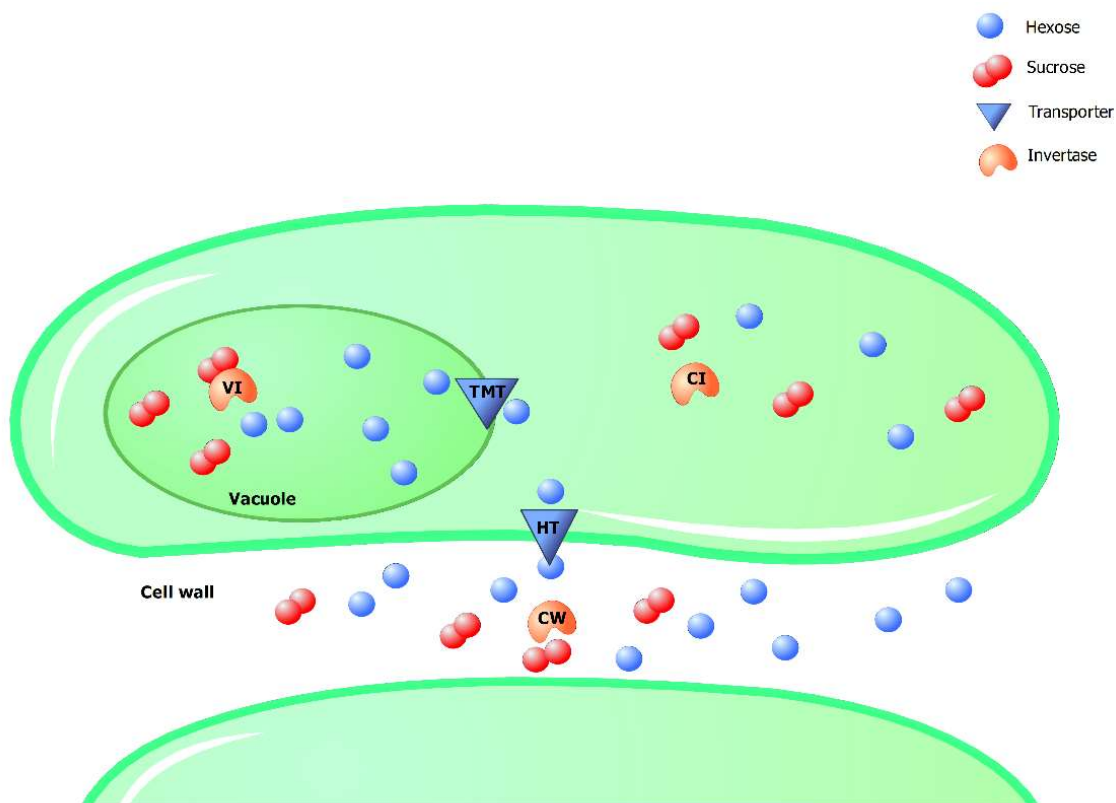


**Figure 3:** Diagram of the main mechanisms involved in sugar metabolism during grape ripening. Sucrose cleavage enzymes (Vacuolar invertase, VI; Cell wall invertase, CWI; Cytosolic invertase, CI) and transporters (Hexose transporters, HT; Tonoplast monosaccharide transporters, TMT). (Image designed with Tinker Cell).

Fruit ripening largely depends on sugar accumulation. Sugars provide the fuel and energy necessary for grape berry metabolism. Additionally hexoses act generating osmotic potential, which drives cell enlargement during grape development and ripening (Gibson 2005). Furthermore sugars have a hormone-like signalling role for activating sugar transporters and invertases what in turn increase the sink activity of the organ. As example many of the sugar transporters described are transcriptionally regulated by glucose and sucrose (Koch 2004). The synergetic signalling effect of sugars and phytohormones on grape berry ripening have been proved, e.g. glucose and ABA activate the synthesis of anthocyanin (Dai et al. 2014).

### 2.1.3 Grape flavonoid biosynthesis

Plant secondary metabolites include phenols, alkaloids and terpenoids. These substances are often needed for plant-environment interaction, to circumvent the negative effects of biotic (e.g. infection) or abiotic (e.g. UV light) stresses. Polyphenols cover a very broad group of molecules and are well present in grape berries.

There are three main groups of flavonoids in grapes: flavonols, tannins or also called proanthocyanins or condensed tannins and anthocyanins. Flavonols are produced during flowering and at the end of ripening in the skin of berries. These pigmented metabolites contribute to colour stabilization in wines and have a role as protectors to UV light and microbial interaction in berries (Hoshino et al. 1980; Smith and Markham 1998; Koes et al. 1994). Tannins, called condensed tannins or proanthocyanidins, are molecules which precursors are flavan-3-ol (catechin and epicatechin) and main synthesis responsible genes are *VviANR* and *VviLAR* (Bogs et al. 2005; Bogs et al. 2007). They are mostly synthesized in pre-*véraison* and localized in seeds and berry skin cells acting against herbivores and later also provide colour stability in wines (Glories 1988).

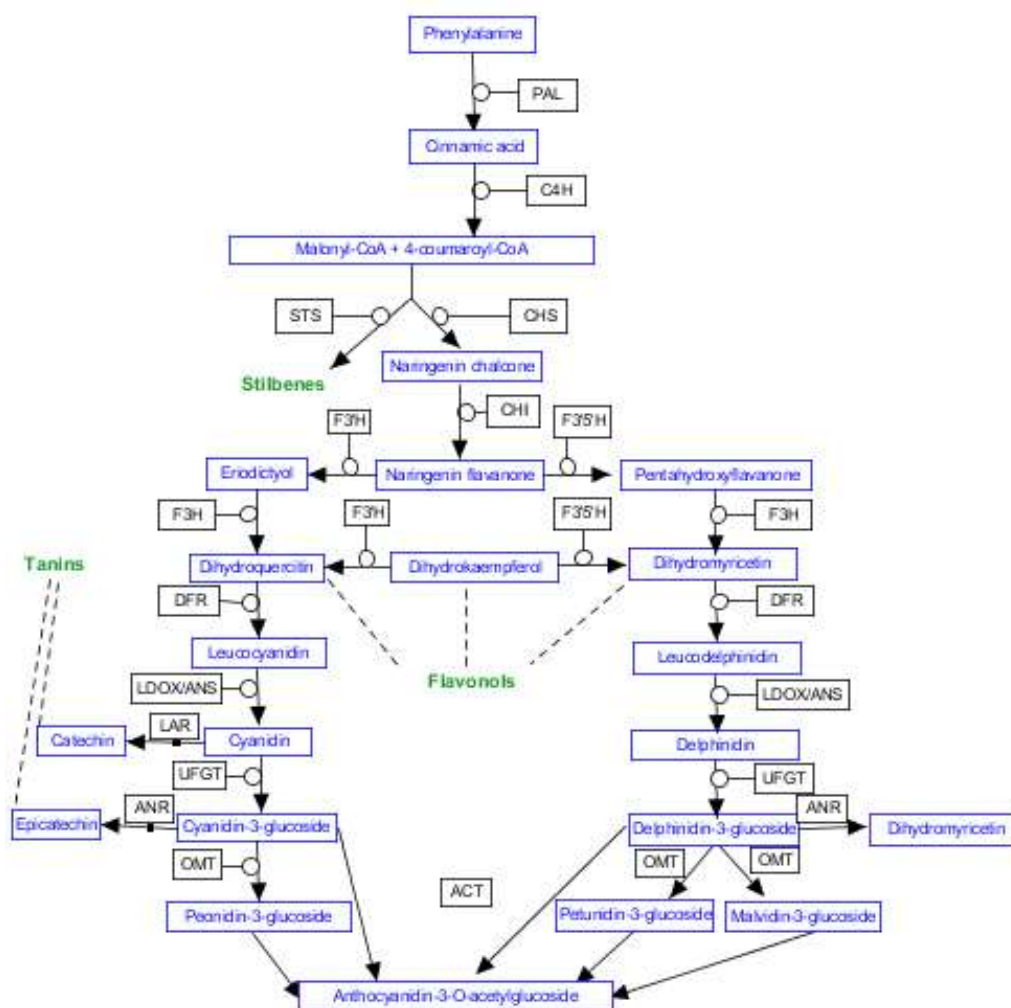


**Figure 4:** Anthocyanin synthesis pathway described for grapevine. In blue are represented the chemical compounds synthesized in every step, in black the genes involved in every step, in green the resulting phenol compounds. Abbreviations: PAL, phenylalanine ammonia-lyase; C4H, cinnamate-4-hydroxylase; 4CL, 4-coumarate-CoA ligase; CHS, chalcone synthase; STS, stilbene synthase; CHI, chalcone isomerase; F3'H, flavonoid 3'-hydroxylase; F3H, flavonone 3-hydroxylase; F3'5'H, flavonoid 3'5'-hydroxylase; DFR, dihydroflavanol 4-reductase; FLS, flavonol synthase; LDOX/ANX, leucoanthocyanidin dioxygenase/anthocyanidin synthase; UFGT, UDP-glucose:anthocyanidin 3-O-glucosyltransferase; OMT, o-methyltransferase; ACT, anthocyanin acyltransferase; LAR, leucoanthocyanidin reductase; ANR, anthocyanidin reductase. Adapted from (Dai et al. 2014). (Pathway designed with PathVisio 3.2.1, National Resource for Network Biology).

Anthocyanins belong to the group of flavonoids. Anthocyanins are very abundant in ripen berries of red wine varieties determine final tone from red to blue of the ripen grapes (Mazza and Miniati 1993). They are mainly synthesized during the second growing phase of berries, coinciding with the fast accumulation of sugars. The key responsible gene controlling the final step of anthocyanin production is *VviUFGT* (Fournier-Level et al. 2009). Anthocyanins are of great importance for wine making

providing colour and in nature they protect plants and berries from high radiations and attract pollinators (Glories 1988; Falcone Ferreyra et al. 2012; Carbonell-Bejerano et al. 2014).

The gene pathway for flavonoid biosynthesis is well characterized. In a first step sucrose is transformed into phosphoenolpyruvate (PEP) through glycolysis. PEP is transformed into an aromatic compound and then through the shikimic acid pathway into the final precursor phenylalanine (Fig. 4). From phenylalanine the anthocyanins, tannins and flavonols are biosynthesized through the phenylpropanoid and flavonoid pathway. Many external factors affect flavonoid biosynthesis, among them nitrogen nutrition, temperature and light have been exhaustively studied showing the adverse influence of excess N fertilization, shadow and very high temperatures (Kliwer 1970; Dokoozlian and Kliwer 1996; Keller and Hrazdina 1998; Mori et al. 2007). Flavonoid production is also determined by internal factors: many biosynthesis genes are shared by tannins, flavonols and anthocyanins that is why a tight coordination will define the final content of them (Harris et al. 2013). It is known that the flavonoid biosynthesis is mainly controlled by the MYB family of transcription factors: *VviMYBA* regulates anthocyanin biosynthesis (Kobayashi 2005; Walker et al. 2007; Boss et al. 1996), *VviMYBF* flavonoid biosynthesis (Czemmel et al. 2009) and *VviMYBPA* tannin biosynthesis (Bogs et al. 2007; Terrier et al. 2009). The expression of biosynthesis genes comprised in the anthocyanin pathway (Fig. 4) will determine the final flavonoid profile (Sparvoli et al. 1994). The role of the MYB family becomes evident as e.g. *VviCHS* (chalcone synthase) has three forms and each of them (*VvCHS1,2,3*) is regulated by different transcription factors (*VviMYB A1*, *PA1/2*, *F1*) leading to the biosynthesis of different flavonoids (anthocyanins, tannins and flavonols) (Harris et al. 2013). Outstanding importance have as well the flavanone-3'-hydroxylase (*VviF3'H*) or flavonoid-3'-5'-hydroxylase (*VviF3'5'H*) due to its role determining the proportion of cyanidin or delphinidin flavonoid-type metabolites produced (Castellarin et al. 2006; Bogs et al. 2006). UDP-glucose:flavonoid 3-O-glucosyl transferase (*VviUGT*) is responsible of the amount of anthocyanin-type produced (Boss et al. 1996; Kobayashi 2005). Correlation between sugar and anthocyanin accumulation in grape berries have been shown in vineyards (Jeong et al. 2004) as well as *in vitro* culture (Hiratsuka et al. 2001). Differences in the effectiveness and anthocyanin type production have been monitored in the presence of sucrose or glucose (Dai et al. 2014). Especially glucose increase the transcription level of downstream genes as *VviF3H*, *VviDFR* or *VviLDOX*

and have only minimal effects on the expression of upstream genes as *VviCHS* or *VviCHI* which show a constitutive expression. Also phytohormones play a role in the regulation of these genes, as e.g. abscisic acid (ABA) is a triggering factor for anthocyanin biosynthesis of the gene *VviUFGT* which contains ABA receptors (Jeong et al. 2004; Castellarin et al. 2011). Sugars and ABA together act synergistically producing a great effect in the anthocyanin production (Pirie and Mullins 1976; Hiratsuka et al. 2001; Finkelstein and Gibson 2002). Ethylene, is also able to trigger the transcription of important pathway genes. External application of ethylene at *véraison* in Carbernet Sauvignon plants triggers the expression of *VviCHS*, *VviF3H*, *VviLDOX* and *VviUFGT* resulting in an increase of anthocyanin content at harvest (El-Kereamy et al. 2003).

#### **2.1.4 Vascular system and assimilate transport in grapevine**

Grape berries become strong sink organs during the ripening process. Assimilates are transported from leaves to sink tissues through the vascular tissue and unloading strongly depends on pumps, transporters or enzymes. Phloem loading of assimilates can occur with two possible mechanisms: sucrose can be uploaded by symplastic passive loading, via plasmodesmata from cell to cell, or by active apoplastic transport, via sucrose and hexose transporters mainly in small veins of the leaves (Turgeon 1996). Long distance transport of sucrose is driven by an osmotic pressure gradient between source and sink tissues, forcing the movement of assimilates towards the sinks where the unloading must take place (Münch 1930). Similar to phloem loading, also the phloem unloading can follow two different pathways: early in the fruit formation the solutes are unloaded through plasmodesmata (direct symplast connection) and after *véraison* throughout the ripening process through apoplastic mechanisms (Zhang et al. 2006). The rate of assimilates delivered from phloem unloading that will reach the grapes is not a static amount but contrary will change between grapes and during time. Nutrients transported to the grape change through ripening. Studies of phloem sap at fruit set determined that the main income assimilates from phloem at pre-*véraison* berries are sugars (sucrose and also hexoses), acids mainly malic, increasing amounts of  $K^+$  and amino acids especially glutamine which is the main resource of N at fruit set (Glad et al. 1992). During rapid growth phloem sap supplies sucrose,  $K^+$  and amino acids and this composition might be stable during the whole ripening process

(Gholami 1996). Special increase of  $K^+$  is identified from *véraison* and during ripening (Mpelasoka et al. 2003). The presence of high  $K^+$  content is of special importance for phloem loading and unloading as it is involved in cation pumps and determines osmotic pressure (Fig. 5) (Spanswick 1981). As in other organisms, in grapevine  $K^+$  is transported passively through channels or actively through carriers. *VviK1.2* is the gene encoding a  $K^+$  plasma membrane channel from the Shaker family (voltage-dependent potassium channels) which induction is mainly occurring during ripening (Cuellar et al. 2013). In the other hand, *VviKUP1* and *VviKUP2* carriers have been found in berries with higher activity at pre-*véraison* (Davies et al. 2006).

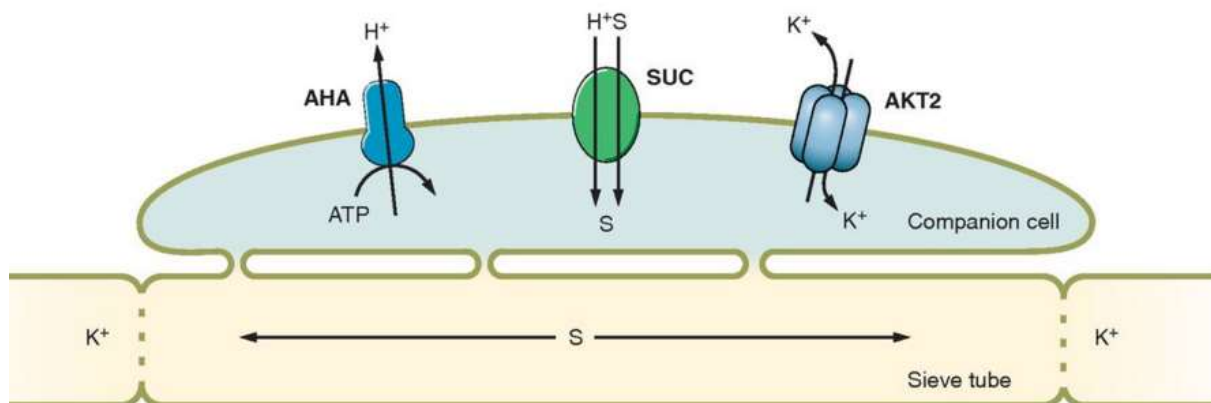


**Figure 5:** Mechanisms for sucrose aploplastic phloem loading in *Arabidopsis thaliana* L.. In the image is represented a sucrose symporter which import sucrose and  $H^+$  and a plant proton pump  $H^+$ -ATPases which creates a  $H^+$  gradient. Furthermore when ATP is limiting, the Shaker  $K^+$  channel enables the loading/unloading of sucrose; *Abbreviations:* SE – sieve element; AHA - Arabidopsis  $H^+$ -ATPase; SUC - sucrose symporter; AKT - Arabidopsis  $K^+$  transporter. *Physiological reviews* 92, 4, 1777-1811. (Hedrich 2012).

Apart from sink strength the amount of assimilates unloaded into the ripening grape is determined by the conductivity and the morphology of the vascular tissues, xylem and phloem. Figure 6 shows the most important elements that form the xylem vascular tissue in a rachis healthy cluster: xylem vessels, tracheids and fibers. The xylem is the main highway of assimilate transport towards developing grape berries during the first growing phase (Coombe and McCarthy 2000). Against previous believe, the xylem vessels keep functional after *véraison* which was proved by dye experiments and the traceability of calcium, a xylem mobile element which content keeps changeable in ripening berries (Rogiers et al. 2000; Keller et al. 2006; Zhang and Keller 2017). Xylem main function during ripening is controlling the water potential and recycling excess

water from the grape to the plant (Keller et al. 2006).  $\text{Ca}^{2+}$  regulation is of great importance as it behaves in response to abiotic and biotic changes and stimuli as light, drought or phytohormones by increasing its concentration (Knight et al. 1997; Tuteja and Sopory 2008). The increase in cytosolic calcium content creates a response activating various pathways for stress tolerance through calcium binding proteins (calmodulin, protein kinases, etc.) (Reddy 2001).

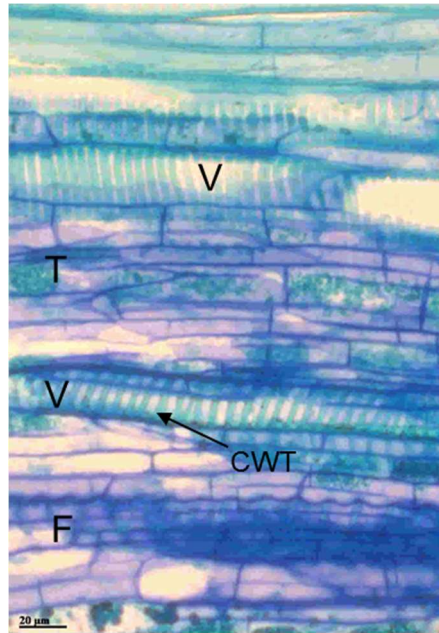


**Figure 6:** Micrograph of a longitudinal section of xylem tissue from a rachis healthy cluster. Section is stained with Toluidine and observed under light microscope. The main elements of xylem can be differentiated. *Abbreviations:* V- vessel; T- tracheid; F- fibers; CWT- cell wall thickening. Scale bar: 20μm.

Phloem tissue is composed by a mixture of cells which are parenchyma cells, companion cells and sieve elements (Fig. 7). Sieve elements are connected through sieve plates creating a continuous tube that will connect source tissues with sink tissues. To facilitate transport, sieve elements have lost structures as nucleus, ribosomes or vacuoles but still plastids, mitochondria or phloem proteins (P-proteins) are conserved and may obstruct transport. Sieve elements are connected via plasmodesmata to the associated companion cell, which support the sieve elements with the necessary metabolism for living. Sieve plates are perforated by sieve pores, which are thought to be the evolution of old plasmodesmata. Sieve pores are the doors between adjacent sieve elements and they allow the flow of water and assimilates (Esau et al. 1962; Cronshaw and Esau 1967; Esau and Gill 1971).

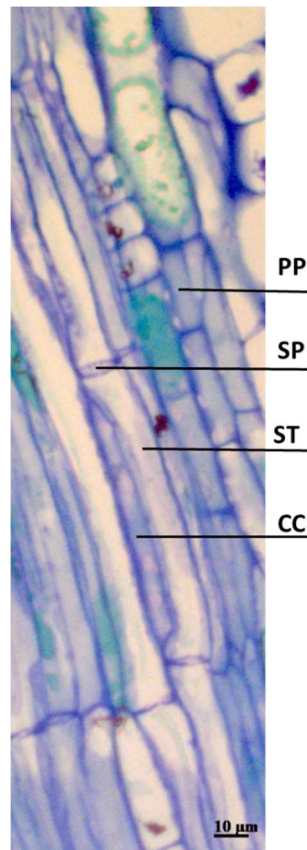


**Figure 7:** Micrograph of a longitudinal section of phloem tissue from a rachis healthy cluster. Section is stained with Toluidine and observed under light microscope. The main elements of phloem can be differentiated. *Abbreviations:* SP- sieve plate; ST- sieve tube; CC- companion cell; PP- phloem parenchyma. Scale bar: 10μm.

The long distance transport of many molecules occurs through the phloem, mainly sucrose but also potassium or phytohormones (Keller 2010). The integrity of phloem tissues is vital as it is the connection between mature source leaves and ripening sink grapes (Coombe 1988; McCarthy and Coombe 1999; Zhang et al. 2006). The driving force of transport is the difference in cell osmotic pressure between source and sink tissues, which is created by sucrose, potassium and activity of transporters in compartmentation (Wardlaw 1990; Lalonde et al. 2003). Assimilate transport does not only depend on sink strength of a tissue but also on sieve elements anatomy, in special sieve plates can greatly limit the transport capacity of the phloem (Thompson 2006). The conduction through phloem is determined by the pressure potential as described by (Münch 1930) but many other factors should be included in this calculations. Different formulas for conductivity calculation have been proposed in the last years taking into account sieve element dimensions, sieve plate and sieve pores (Thompson and Holbrook 2003; Mullendore et al. 2010). Furthermore, the transport capacity is not

a static factor: the plant has different mechanisms, like p-proteins or callose, to modify the conductivity of the phloem tissue, usually related to stress situations where assimilates should be preserved or translocation of pathogens prevented (Evert 1982; van Bel 2003; Furch et al. 2007). P-proteins are ubiquitous proteins in the phloem sap with a changeable form: they can become loosened, forming a gel and blocking the transport, or condensed, permitting the transport. It has been proved that P-proteins react to turgor loss, membrane damage or wounding and this regulation may be  $\text{Ca}^{2+}$  mediated but details remain partly obscure (Knoblauch et al. 2001; Froelich et al. 2011). Even some authors suggest that P-proteins may control phloem flow while others conclude that they do not disturb assimilate movement (Froelich et al. 2011). A different reaction observed is callose deposition, which are polysaccharides joined by glycoside bonds, which develop in the sieve plates and thereby modify the size of sieve pores. It is regarded as a defensive response of the plant that is reducing the conductivity of the phloem being able to produce a complete occlusion of the sieve pores (Currier 1957). As an example, the presence of callose has been observed in *Vitis vinifera* L after infection with downy mildew (*Plasmopara viticola*) (Kortekamp et al. 2015; Gindro et al. 2015). Salicylic acid may activate the expression of callose synthesis genes in response to powdery mildew resistant 4 (pmr4) gene in *Arabidopsis thaliana* L (McNairn and Currier 1968; Amor et al. 1995; Nishimura et al. 2003). Callose is also important for new tissue development: callose formation prevents transport and accumulation of assimilates enhance turgor pressure causing cell wall loosening and cell growth (Ruan et al. 2004). Its synthesis has been related with activity of sucrose synthase associated to cell wall in cotton (Amor et al. 1995). Different factors are able to trigger callose induction as heat, pH, glucosides, divalent anions ( $\text{Ca}^{2+}$ ,  $\text{Mg}^{2+}$  or  $\text{Mn}^{2+}$ ), ABA or  $\text{Ca}^{2+}$ . Callose can be observed in the laboratory by aniline blue staining or a callose-specific monoclonal antibody and modern scanning electron microscopic techniques enables the visualization without staining methods (O'Brien and McCully 1981; Nishimura et al. 2003; Mullendore et al. 2010).

## 2.2 Berry shrivel

Grapevine is a very important crop worldwide which fruit is used mainly for wine production. *Vitis vinifera* L. cv. Zweigelt is a cross between cv. Blaufränkisch and cv.

Saint Laurent bread in 1922 by the Federal Institute of Viticulture and Pomology at Klosterneuburg (Lower Austria). It has become an important wine grape variety in Austria, representing nowadays about 14% of the total grape production of the country (source Statistics Austria, Vineyard Land Survey 2009) and currently is the leading red grape variety cultivated. Zweigelt is highly susceptible to a ripening disorder called berry shrivel which incidence rate reaches up to 50% of the total production depending on vineyards and years (Knoll et al. 2010).

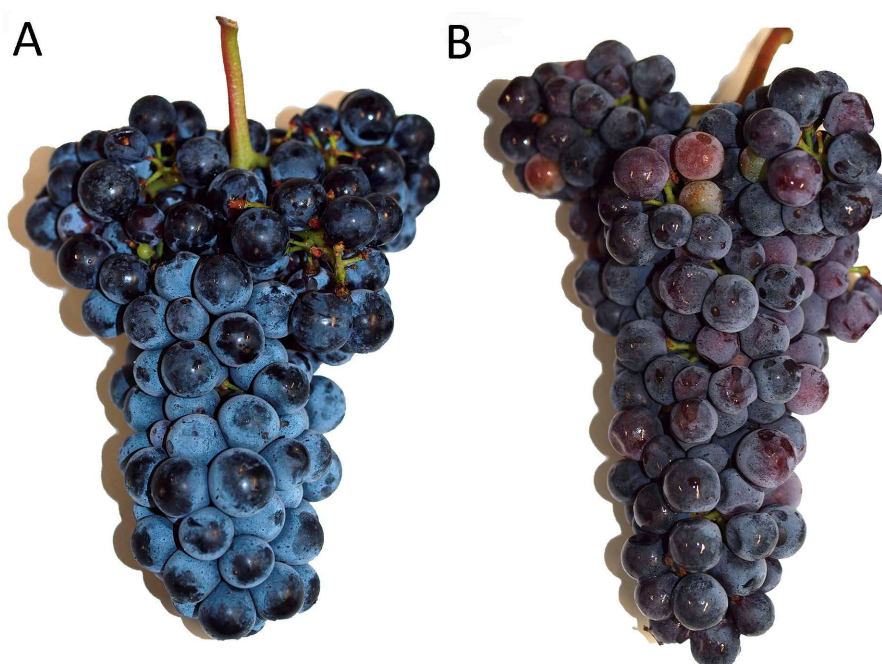


**Figure 8:** Difference between a healthy grape cluster (A) and a cluster showing BS symptoms (B) collected at the end of the ripening period in Burgenland (Austria). BS cluster is already showing severe symptoms as softening of berries, loss of turgor and a difference in colour development.

The BS disorder is not limited to Austria or Zweigelt cv. BS has been highly studied, particularly in central Europe and in regions of US as California or Washington but also in other areas as China. This disorder also affects different grape varieties, including white varieties e.g. Sauvignon blanc, Chardonnay or Semillón as well as red varieties e.g. Cabernet Sauvignon, Grenache, Nebbiolo, Humagne rouge or Zweigelt (Knoll et al. 2010; Griesser et al. 2012; Krasnow et al. 2008; Krasnow et al. 2009; Hall et al. 2011; Zufferey et al. 2015; Bondada and Keller 2012). Although several studies have been conducted within the last 15 years, the induction process and the causes of BS remain unknown.

BS is attributed to be a physiological disorder, which results in a disturbed ripening process of the berry. No evidence of a biotic cause has been found: several biotic tests have resulted negative and affected plants are free of phytoplasma and bacteria, the disorder is not appearing every year in the same vines and vegetative propagation of a plant with BS berries does not transmit the disorder (Krasnow et al. 2009; Keller et al. 2016). BS is mainly characterized by its symptoms as loose of turgor, dehydration, mesocarp cell death, disturbed sugar accumulation, low pH, reduced elasticity and anthocyanin content and greater tannin levels between others (Rogiers et al. 2004; Krasnow et al. 2009; Knoll et al. 2010; Fuentes et al. 2010; Griesser et al. 2012; Bhaskar Rao and Markus 2012). BS is differentiated from other similar disorders as bunch stem necrosis (BSN) since the symptoms are manifested in the berries but pedicel and rachis appear to be healthy, even though collapsed cells in the rachis have been already described (Hall et al. 2011). The appearance of a healthy and BS Zweigelt cluster at the end of ripening are shown in Figure 8: BS berries show turgor loss, abnormal growth and different anthocyanin synthesis but rachis and pedicels of the cluster seem to be normal. The first growing phase starting from flowering to *véraison* seems to be normal as seed reached full development (Hall et al. 2011; Bondada and Keller 2012). Weather conditions observation and its relation with BS incidence suggest a negative influence of cold weather conditions at bloom or hot and dry weather during the ripening (Raifer and Roschatt 2001).

### **2.2.1 BS berries nutrient profile**

The nutrient profile of BS grapes is one of the most discussed symptoms in BS berries. Nutrient analysis have been conducted by different authors showing variable results (Knoll et al. 2006; Bondada and Keller 2012; Bachteler 2012; Raifer et al. 2014; Bachteler et al. 2015; Bondada 2016; Keller et al. 2016; Griesser et al. 2017). Concentration of tested nutrients in BS affected plants are usually classified into xylem mobile or phloem mobile to relate their content with the vascular tissue status. Some indicators suggest that nutrients have a delayed or reduced arrival in BS grapes compared with healthy samples pointing towards the importance of the conductive anatomy of the phloem and xylem for the development of BS (Bondada 2016). Among the discussed nutrients, K<sup>+</sup> deficiency seems to be of specific interest: lower K<sup>+</sup> content has been reported by various publications and it is already assumed as a general

symptom that is as a possible inducer of BS (Krasnow et al. 2009; Bachteler et al. 2015; Griesser et al. 2017).  $K^+$  deficiency is not only detected in grapes but also in rachis and pedicels (Bondada 2016; Griesser et al. 2017). The reasons that lead to a  $K^+$  deficiency in BS clusters are not still identified: - Reduced content in grape cannot be attributed to leaf deficiency as it has been probed that application of foliar  $K^+$  has no impact in berry  $K^+$  content and BS incidence rate (Knoll et al. 2006). - Neither nutrient soil status did influenced BS rate when fertilizing soil in a Zweigelt cv. field experiment (Bachteler et al. 2015). - Further no correlation has been detected between  $K^+$  content in the adjacent leaves and BS affected clusters (Griesser et al. 2017). Other authors have related canopy topping at the beginning of berry ripening with a higher incidence of BS (Raifer et al. 2014). Recently  $K^+$  deficiency hypothesis for BS induction have been investigated, suggesting that the observed  $K^+$  deficiency in grapes (berries, rachis and pedicels) is rather due to a transport failure than a general deficiency of the whole plant (Griesser et al. 2017). A deeper insight in the genetic mechanisms of  $K^+$  transport have confirmed a reduced induction of  $K^+$  genes *VviKUP1* and *VviKUP2* and *VviK1.2* during ripening in BS affected berries (Griesser et al. 2017). The importance of  $K^+$  during grape berry ripening lies on the role of  $K^+$  carriers and channels for phloem unloading. Further phloem mobile elements have been tested in rachis and berry grapes with no consistent results. All the studies have shown reduced content of  $K^+$  in berries and rachis. Reduced amounts of P, S, B, Fe, Cu and Mg have been detected in Cabernet Sauvignon BS affected berries (Krasnow et al. 2009; Bondada 2016). Contrary increased amounts of P, S, Fe, Cu, Al and Na have been detected in Zweigelt BS affected berries (Griesser et al. 2017). Also rachis element content has been tested in Cabernet Sauvignon and Zweigelt and these tend to be present in higher amounts (Krasnow et al. 2009; Griesser et al. 2017). The irregular content, increased and decreased, of phloem transported nutrients opens the uncertainty if phloem transport is generally altered or if certain molecules or nutrients fail to be transported towards BS grapes.

The most altered xylem mobile element in BS grape berries is  $Ca^{2+}$ , showing higher concentrations for most authors but also reduced for others (Krasnow et al. 2009; Bachteler 2012; Bondada 2016; Griesser et al. 2017).  $Ca^{2+}$  has an important role for signalling and response to different biotic and abiotic stress. Its irregular content may affect this function in BS affected berries. Increased soil fertilization with Ca has been correlated with a higher incidence of BS (Bachteler et al. 2015), and content reduction

of phloem and xylem nutrient mobile elements in BS samples have been interpreted as a lack of functionality of the vascular tissues but further evidences are needed (Bondada 2016).

### **2.2.2 BS berries carbohydrate metabolism**

BS berries show high acidity what makes them unpleasant for the taste. Content of tartaric acid is similar at healthy and BS berries (Krasnow et al. 2009), although there is no agreement whether malate acid content increases or decreases during BS (Krasnow et al. 2009; Keller et al. 2016). Degradation of malate acid is happening in both BS and healthy berries during ripening and sometimes is slightly slower in BS samples. It is thought that these differences may not be enough to explain the sour taste of BS berries. Rather low pH (low K<sup>+</sup>) and decreased content of sugar may not mask the sensorial quality of acid content in grapes (Keller et al. 2016).

Low sugar content is one of the most aggressive and persistent symptoms observed in BS berries (Krasnow et al. 2009; Hall et al. 2011; Knoll et al. 2010; Griesser et al. 2012; Keller et al. 2016). Sugar accumulation through ripening has been monitored by numerous studies due to the simple and reliable method of soluble solid for sugar quantification. In grapevine ripe fruits the hexoses, specially glucose and fructose, are the major solids in vacuoles reaching at maturation concentrations around 1M (Coombe and McCarthy 2000). The fast sugar accumulation seems to be disturbed in BS berries. Sugar accumulation in BS berries show differences already three weeks before symptoms are visible which values keep stable between 11 and 13° Brix throughout ripening (Knoll et al. 2010; Griesser et al. 2012; Keller et al. 2016). The accumulation of soluble solids after *véraison* is reduced and stops completely later during the ripening process. These facts together with the normal development of seed places the induction of the illness close to *véraison* (Hall et al. 2011; Bondada and Keller 2012). Most of the studies focused on the determination of soluble solids, but no insight in the sugar metabolism of BS berries in comparison to healthy berries has been performed so far.

### 2.2.3 BS berries polyphenol profile

Phenolic profile of BS grapes is characterized by a reduced anthocyanin content while tannin content shows higher values than in healthy grapes producing bitter and astringent off-flavours (Krasnow et al. 2009; Knoll et al. 2010; Griesser et al. 2012). Tannin content in the seed seems to be consistent to healthy berries but tannin content in the skin is higher in BS than in healthy berries which has been related to abiotic stress response (Krasnow et al. 2009; Bondada 2014).

The differences in colour development of BS affected berries are shown in Figure 9. BS berries show a pale colour while healthy berries show a dark blue colour at the end of ripening. Specifically cyanidin, delphinidin and petunidin glucosides are found in lower amounts in Cabernet Sauvignon BS berries in the last part of ripening (Krasnow et al. 2009). The reduced amount of anthocyanin has been attributed to the low amount of sugars accumulated by BS berries (Keller et al. 2016). In general, berries that do not accumulate sugars further than 15° Brix are not able to colour properly which is maybe related to the role of sugars in the regulation of the anthocyanin biosynthesis (Pirie and Mullins 1976; Keller and Shrestha 2014; Dai et al. 2014). Water status or cell turgor is also related to reduced tannin and anthocyanin content but both are affected in the same manner by this factor while in BS berries anthocyanin reduction is more pronounced (Roby et al. 2004). Light is another important factor for anthocyanin biosynthesis but affected clusters are not influenced by orientation and hence by sun exposure (Downey et al. 2004). Apart from ABA, ethylene is also influencing anthocyanin biosynthesis and its synthesis within the berry is related to anthocyanin biosynthesis triggering (Chervin et al. 2004).



**Figure 9:** Grape berries of a healthy cluster (A) and a BS symptomatic cluster (B). The difference in anthocyanin content is visible.

#### 2.2.4 BS physiological modifications

BS symptoms are affecting not only grape berry nutrients and metabolites but also morphological structures. Mesocarp cell viability at BS affected berries is decreasing faster than healthy berries towards the end of ripening (Krasnow et al. 2009). Also it was described collapsed mesocarp and high concentration of calcium oxalate crystals in mesocarp cells of BS berries (Bondada and Keller 2012). It is thought that the necrotic mesocarp leads to the turgor loss and the flaccid appearance of BS berries. Further, flaccidity results in wrinkled exocarp. In contrast, epicuticular waxes of BS berries show no modifications (Bondada and Keller 2013). Figure 10 shows morphological differences: while healthy berries are round and turgid (Fig. 10A) BS berries exocarp become wrinkled as turgor is lost (Fig. 10B). Additionally, the tight connection from the pedicel to the berry by the brush present in healthy berries (Fig. 10C) is weak in BS grape berries (Fig. 10D).



**Figure 10:** A) Healthy berry close to full-ripen which shows a round morphology and turgidity. B) BS berry which has lost turgor and exocarp looks wrinkled. C) Healthy berry well-connected to the pedicel. D) BS berry which tight connection with the pedicel is lost and juice is getting lost through it. Pedicel still keeps green and no necrosis is visible.

The main symptoms of BS described so far have been focussed on berries as, contrary to BSN, rachis and pedicels of BS cluster do not show obvious symptoms. In any case all tissues should be under study as usually BS symptoms appear on the cluster tip but through ripening they spread towards the peduncle and finally it covers the whole cluster (Keller et al. 2016). In fact, due to the reduced amount of solutes that are able to reach BS berries the idea of reduced cell viability and transport capacity of vascular tissues was arising. Different studies have focused in the morphology of vascular tissues in the grape and rachis (Hall et al. 2011; Bondada and Keller 2012; Zufferey et al. 2015). First studies covering rachis observed reduced cell viability in rachis of BS berries (Hall et al. 2011). Xylem integrity has been tested in Humagne cv. and did not show important abnormalities, hydraulic conductance was tested with no presence of

embolism and the slight reduction in xylem conductivity may not explain the appearance of BS (Zufferey et al. 2015). Cabernet Sauvignon cv. xylem observation in peduncles did not show any difference in xylem tissues between healthy and BS samples (Bondada 2014). About rachis tissue organization, a detailed study has been conducted in Cabernet Sauvignon peduncle showing that general organization of tissues was conserved in BS affected clusters (hard phloem, primary phloem, xylem and pith (Bondada 2014). Hard secondary phloem regions have been observed in Humagne cv. BS affected berries and has been attributed to the disorder (Zufferey et al. 2015). Hard phloem regions usually appear only in perennial plants and in annual structures where it is associated with cold weather when the plant suffers a false hibernation or hardiness due to wind. In a different study brownish colouring in the phloem was hypothesized to be necrosis of phloem cells in the peduncle but so far this has not been proved (Bondada 2016). A stronger presence of callose has been observed in sieve plates of BS affected clusters than in healthy clusters at the end of the ripening period (Bondada and Keller 2013; Bondada 2014). Further proof is needed to evaluate the possible effects of these observations on phloem conductance.

## 3 Materials and methods

### 3.1 Collection of plant material

Analytical analyses, enzymatic assays and qPCR were performed with plant material obtained from distal parts of grape clusters from a commercial vineyard in lower Austria (Mailberg GPS coordinates 48.6667, 16.1833). The vineyard was planted in 1974 with the red wine cultivar Zweigelt (*Vitis vinifera* L.) grafted on Kober 5BB (*V. riparia* x *V. berlandieri*) with vertical shoot positioning (VSP) and bilateral canes as trellising system. 300 grape clusters were labelled randomly distributed within the vineyard short after bloom (10.06.2011). Soluble solids (Digital refractometer, Atago PAL-1, Tokyo, Japan) were measured once per week from all labelled grape clusters to follow the growth and ripening process. Berries (10 berries each) were collected at six sampling times in 2011, namely on 22.07. (42 DAA), 29.07. (49 DAA), 4.08. (55 DAA), 11.08. (62 DAA), 17.08. (68 DAA) and 24.08. (75 DAA), representing a time period from BBCH79 (majority of berries touching) to BBCH89 (berries ripe for harvesting). Every cluster was sampled only once and only the cluster tip (2-3 cm) is taken to not influence the further development of each grape cluster. Samples were frozen in liquid nitrogen immediately and were categorized as healthy and BS short before harvest. Eight field samples were pooled into four biological repeats for further analyses. Seeds were removed and plant material was further homogenized with a ball mill (Retsch MM400, Haan, Germany) under cold conditions to prevent thawing.

Samples used for light microscopy and transmission electron microscopy were collected in two seasons, 2013 and 2014. Collected grapes were classified according to symptom severity into: 'early symptoms' grapes (soluble solids around 12°Brix and first symptoms of turgor loss and 'late symptoms' samples (severe turgor loss with shrinking berries and low anthocyanins accumulation). In 2013 healthy (n = 8) and BS (n = 8) samples were taken from both, green house plants (BOKU, Tulln, Lower Austria) and from vineyard (Mailberg, Lower Austria). In 2014 healthy (n = 7) and BS (n = 11) samples were taken from a commercial vineyard (Burgenland, Austria). Pedicel and rachis samples were immediately cut in sections thinner than 1mm and conserved in 0.1M sodium cacodylate buffer until further processing in the laboratory. Samples (healthy (n = 5) and BS (n = 6)) used for scanning electron microscopy were obtained 2015 from two vineyards (Lower Austria and Burgenland) from the start of BS

symptoms till the end of the season, classifying them as 'early symptoms' or 'late symptoms' following the same pattern described. Samples were cut in 1 mm sections and were cleaned to make the cell walls visible as described below.

## 3.2 Metabolite analysis

### 3.2.1 Measurement of total anthocyanin content

The measurement of total anthocyanin content followed a pH differential method (Lee et al. 2005; Fang and Bhandari 2011). Four biological replicates were used for each time point and treatment. Anthocyanins were extracted by adding 4 ml of extraction solution (acidified EtOH, 0.1% HCL (v/v)) to 400 mg homogenized plant material. Extraction was performed with an ultrasonic bath (Branson 5210 ultrasonic bath, Branson Ultrasonics, Danbury, 06810 USA) for 30 min and was repeated twice. The extracts for each sample were collected after centrifugation (16000xg for 15 min) (Centrifuge 5804R, Eppendorf, Hamburg, Germany) and combined. The absorbance was measured with a Spectrophotometer (Genesys 10S UV-VIS, Thermo Fisher Scientific, MA 02454 Waltham, USA) at 510 nm and 700 nm in buffers at pH 1.0 (0.025M potassium chloride buffer) and pH 4.5 (0.4 sodium acetate buffer) and finally calculated as followed:  $A$  (absorbance) =  $(A_{510} - A_{700})_{pH1.0} - (A_{510} - A_{700})_{pH4.5}$ . The total anthocyanin content, expressed as cyanidin-3-glucoside equivalent was calculated: anthocyanin content (mg cyanidin-3-glucoside g<sup>-1</sup> DW grape berries without seeds) =  $(A \times 449 \text{ g mol}^{-1} \text{ cyanidin-3-glucoside} \times \text{dilution factor } 1:10 \times 8 \text{ ml extract volume} \times 1000) / (29600 \text{ molar extinction coefficient of cyanidin-3-glucoside} \times 1 \times \text{DW dry weight berry material})$  (De Beer et al. 2004). The dry matter content (DW) of the plant material was determined for all samples twice with 200 mg fresh weight at 80°C for 48 h.

### 3.2.2 Sugar analysis

Extraction and analysis of carbohydrates were performed as described (Guignard et al. 2005). Approximately 100 mg of powdered grape material were mixed with 1 ml of EtOH 80%. This mixture was homogenized using a vortex/mixer for 30 s and shaken for 30 min at 4°C. After centrifugation at 10,000g for 10 min at 4°C (Centrifuge 5417 R, Eppendorf, Hamburg, Germany), the supernatant was collected. An additional extraction was done on the residue using the same extraction solvent (0.5 ml). The

supernatants were pooled and evaporated to dryness in a SpeedVac concentrator (Heto, Thermo Electron Corporation, Waltham, MA). Carbohydrates were re-suspended in 1 ml of water and the suspension was filtered through a 0.45  $\mu\text{m}$  Acrodisc PVDF syringe filter prior to analysis using high performance anion exchange chromatography coupled with pulsed amperometric detection (HPAEC-PAD). The values obtained were corrected for the dry weight of the samples.

### 3.2.3 Polyphenol analysis using LC-MS/MS

Anthocyanins and other selected polyphenols were extracted and analyzed utilizing the validated method of (Schoedl et al. 2011). The established method covers representative metabolites of the structure class anthocyanins, cinnamic acids, flavonoids and stilbenes and was extended to enable the simultaneous separation and quantification of 23 polyphenols. 100 mg of homogenized plant material (samples from 24.08.2011) was extracted for 10 min twice in 1ml of extraction buffer (0.02% hydrochloric acid (m/v) in 80% aqueous MeOH (v/v)) using ultrasonication in ice water (Branson 5210 ultrasonic bath, Branson Ultrasonics, Danbury, 06810, USA). The combined extracts were diluted 1:1 with 0.5% aqueous (v/v) formic acid in water and 5  $\mu\text{L}$  were injected into the LC-MS/MS system without the need for any further sample preparation. The detection and quantification of analytes were performed using a 4000 QTrap LC-MS/MS system (AB Sciex, Foster City, CA) equipped with a TurbolonSpray electrospray ionization (ESI) source and a 1290 series HPLC system (Agilent, Waldbronn, Germany). Chromatographic separation was obtained at 40°C on a Gemini RP-18 column, 100  $\times$  2 mm inner diameter, 3  $\mu\text{m}$  particle size (Phenomenex, Torrance, CA) protected with a Gemini 3.0  $\times$  2 mm guard column (Phenomenex, Torrance, CA) using gradient elution. The mobile phase consisted of (A) 0.5% formic acid in H<sub>2</sub>O and (B) 0.5% formic acid in MeOH. The flow rate was 400  $\mu\text{L}/\text{min}$  and the total run time 22 min. Selected reaction monitoring (SRM) mode in negative polarity was performed with the following settings: source temperature, 550 °C; curtain gas, 10 psi (69 kPa of maximum 99.5% nitrogen); ion source gas 1 (source heating gas), 50 psi (345 kPa of nitrogen); ion source gas 2 (drying gas), 50 psi (345 kPa of nitrogen); ion spray voltage, -4000 V. For quantification external calibration using standards in pure solvent was applied (Schoedl et al. 2011). To putatively identify conjugated anthocyanins in a

second analysis step, SRM transitions according to (Sapozhnikova 2014) were included into the method and acquainted using the positive ionization mode.

### 3.3 RNA extraction and qPCR analysis

RNA extraction of berries was performed according to a modified protocol (Reid et al. 2006). The extraction buffer (300mM Tris HCl (pH 8.0), 25mM EDTA, 2M NaCl, 2% CTAB, 2% PVPP, 0.05% spermidine trihydrochlorine and 2%  $\beta$ -mercaptoethanol) was added to 200mg ground plant material and incubated at 65°C for 20 min (Thermomixer Comfort, Eppendorf, Hamburg, Germany). Adjacent 1 vol of chloroform:isoamyl alcohol (24:1, v/v) was added and the aqueous phase was recovered. This step was performed twice. RNA and DNA was precipitated with 0.1 vol Na-acetate (3M, pH 5.2) and 0.7 vol isopropanol for 30 min at -80°C. The pellet was washed two times with 70% EtOH. The dried pellet was dissolved in DEPC water followed by DNA digestion with Amplification Grade DNase 1 (Sigma Aldrich, St. Louis, MO 63103, USA) according to manufacturer's instructions. After the reaction and the inactivation of the enzyme the volume was filled up to 300 $\mu$ l with DEPC water. RNA was precipitated overnight at 4°C by adding 95 $\mu$ l of 8M LiCl. After centrifugation (max speed, 30 min, 4°C) (Centrifuge 5417 R, Eppendorf, Hamburg, Germany) an RNA pellet was obtained and washed twice with ice cold 70% EtOH. Finally the RNA was dissolved in 50 $\mu$ l 0.1 TE buffer and stored at -80°C. Purity and concentration of RNA was determined with a NanoDrop 2000c (Thermo Scientific, Wilmington, USA).

Subsequent reverse transcription was performed with 1,000 ng total RNA by using the GoScript Reverse Transcription System (Promega, Madison, USA) according to manufactures recommendations. cDNA was further diluted 1:20 for qPCR analyses. qPCR was performed using the Rotor-Gene Q cycler (Qiagen, Hilden, Germany) in 12 $\mu$ l reaction volume with 2 $\mu$ l cDNA, 200nM primers each and 2X KAPA SYBR FAST qPCR Universal (Peqlab, Erlangen, Germany). All primers were tested for their efficiency prior to analysis by conducting standard curves with four step template dilutions. Cycling conditions were as follows: activation 4 min at 95°C, 40 cycles for 8 sec at 95°C, 20 sec at 60°C, 30 sec at 72 and 5 sec at 75°C with fluorescence measurement. Dissociation curves were performed with continuous fluorescence

acquisition from 65-95°C. Normalized relative quantities (NRQ) were calculated with the R program (Team 2016) and the package easyqPCR (Pape 2012).

**Table1:** List of primers and genes tested by qPCR

| List of primers tested by RT-PCR                    |                    |                             |                            |
|---|--------------------|-----------------------------|----------------------------|
| Gene  | Nomenclature       | Primer sequence 5'-3'       |                            |
|   |                    | Forward                     | Reverse                    |
| Hexose transporter <i>VviHT1</i>                    | VIT_20s0181g00010  | F: aaccaccagccttacagaa      | R: ctgaccagcagccattgata    |
| Hexose transporter <i>VviHT3</i>                    | VIT_11s0149g00050  | F: gaattctgtgtgggtcacgtccat | R: aggccaccagcagcagagaga   |
| Cytosolic invertase <i>VviCINV1</i>                 | VIT_06s0061g01520  | F: ttcataggaagcagtcacg      | R: tagtctcttccaagccaa      |
| Vacuolar invertase <i>VviGIN1</i>                   | VIT_16s0022g00670  | F: gaggaagaggggtggctcagg    | R: caggcaaacatggcgtagtccaa |
| Vacuolar invertase <i>VviGIN2</i>                   | VIT_200s0233g00010 | F: acgcctcactgtgtttca       | R: caacgaggttccaacgg       |
| Cell wall invertase <i>VviCWI</i>                   | VIT_204s0008g01140 | F: aaccaccagccttacagaa      | R: ctgaccagcagccattgata    |
| Tonoplast monosaccharide transporter <i>VviTMT1</i> | VIT_218s0122g00850 | F: gctccctgaaacgggaaactacgc | R: atgggaaggagggggcacca    |
| Tonoplast monosaccharide transporter <i>VviTMT2</i> | VIT_203s0038g03940 | F: tcttcccaccctgtccgagg     | R: gccaaagacaccagcaaggcca  |
| Tonoplast monosaccharide transporter <i>VviTMT3</i> | VIT_07s0031g02270  | F: ccaaggggtggaaggacaagca   | R: ccacccaacaacaatgcacgc   |
| Flavonoid 3' hydroxylase <i>VviF3'H</i>             | VIT_04s0023g03370  | F: agcgtcaaaccgagcatggagc   | R: tgggtgtgagctgatgtctct   |
| Leucoanthocyanidin reductase 1 <i>VviLAR1</i>       | VIT_01s0011g02960  | F: cgccctagtgaaagccatga     | R: attgtcggaccctacgcttc    |
| Flavonoid-3-O-glycosyltransferase <i>VviUFGT</i>    | VIT_16s0039g02230  | F: cctaagggacaaggcaagg      | R: cccaactgctcatgtgcta     |
| Myb transcription factor <i>VviMYBPA1</i>           | VIT_15s0046g00170  | F: tattgggttgacgggggtg      | R: tcgctcaagcagttgcagat    |
| Myb transcription factor <i>VviMYBA1A2</i>          | VIT_07s0005g01210  | F: tctcaaaggcaaaagctgaag    | R: tcggtgccacagtaaggctc    |
| Anthocyanidin reductase <i>VviANR</i>               | VIT_00s0361g00040  | F: ctgatgggacaggtctggt      | R: tgtctggaggcagatagc      |
| Dihydroflavonol 4-reductase <i>VviDFR</i>           | VIT_18s0001g12800  | F: ctgagcaagctgcatggaag     | R: cagtgatcggggaaagagca    |
| Leucoanthocyanidin reductase 2 <i>VviLAR2</i>       | VIT_17s0000g04150  | F: tcgctcatttccgacctcc      | R: ttctccacggttacacggg     |
| Leucoanthocyanidin dioxygenase <i>VviLDOX</i>       | VIT_02s0025g04720  | F: accgtgtaaggtgtctgga      | R: gtctcccactcaagctgtc     |
| Flavanone-3 $\beta$ -hydroxylase 1 <i>VviF3Hmix</i> | VIT_04s0023g03370  | F: ttatctgagcaatgggaggttca  | R: gctcatcttctctgtacatct   |
| Chalcone synthase 1/2/3 <i>VviCHSmix</i>            | VIT_14s0068g00930  | F: atgatgtaccaacagggtctgc   | R: cagctgtgatctcagagcagac  |
| Chalcone isomerase <i>VviCHI</i>                    | VIT_13s0067g03820  | F: acgctcggcgaagtgaa        | R: gcgaccctcaaaggcaaaatcg  |
| Actin <i>VviACT</i>                                 | VIT_04s0044g00580  | F: tgtgcttagtggtgggtcaa     | R: atctgctggaaggtgctgag    |
| Ubiquitin <i>VviUBI</i>                             | VIT_16s0098g01190  | F: ttgatgcaattggctaggaa     | R: tgtaacactgcatgcaccaa    |

Prior to analyses the most stable reference genes were determined by testing: actin (VIT\_04s0044g00580), ef1 (VIT\_06s0004g03220), gadph (VIT\_17s0000g10430) and ubiquitin (VIT\_16s0098g01190). According to Normfinder calculation (Andersen et al. 2004) actin and ubiquitin were the most stable reference genes for our qPCR analyses. Three groups of genes were tested (Table 1). Hexose transporters *VviHT1* and *VviHT3* (Fillion et al. 1999; Vignault et al. 2005; Deluc et al. 2007; Hayes et al. 2007), the

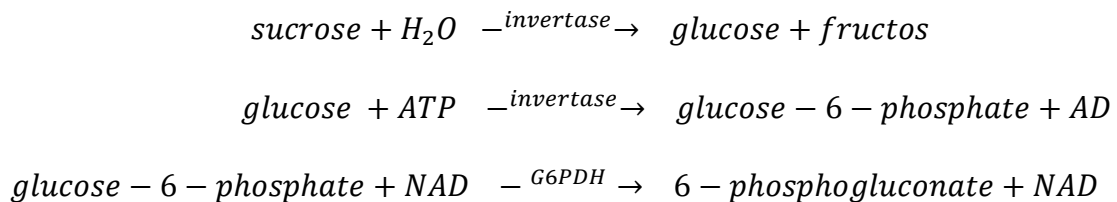
tonoplast monosaccharide transporter genes *VviTMT1*, *VviTMT2* and *VviTMT3* (Afoufa-Bastien et al. 2010; Zeng et al. 2011) and the invertases *VviGIN1*, *VviGIN2*, *VviCINV1* and *VviCWI* (Davies and Robinson 1996; Hayes et al. 2007; Nonis et al. 2008). Anthocyanin biosynthesis primers were designed in the laboratory (*VviF3'H*, *VviLAR1*, *VviUFGT*, *VviMYBPA1*, *VviMYBA1A2*, *VviANR*, *VviDFR*, *VviLAR2*, *VviLDOX*, *VviF3Hmix*, *VviCHSmix*, *VviCHI*).

### 3.4 Enzyme activity assay of the carbohydrate metabolism

Vacuolar (VINV), cell wall (CWINV) and cytosolic invertase (CINV) assays were performed from a starting material around 40mg FW (adapted from (Gibon et al. 2004)). Soluble proteins were obtained after incubation in 400µl extraction buffer (50mM HEPES, 0,25% BSA, 10mM MgCl<sub>2</sub>, 1mM EDTA, 1mM EGTA, 1mM capronic acid, 1mM benzamidine, 25 mM sorbitol, 2mM leupeptine, 50mM PMSF, 10mM DTT, 1% triton, 20% Glycerol, 1% PVP, 1% PVPP). Samples were centrifuged for 20 min at 10,000g and 4°C (Centrifuge 5417 R, Eppendorf, Hamburg, Germany) and extracts were used for quantification of vacuolar and cytosolic invertases. From the resulting pellet, insoluble proteins were extracted in 400µl NaCl high salt buffer (1M NaCl, 50mM HEPES, 0.25% BSA, 10mM MgCl<sub>2</sub>, 1mM EDTA, 1mM EGTA, 1mM capronic acid, 1mM benzamidine, 25 mM sorbitol, 2mM leupeptine, 50mM PMSF, 10mM DTT, 1% triton, 20% Glycerol, 1% PVP, 1% PVPP) and centrifuged for 20 min at 10,000g and 4°C (Centrifuge 5417 R, Eppendorf, Hamburg, Germany) for CWINV reaction.

Both acid enzymes (VINV and CWINV) were performed in a two-steps assay in 96 microtiter plate. Acid invertase reaction was performed in acetate/KOH buffer pH 4.5. The invertase reaction was started by the addition of 20mM sucrose and run during 20 min at 37°C (Microplate reader FLUOstar Omega, BMG LABTECH, Offenburg, Germany). The reaction was stopped by deactivation of the enzyme at 95°C (Digital Dry Block Heaters, VWR, Radnor, PA, USA). In a second step the detection of glucose and fructose, degradation products of the invertase reaction, was performed at pH7 by the addition of the detection buffer (0.2M HEPES pH7, 1U/ml G6PDH, 1U/ml HXK, 1mM ATP and 1mM NAD). In this step the coupling reaction of NADH production was monitored at 340nm (Microplate reader FLUOstar Omega, BMG LABTECH, Offenburg, Germany). Cytosolic invertase reaction was run in a one-step assay,

invertase reaction and detection reaction were performed simultaneously incubated with the detection buffer (50mM HEPES pH7, 20mM sucrose in the samples, 1U/ml G6PDH, 1U/ml HXK, 1mM ATP and 1mM NAD) at pH 7 and 37°C and simultaneously the coupling reaction of NADH production was monitored at 340nm (Microplate reader FLUOstar Omega, BMG LABTECH, Offenburg, Germany) (Gibon et al. 2004; Biais et al. 2014). Standards of glucose and fructose were included for further calculations. Calculations of enzyme activity were performed with the software Optima MARS Data Analysis (BMG LABTECH, Offenburg, Germany) by the slope linear regression function, obtaining nmol/min. Results were then expressed in DW basis.



### 3.5 Microscopic procedures

#### 3.5.1 Light microscopy

Fixation was performed with 2% (w/v) paraformaldehyde (Sigma–Aldrich, St. Louis, MO, USA) and 2% (v/v) glutaraldehyde (Fluka, Buchs, Switzerland) in 0.1 M sodium cacodylate buffer (pH 7.2) for 2 h at room temperature under -0.4 MPa vacuum. Afterwards samples were washed 4 times in 0.1 M sodium cacodylate buffer for 10 min at room temperature and then stored in 0.1 M cacodylate buffer at 4°C (Golinowski et al. 1996). Dehydration of the samples was performed from 30% EtOH increasing in 10% concentration in every step till 100% EtOH for 30 min. Infiltration and embedding was performed with 2-hydroxyethyl methacrylate (HEMA) also called glycol methacrylate (JB4 embedding kit Polyscience, Warrington, USA) following the manufacturer instructions. Infiltration was performed with a mixture of 100 ml of JB4 solution A (monomer) and 1.25 g of benzoyl peroxide and increasing amounts of infiltration solutions were added for incubation (30 min) (50% EtOH – 50% resin; 25% EtOH – 75% resin; 10% EtOH – 90% resin; 100% resin). The infiltration step with pure resin was repeated 3 times. Infiltrated samples were placed in the embedding molds

(JB-4 Embedding Molds from Polyscience Inc.) and freshly prepared embedding solution (25 ml of JB4 resin solution A was mixed with 1 ml of JB4 solution B (accelerator)) was poured. To remove air the slots in molds were covered with block holders and kept at 4°C overnight to control the exothermic reaction. Polymer cubes were then mounted on wood holders before sectioning on the rotatory microtome equipped (Leica Biosystems) with a D-knife (Leica Biosystems) and sectioned on 5 µm thick sections (Sullivan-Brown et al. 2011).

Three different methods were used to stain the sections. Toluidine blue dye was used in a concentration of 0.05% (w/v), incubated 5 min and rinsed with distilled water (Gerlach 1984). A combination of safranin/astrablau dyes: sections were first stained with safranin 0.1% for 1 min, rinsed with 70% EtOH, then stained in 1% astrablau for 10 min and rinsed with ddH<sub>2</sub>O (Gerlach 1984). Triple fuchsin–chrysoidin–astral blue (FCA or Etzold) staining was performed by incubating sections in a mixture of 0.01% new fuchsin, 0.014% chrysoidin, 0.012% g astral-blue in 5% acetic acid solution for 5–8 min and they were rinsed with distilled water thereafter (Etzold 2002). The three staining methods enable the differentiation of phloem and xylem tissues: toluidine stains lignin greenish, nucleic acids blue and polysaccharides purple, safranin/astrablau stains cellulose blue and lignin red and FCA or Etzold stains lignin red, cutin yellow, and cellulose blue (Seidelmann et al. 2012). Images were obtained with the microscope Zeiss Axiovert 200M Inverted microscope and a coupled Axio Cam camera (Zeiss, 73447 Oberkochen, Germany). Further analyses of the images were performed with the ImageJ software (Schneider et al. 2012; Schindelin et al. 2015).

### **3.5.2 Scanning Electron Microscopy**

Samples were washed in water and incubated in 0.1% proteinase K (Invitrogen) dissolved in 50 mM Tris-HCl buffer, 1.5 mM Ca<sup>2+</sup> acetate, and 8% Triton X-100, pH 8.0 at 55°C for 10 days with agitation at 350 rpm (Thermomixer Comfort, Eppendorf, Hamburg, Germany). The proteinase K was deactivated with 100% EtOH. After washing with ddH<sub>2</sub>O, starch grains were digested in a 0.1% amylase solution (Sigma–Aldrich, St. Louis, MO, USA) in 10 mM Tris-HCl, pH 7.0 for 3 days. The cleaning protocol was adapted from (Mullendore et al. 2010). Samples were dehydrated for 12h in freeze drier Christ beta 2-4 L (Martin Christ Gefriertrocknungsanlagen GmbH, Osterode am Harz, Germany). Observations were conducted with tabletop SEM

microscope Hitachi TM3030. Samples were mounted on aluminium cylinder holders (Specimen Mount, Ø15 x 6 mm x M4) and fixed with carbon stickers (15 mm carbon conductive Tabs double coated, Pelco Tabs). Elemental analysis was performed using Energy Dispersive X-ray Spectrometer Quantax70 (Bruker Corporation, Billerica, Ma, USA).

Conductivity ( $k$ ) was calculated following the equation from (Thompson and Holbrook 2003) where  $N_p$  is the number of sieve pores per sieve plate,  $r$  ( $\mu\text{m}$ ) is sieve element radius,  $l$  ( $\mu\text{m}$ ) is sieve element length,  $r_p$  ( $\mu\text{m}$ ) is sieve pore radius, and  $l_p$  is sieve plate thickness. Measurement of this elements was performed with Image J software (Schneider et al. 2012; Schindelin et al. 2015).

$$k = \left[ \frac{8 N_p r_p^4 l}{(8 N_p r_p^4 (l - l_p) + (8 l_p + 3 \pi r_p) r^4)} \right] \left[ \frac{r^2}{8} \right]$$

### 3.5.3 Transmission Electron Microscopy

Fixation was performed as described above (Golinowski et al. 1996). Then the samples were washed 4 times in 0.1M sodium cacodylate buffer for 10 min at room temperature and were stored in 0.1 M cacodylate buffer at 4°C. Post-fixation was performed with 2% (w/v) osmium tetroxide (Roth GmbH, Karlsruhe, Germany). Dehydration of samples was performed with EtOH as described above. The EtOH was substituted with propylene oxide (Sigma–Aldrich, St. Louis, MO, USA) and the samples were infiltrated in a graded ascending series of Spurr's resin dissolved in propylene oxide (Sullivan-Brown et al. 2011). After infiltration the samples were embedded in flat embedding moulds and polymerization of the resin was performed at 70°C for 18 h. Ultra-thin (60–90 nm thick) sections were taken with a Leica UCT ultramicrotome (Leica, Wetzlar, Germany) and collected on formvar-coated copper single slot grids. They were stained with uranyl acetate and lead citrate and examined in FEI M268D 'Morgagni' transmission electron microscopy (FEI Corp., Hillsboro, OR, USA) equipped with an SIS 'Morada' digital camera (Olympus-SIS, Muenster, Germany). The images were captured using an SIS iTEM software (Olympus-SIS, Muenster, Germany) and adjusted for similar brightness and contrast, and resized using Adobe Photoshop software.

### 3.6 Statistical analysis

Normalized relative quantities (NRQ) were calculated with the R program (Team 2016) and the package `easyqPCR` (Pape 2012). Shapiro Wilk test of normality was applied to all data sets (Shapiro and Wilk 1965). For not normally distributed populations outliers were detected and discarded when necessary. Differences between treatments were statistically analyzed by t-test for normally distributed populations (Welch 1947) and Mann Withney U test for not normally distributed populations with the `r` program (SPSS 10.01, SPSS Inc. Chicago, IL, USA) (Mann and Whitney 1947). Statistical differences between groups were significant when  $p < 0.05$ . All data in tables and graphs are presented as mean  $\pm$  standard error. Heatmap graphs are presenting log<sub>2</sub> fold-change (FC) data with the computer program R version 3.3.2 (Team 2016) using 'heatmap.2' function of the package 'gplots' (Gregory R. Warnes 2016). For correlation between genes Pearson correlation coefficient was used (SPSS 10.01, SPSS Inc. Chicago, IL, USA) and was calculated from log<sub>2</sub> fold-change (FC) data.

## 4 Results

### 4.1 Molecular biology: sugar and anthocyanin metabolism

#### 4.1.1 Comparative accumulation of sugar and anthocyanin in healthy and BS berries on a time scale

In order to analyse the accumulation of solutes in BS berries and locate the start of the symptoms, time scale analysis determining the content of soluble solids and total anthocyanin were conducted throughout the growing season with healthy and BS grapes (Fig. 11). Samples from vineyards were obtained at different time points during berry growth and berry ripening including symptomatic as well as pre-symptomatic BS grape clusters. So far, no previous studies have analysed BS samples before symptoms appear. Furthermore as it is reasonable to think that BS is induced before symptoms become visible, it was expected to detect abnormal pre-symptomatic metabolite contents.

Sugar accumulation is one of the key features of fruit ripening which determines fruit quality and limits further industrial processing (Jackson and Lombard 1993). As sugar is the most abundant assimilate in grapes during ripening, an easy and robust field method to follow the ripening process of sugar accumulation is to determine total soluble solids. As shown in Figure 11.A, healthy berries accumulate soluble solids until the end of ripening whereas the values for BS berries increase slowly and stop in the middle of the ripening stage when Brix values are around 10-13°. A significant differentiation in soluble solids between healthy and BS berries (from 17.08.2011 on) happens after the first BS symptoms are observed (11.08.2011) but the trend can already be observed at *véraison*. Similar results were obtained for the total anthocyanin content (Fig. 11B). Anthocyanin synthesis in healthy berries starts short after *véraison* but its concentration grows especially in the last three weeks of ripening. In BS berries the concentration of total anthocyanins accumulated in the skin is significantly reduced close to harvest (24.08. and 09.09.2011). As a conclusion of sugar and anthocyanin profile content, reduced accumulation in symptomatic BS berries is gradual and differences become significant after symptom development.

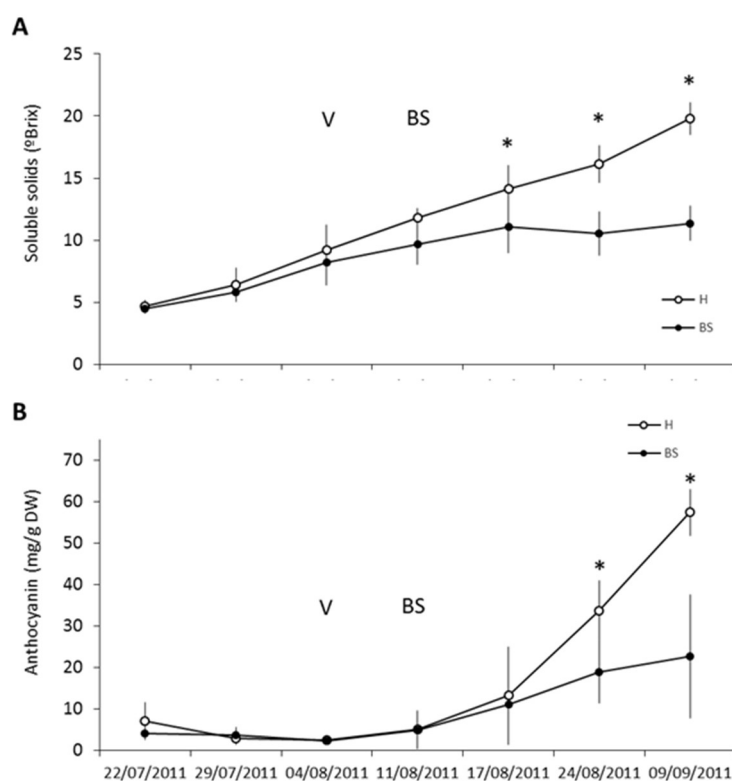


**Figure 11:** (A) Timescale of soluble solids ( $^{\circ}$ Brix) measurement of 300 grape clusters in the vineyard and (B) total anthocyanin content of healthy and BS grapes at 6 sampling dates (N=4 each) which data is presented as mean values ( $\text{mg g}^{-1}$  DW)  $\pm$  standard deviation. Asterisk (\*) indicates statistical significance between H and BS samples ( $p < 0.05$ , t-test). *Abbreviations:* V-*véraison*; BS- berry shrivel symptom development.

#### 4.1.2 Comparative analysis of glucose, fructose and sucrose on a time scale

As differences in total soluble solids were significant among healthy and BS berries at ripening, we determined the concentrations of single sugars (sucrose, glucose and fructose) throughout the growing season (Fig. 12). We expected a decrease in the amount of sucrose or hexoses which would give us an insight of the altered sugar mechanisms in BS berries. Healthy samples did show a typical pattern of sugar accumulation in berries: low concentrations before *véraison*, while later especially hexose concentration rapidly increased. Sugar concentrations in BS berries are significantly reduced at the end of the ripening phase. Lower concentrations in sucrose were observed from *véraison*, although were not significant at early sampling dates (Fig. 12A). Results for hexose concentrations were similar: reduced values in BS berries for glucose and fructose were observed already before *véraison* but reached statistical significance later during the ripening process (Fig.12B-C). In order to have a

different perspective on concentration results, they were transformed into % of increase at the different time points (Fig. 12D-E-F). The results of BS berries were related to the final contents in healthy as well as BS berries. Surprisingly the accumulation rates in H and BS berries are very similar when taking into account the final content in both sample types. Nevertheless it seems that around *véraison* a lower rate of accumulation for sucrose and fructose is observed.

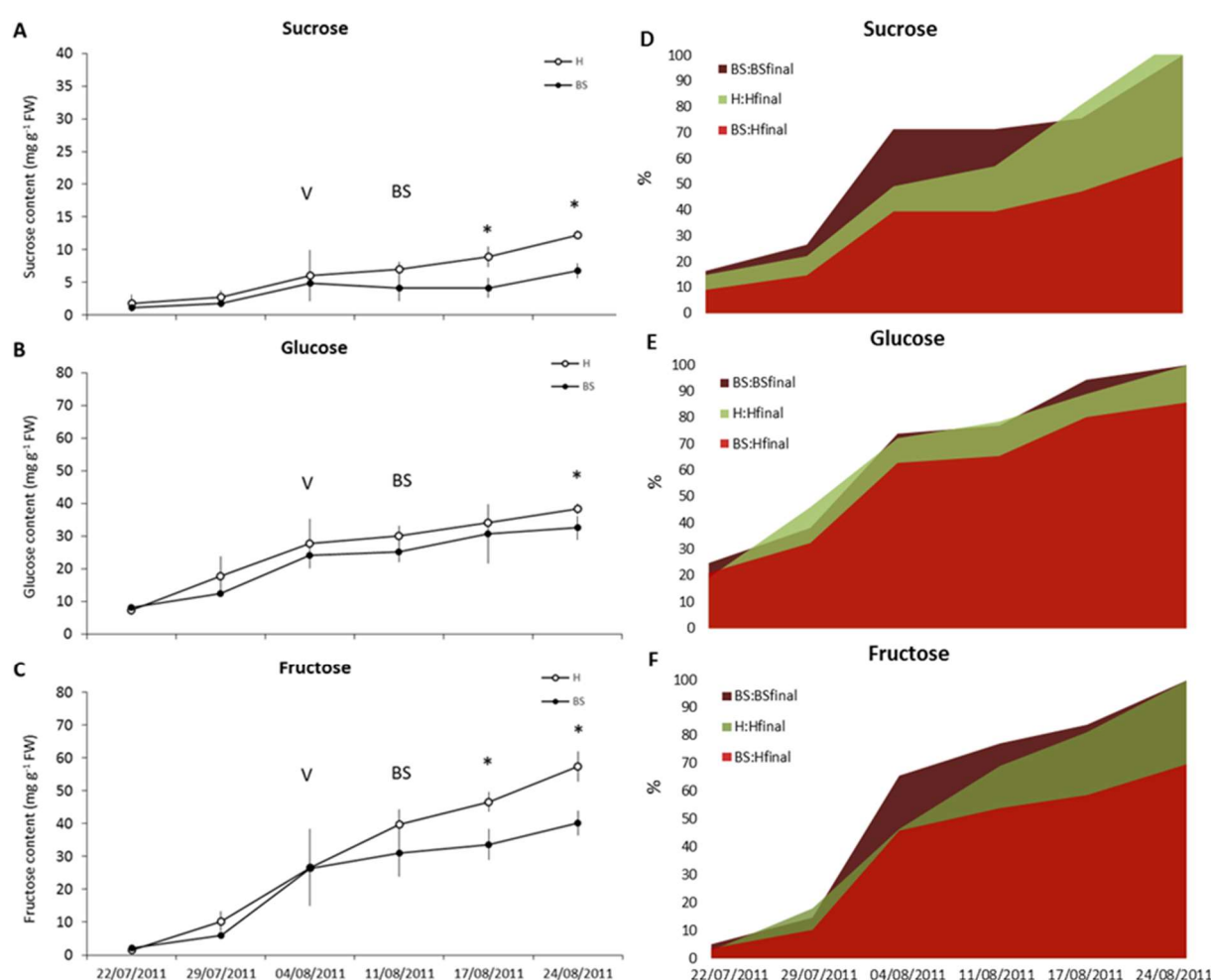


**Figure 12:** Timescale content (mg g<sup>-1</sup> FW) of sucrose (A), glucose (B) and fructose (C) in healthy and BS grapes. Timescale accumulation (%) of sucrose (D), glucose (E) and fructose (F) in healthy and BS grapes in relation to healthy berries final content (H:H<sub>final</sub>; H:BS<sub>final</sub>) or BS berries final content (BS:BS<sub>final</sub>). Data presented are mean values on fresh weight basis  $\pm$  standard deviation (N=4 each). Asterisk (\*) indicates statistical significance between H and BS samples (p < 0.05, t-test). *Abbreviations:* V- *véraison*; BS- berry shivel symptom development.

### 4.1.3 Comparative analyses of single polyphenols

It is obvious from visible symptoms (Fig. 6) and total anthocyanin analysis (Fig.11) that the biosynthesis of anthocyanins in BS berries is limited. To determine the bottleneck points that unable normal anthocyanin production in BS grapes, sub-products of the biosynthesis pathway were quantified applying a highly selective and sensitive LC-MS/MS method (Table 2, Fig.13). In summary, 32 compounds were tested of which 13 metabolites were below the detection limit (Appendix A). In accordance with the total anthocyanin measurements, the anthocyanins delphinidin-glucoside and cyanidin-glucoside as well as other highly conjugated derived metabolites are clearly less abundant in the BS samples. Other polyphenols had a higher content in BS samples, especially a phenolic acid (caftaric acid), some flavonols (particularly quercetin-3-O-glucuronide) and flavanols (catechin and epicatechin tannin precursors). Summarizing the results: less complex molecules, that are typically synthesized during early berry development and that are more stable, were increased while more complex compounds, which are synthesized during berry ripening and are easier degraded as e.g. anthocyanins, were reduced. For a direct comparison between healthy and BS samples, the log<sub>2</sub>FC of different polyphenols was calculated (Fig. 13). Blue colours represent decreased content in BS berries in relation to healthy samples and red coloured products represent increased content. Anthocyanins are predominantly in blue, whereas flavanols, flavonols, stilbenes and phenolic acids are coloured in red.

**Table 2:** Results of specific analyses of polyphenols from grape berry samples collected during the ripening phase (24.08.2011). BS symptoms were already visible. Data presented are mean values on dry weight basis  $\pm$  standard deviation (N=4 each). T-test was used to detect significant statistical differences were calculated ( $p < 0.05$ ) between healthy and BS samples are indicated with different letters.

| Polyphenols analyzed with LC-MS   | Groups of polyphenols      | Unit                                       | Contents (mean $\pm$ standard deviation) |                     |
|---|----------------------------|--|--|---------------------|
|   |                            |  | Healthy                                  | Berry Shivel        |
| caftaric acid   | phenolic acids             | $\mu\text{g g}^{-1}$ berry DW              | b 1772 $\pm$ 278                         | a 4496 $\pm$ 335    |
| <i>trans</i> -resveratrol-3- <i>O</i> -glucoside                                  | stilbenes                  | $\mu\text{g g}^{-1}$ berry DW              | a 3.0 $\pm$ 1.8                          | a 4.3 $\pm$ 1.1     |
| <i>cis</i> -resveratrol-3- <i>O</i> -glucoside                                    | stilbenes                  | $\mu\text{g g}^{-1}$ berry DW              | b 4.1 $\pm$ 1.0                          | a 13.8 $\pm$ 4.4    |
| dihydromyricetin  | flavanonol                 | $\mu\text{g g}^{-1}$ berry DW              | a 15.9 $\pm$ 1.5                         | a 18.1 $\pm$ 1.3    |
| quercetin-3- <i>O</i> -glucuronide  | flavonols                  | $\mu\text{g g}^{-1}$ berry DW              | b 141.9 $\pm$ 18.4                       | a 442.9 $\pm$ 83.8  |
| quercetin-3- <i>O</i> -glucoside  | flavonols                  | $\mu\text{g g}^{-1}$ berry DW              | a 102.5 $\pm$ 72.3                       | a 122.8 $\pm$ 71.5  |
| kaempferol-3- <i>O</i> -glucoside   | flavonols                  | $\mu\text{g g}^{-1}$ berry DW              | a 21.3 $\pm$ 18.4                        | a 33.8 $\pm$ 36.2   |
| (+)-catechin  | flavan-3-ols               | $\mu\text{g g}^{-1}$ berry DW              | b 85.0 $\pm$ 47.4                        | a 200.4 $\pm$ 42.7  |
| (-)-epicatechin   | flavan-3-ols               | $\mu\text{g g}^{-1}$ berry DW              | a 132.6 $\pm$ 138.4                      | a 224.9 $\pm$ 145.9 |
| (-)-epicatechin gallate   | flavan-3-ols               | $\mu\text{g g}^{-1}$ berry DW              | a 15.4 $\pm$ 10.9                        | a 32.1 $\pm$ 15.4   |
| DEL-3- <i>O</i> -glucoside  | anthocyanin/anthocyanidins | area $\times 10^6 \text{ g}^{-1}$ berry DW | a 1391 $\pm$ 123                         | b 498 $\pm$ 368     |
| DEL-3- <i>O</i> -(6- <i>O</i> -acetyl)-5- <i>O</i> -diglucoside                   | anthocyanin/anthocyanidins | area $\times 10^6 \text{ g}^{-1}$ berry DW | a 0.6 $\pm$ 0.5                          | a 0.7 $\pm$ 0.4     |
| DEL-3- <i>O</i> -(6- <i>O</i> - <i>p</i> -coumaryl)-5- <i>O</i> -diglucoside      | anthocyanin/anthocyanidins | area $\times 10^6 \text{ g}^{-1}$ berry DW | a 262 $\pm$ 29                           | b 47 $\pm$ 32       |
| <i>cis</i> -DEL-3- <i>O</i> -(6- <i>O</i> --coumaryl)-glucoside                   | anthocyanin/anthocyanidins | area $\times 10^6 \text{ g}^{-1}$ berry DW | a 413 $\pm$ 49                           | a 272 $\pm$ 122     |
| <i>trans</i> -DEL-3- <i>O</i> -(6- <i>O</i> - <i>p</i> -coumaryl)-glucoside       | anthocyanin/anthocyanidins | area $\times 10^6 \text{ g}^{-1}$ berry DW | b 10 $\pm$ 2                             | a 23 $\pm$ 7        |
| CYA-3- <i>O</i> -glucoside  | anthocyanin/anthocyanidins | area $\times 10^6 \text{ g}^{-1}$ berry DW | a 3.4 $\pm$ 1.3                          | b 0.9 $\pm$ 0.5     |
| CYA-3- <i>O</i> -(6- <i>O</i> - <i>p</i> -coumaryl)-5- <i>O</i> -(Ac)-diglucoside | anthocyanin/anthocyanidins | area $\times 10^6 \text{ g}^{-1}$ berry DW | a 33 $\pm$ 9                             | b 7 $\pm$ 3         |
| <i>cis</i> -CYA-3- <i>O</i> -(6- <i>P</i> - <i>p</i> -coumaryl)-glucoside         | anthocyanin/anthocyanidins | area $\times 10^6 \text{ g}^{-1}$ berry DW | a 94 $\pm$ 30                            | a 56 $\pm$ 20       |
| <i>trans</i> -CYA-3- <i>O</i> -(6- <i>O</i> - <i>p</i> -coumaryl)-glucoside       | anthocyanin/anthocyanidins | area $\times 10^6 \text{ g}^{-1}$ berry DW | a 14 $\pm$ 4                             | a 26 $\pm$ 14       |

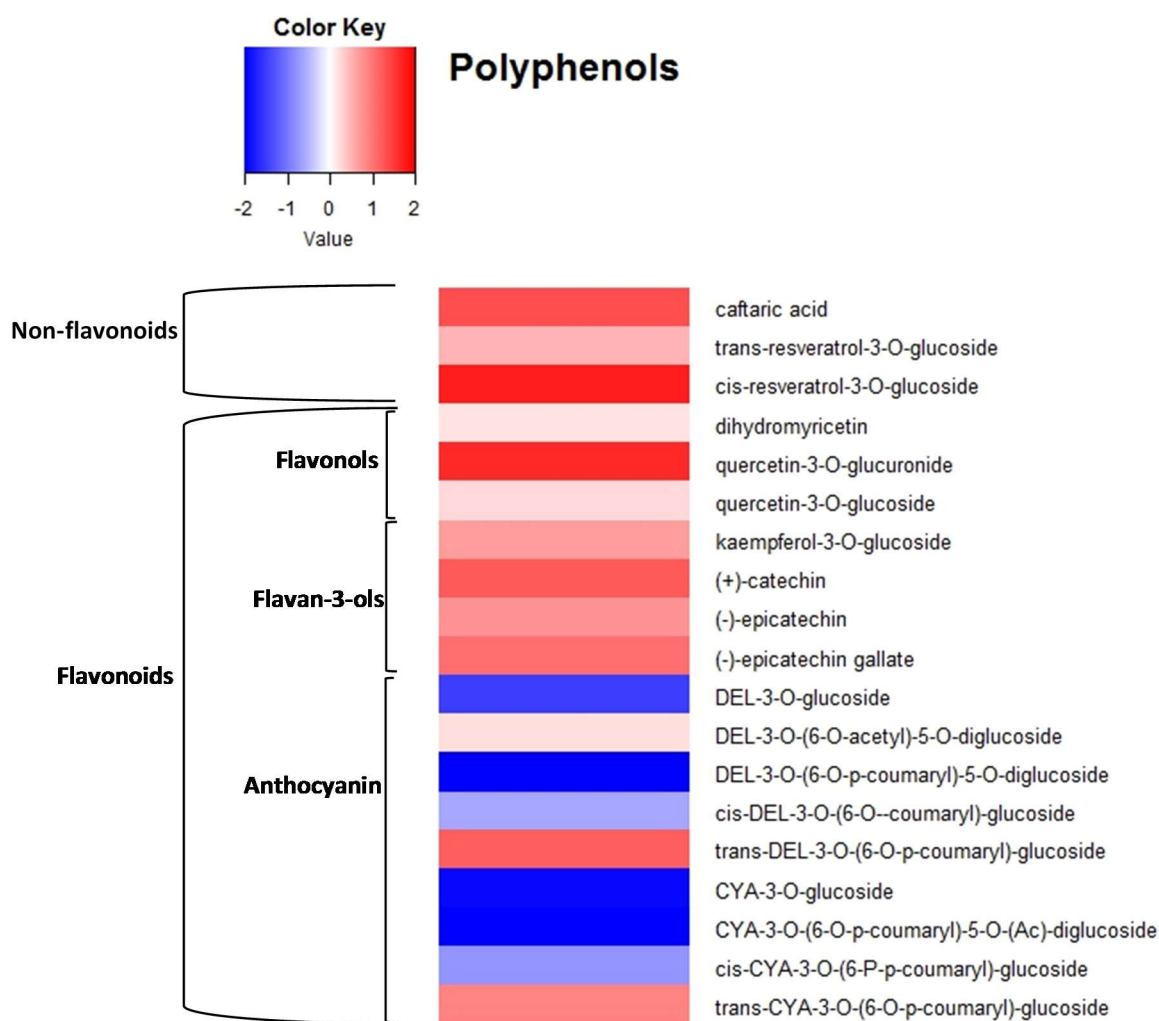


**Figure 13.** Heat map of the polyphenols with statistical significance between healthy and BS samples (statistical significant differences  $p < 0.05$ ). Data are expressed as FC log2 scale calculated from mean values.

#### 4.1.4 Gene expression profiles

Gene expression analyses (qPCR) were conducted to analyse key genes within the sugar transport and metabolism as well as the polyphenol biosynthesis pathway. Thereby we aim to determine the sink activity in BS berries and possibly identify key processes leading to the observed BS symptoms. Hypothetically the reduced accumulation of sugars may be the result of abnormal expression of sugar metabolism related genes (enzymes and transporters) which in turn may reduce sink activity and so phloem unloading. It is also supposed that the reduced anthocyanin contents

determined in BS berries rely on altered gene expression within the phenylpropanoid biosynthesis pathway.

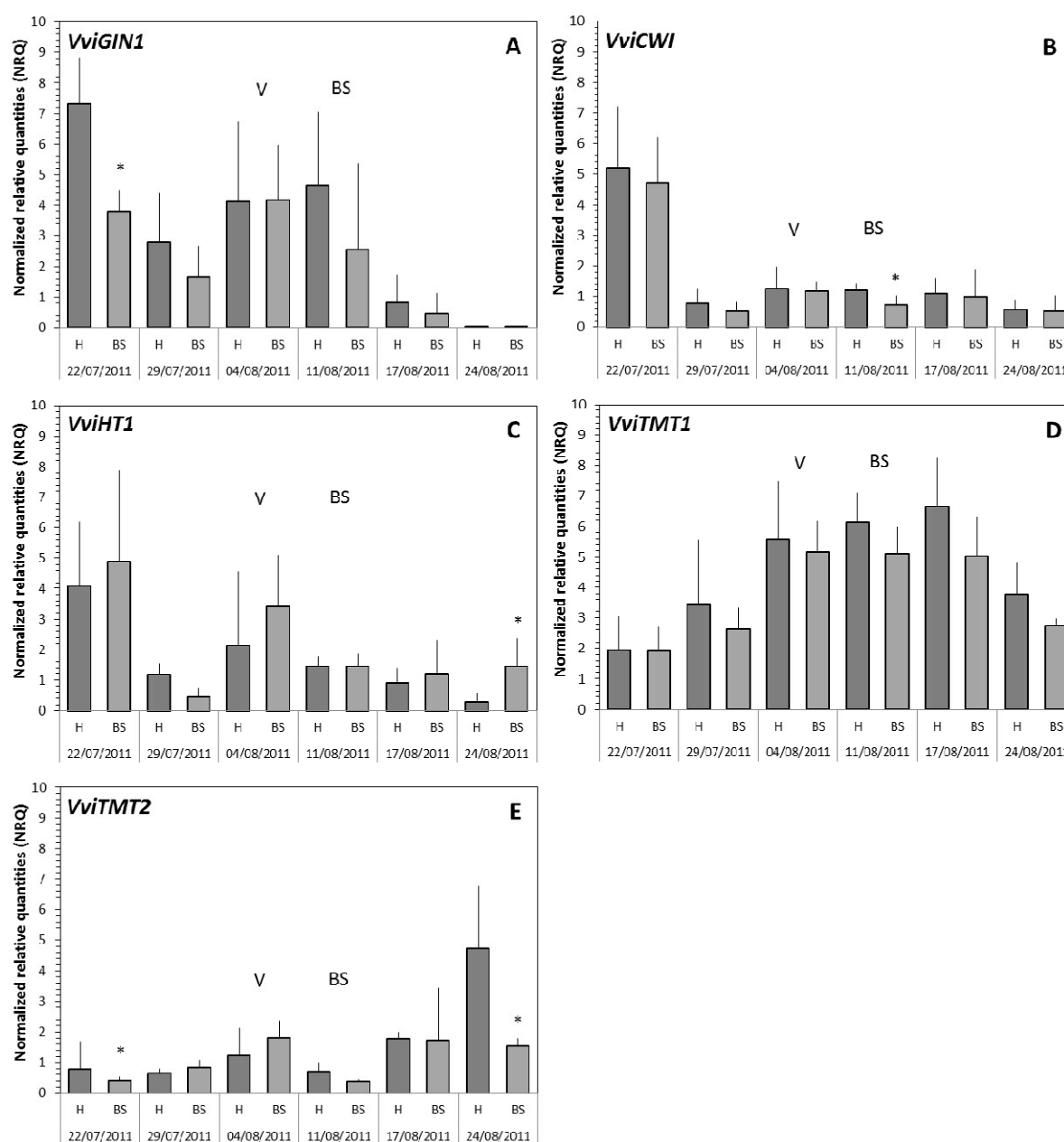


**Figure 14:** In the figures are represented the NRQ values obtained for the genes *VviGIN1* (A), *VviCWI* (B), *VviHT1* (C), *VviTMT1* (D) and *VviTMT2* (E) which are quantitatively more expressed from the sugar related genes analyzed. It is observable that induction of VINV, CWI and HT is produced in the developmental phase of the grape while TMT induction is produced through ripening. Statistical differences between healthy and BS berries are identified at time-points with reduced expression for *VviCWI* and *VviHT1*. Low induction of *VviGIN1* and *VviTMT2* in BS berries coincides with the peak of expression at healthy berries. Asterisks (\*) show statistical differences calculated with t-test ( $p < 0.05$ ). Abbreviations: V- véraison; BS- berry shrivel symptom development.

The expression of nine sugar metabolism related genes were examined through ripening (*VviHT1*, *VviHT3*, *VviTMT1*, *VviTMT2*, *VviTMT3*, *VviGIN1*, *VviGIN2*, *VviCINV1* and *VviCWI*) (Table 3.1). *VviHT1*, *VviGIN1*, *VviCWI*, *VviTMT1* and *VviTMT2* are quantitatively the highest expressed genes in healthy samples at some time points of berry development and ripening. As we assume a stronger role for these genes in grape sugar metabolism, their results are shown in detail (Fig. 14). The highest expression of *VviGIN1* is observed before *véraison*, which underlines the role of vacuolar invertases (VINV) during the first growing phase of grapes, when there is still a symplastic connection between berries and vine (Fig. 14A). In BS affected samples a lower expression of *VviGIN1* was observed at the first sampling date. Additionally to *VviGIN1*, a high expression of *VviCWI* and *VviHT1* was observed in healthy and BS pre-*véraison* samples. These are key genes of the apoplastic phloem unloading process which starts at *véraison*. Cell wall invertases (CWINV) and hexose transporters (HT) play major roles in apoplastic phloem unloading and here we demonstrate an early induction of gene expression in both, healthy and BS samples, without differences between them. At *véraison*, *VviCWI* is slightly higher expressed in healthy berries while *VviHT1* is increased in BS berries at the last sampling time point. From the five strongly expressed sugar related genes (*VviHT1*, *VviGIN1*, *VviCWI*, *VviTMT1* and *VviTMT2*) only the TMT genes reach the highest expression after *véraison*. *VviTMT1* is strongly expressed during the whole ripening period in all samples analyzed. *VviTMT2* is only showing a very strong expression close to full ripening in healthy berries whereas BS samples did not show this induction.

In summary, only *VviGIN1* and *VviTMT2* were significantly less expressed in BS samples when expression was highest in healthy samples. On a time scale, the first significant difference observed among healthy and BS grapes was the expression of *VviGIN1*, with a strong decrease in BS berries before *véraison*. The expression of *VviCWI* and *VviHT1* was influenced in BS grapes during later sampling stages, when the general expression of the genes was already reduced. *VviCWI* and *VviHT1* significant differences were determined after symptom observation what minimizes their role as BS inducers and enhance their role in symptom development. The results obtained for *VviCWI* were unexpected, as the gene contributes to sink establishment and hexose accumulation during the ripening phase, and is not in correspondence with the observed reduced sugar accumulation in BS berries. It is also important to notice

that significant differences between healthy and BS samples at pre-*véraison* showed always reduced gene expression in BS berries (*VvGIN1* and *VvTMT2*) while during the ripening phase the expression was induced in BS affected samples (*VvHT1*, *VvHT3*, *VvCINV* and *VvGIN2*).

**Table 3:** Data obtained from relative gene expression (qPCR) calculated as NRQs of nine sugar related genes and thirteen polyphenol biosynthesis genes. Healthy and BS berries at six sampling dates were analyzed. Data shown are mean values  $\pm$  standard deviation (N=4 each). Significant differences were tested with Mann-Whitney U and t-test ( $p \leq 0.05$ ) for statistical significance. Significant statistical differences are indicated with an asterisk (\*).

| Relative gene expression sugar metabolism and anthocyanin biosynthesis. Normalized relative quantities (mean values $\pm$ standard deviation) |                |                  |                |                |                |                  |                |                  |                |                |                |                  |
|---|----------------|------------------|----------------|----------------|----------------|------------------|----------------|------------------|----------------|----------------|----------------|------------------|
| 1 Sugar metabolism  |                |                  |                |                |                |                  |                |                  |                |                |                |                  |
|   | 22.07.#        |                  | 29.07.#        |                | 04.08.#        |                  | 11.08.#        |                  | 17.08.#        |                | 24.08.#        |                  |
|   | Healthy        | BS               | Healthy        | BS             | Healthy        | BS               | Healthy        | BS               | Healthy        | BS             | Healthy        | BS               |
| <i>VviHT1</i>   | 4.09 $\pm$ 2.1 | 4.90 $\pm$ 3.0   | 1.16 $\pm$ 0.4 | 0.44 $\pm$ 0.3 | 2.15 $\pm$ 2.4 | 3.41 $\pm$ 1.7   | 1.47 $\pm$ 0.3 | 1.47 $\pm$ 0.4   | 0.90 $\pm$ 0.5 | 1.20 $\pm$ 1.1 | 0.27 $\pm$ 0.3 | * 1.45 $\pm$ 0.9 |
| <i>VviHT3</i>   | 0.88 $\pm$ 0.3 | 0.83 $\pm$ 0.3   | 0.75 $\pm$ 0.3 | 0.63 $\pm$ 0.4 | 1.69 $\pm$ 0.5 | 2.64 $\pm$ 1.1   | 0.97 $\pm$ 0.3 | 1.05 $\pm$ 0.2   | 1.01 $\pm$ 0.3 | 1.06 $\pm$ 0.2 | 1.01 $\pm$ 0.5 | 1.06 $\pm$ 0.3   |
| <i>VviCINV1</i>   | 0.81 $\pm$ 0.5 | 1.04 $\pm$ 0.1   | 0.59 $\pm$ 0.2 | 0.48 $\pm$ 0.1 | 0.64 $\pm$ 0.1 | * 2.35 $\pm$ 0.7 | 0.91 $\pm$ 0.2 | 1.34 $\pm$ 0.3   | 1.31 $\pm$ 0.5 | 1.47 $\pm$ 0.5 | 0.95 $\pm$ 0.2 | * 1.89 $\pm$ 0.1 |
| <i>VviGIN1</i>  | 7.33 $\pm$ 1.5 | * 3.78 $\pm$ 0.7 | 2.80 $\pm$ 1.6 | 1.67 $\pm$ 1.0 | 4.13 $\pm$ 2.6 | 4.18 $\pm$ 1.8   | 4.64 $\pm$ 2.4 | 2.56 $\pm$ 2.8   | 0.82 $\pm$ 0.9 | 0.47 $\pm$ 0.6 | 0.03 $\pm$ 0.0 | 0.02 $\pm$ 0.0   |
| <i>VviGIN2</i>  | 3.2 $\pm$ 0.9  | 3.03 $\pm$ 0.9   | 1.52 $\pm$ 0.2 | 1.57 $\pm$ 0.3 | 0.76 $\pm$ 0.2 | * 1.31 $\pm$ 0.3 | 0.89 $\pm$ 0.1 | * 1.34 $\pm$ 0.3 | 0.61 $\pm$ 0.2 | 0.50 $\pm$ 0.1 | 0.33 $\pm$ 0.1 | 0.43 $\pm$ 0.1   |
| <i>VviCWI</i>   | 5.21 $\pm$ 1.0 | 4.71 $\pm$ 1.5   | 0.77 $\pm$ 0.5 | 0.51 $\pm$ 0.3 | 1.26 $\pm$ 0.7 | 1.17 $\pm$ 0.3   | 1.21 $\pm$ 0.2 | * 0.73 $\pm$ 0.3 | 1.10 $\pm$ 0.5 | 1.00 $\pm$ 0.9 | 0.57 $\pm$ 0.3 | 0.53 $\pm$ 0.5   |
| <i>VviTMT1</i>  | 1.95 $\pm$ 1.1 | 1.91 $\pm$ 0.8   | 3.47 $\pm$ 2.1 | 2.61 $\pm$ 0.7 | 5.59 $\pm$ 1.9 | 5.17 $\pm$ 1.0   | 6.12 $\pm$ 1.0 | 5.10 $\pm$ 0.9   | 6.65 $\pm$ 1.6 | 5.03 $\pm$ 1.3 | 3.78 $\pm$ 1.0 | 2.74 $\pm$ 0.2   |
| <i>VviTMT2</i>  | 0.78 $\pm$ 0.9 | * 0.42 $\pm$ 0.1 | 0.64 $\pm$ 0.2 | 0.82 $\pm$ 0.3 | 1.24 $\pm$ 0.9 | 1.81 $\pm$ 0.6   | 0.71 $\pm$ 0.3 | 0.39 $\pm$ 0.1   | 1.78 $\pm$ 0.2 | 1.73 $\pm$ 1.7 | 4.74 $\pm$ 2.1 | * 1.54 $\pm$ 0.3 |
| <i>VviTMT3</i>  | 1.52 $\pm$ 0.2 | * 0.76 $\pm$ 0.4 | 1.33 $\pm$ 0.6 | 1.42 $\pm$ 0.3 | 1.65 $\pm$ 1.0 | 1.91 $\pm$ 0.6   | 1.03 $\pm$ 0.5 | * 0.45 $\pm$ 0.2 | 0.90 $\pm$ 0.4 | 1.50 $\pm$ 0.8 | 0.59 $\pm$ 0.1 | 0.63 $\pm$ 0.3   |
| 2 Anthocyanin biosynthesis  |                |                  |                |                |                |                  |                |                  |                |                |                |                  |
| <i>VviCHS</i>   | 0.83 $\pm$ 0.5 | 0.54 $\pm$ 0.3   | 0.26 $\pm$ 0.0 | 0.32 $\pm$ 0.2 | 0.42 $\pm$ 0.0 | 0.56 $\pm$ 0.2   | 1.70 $\pm$ 0.8 | 1.00 $\pm$ 0.3   | 2.86 $\pm$ 2.3 | 1.83 $\pm$ 1.2 | 8.66 $\pm$ 2.5 | * 5.12 $\pm$ 2.3 |
| <i>VviCHI</i>   | 0.53 $\pm$ 0.2 | 0.37 $\pm$ 0.2   | 0.27 $\pm$ 0.1 | 0.32 $\pm$ 0.1 | 0.92 $\pm$ 0.5 | 0.65 $\pm$ 0.4   | 1.55 $\pm$ 0.5 | 1.18 $\pm$ 0.4   | 2.15 $\pm$ 0.1 | 3.65 $\pm$ 1.8 | 5.11 $\pm$ 1.0 | * 2.47 $\pm$ 0.6 |
| <i>VviF3H</i>   | 0.58 $\pm$ 0.2 | 0.66 $\pm$ 0.1   | 0.33 $\pm$ 0.0 | 0.40 $\pm$ 0.1 | 0.69 $\pm$ 0.1 | 0.92 $\pm$ 0.3   | 1.33 $\pm$ 0.3 | 1.18 $\pm$ 0.5   | 2.45 $\pm$ 1.0 | 2.50 $\pm$ 0.7 | 2.78 $\pm$ 0.7 | * 1.64 $\pm$ 0.4 |
| <i>VviF3'H</i>  | 1.02 $\pm$ 0.3 | 0.63 $\pm$ 0.2   | 0.65 $\pm$ 0.1 | 0.70 $\pm$ 0.2 | 0.65 $\pm$ 0.1 | 0.83 $\pm$ 0.4   | 1.11 $\pm$ 0.6 | 0.61 $\pm$ 0.1   | 1.31 $\pm$ 0.4 | 2.64 $\pm$ 2.2 | 3.09 $\pm$ 1.1 | 1.83 $\pm$ 0.7   |
| <i>VviDFR</i>   | 0.56 $\pm$ 0.1 | 0.55 $\pm$ 0.1   | 0.55 $\pm$ 0.1 | 0.55 $\pm$ 0.1 | 0.87 $\pm$ 0.1 | * 1.03 $\pm$ 0.1 | 1.59 $\pm$ 0.5 | 1.33 $\pm$ 0.5   | 1.53 $\pm$ 0.5 | 2.22 $\pm$ 0.7 | 1.85 $\pm$ 0.3 | 1.17 $\pm$ 0.2   |
| <i>VviLAR1</i>  | 3.46 $\pm$ 2.0 | 1.93 $\pm$ 1.2   | 0.49 $\pm$ 0.1 | 0.96 $\pm$ 1.0 | 2.35 $\pm$ 0.5 | * 1.05 $\pm$ 0.4 | 2.16 $\pm$ 0.4 | 2.04 $\pm$ 1.2   | 0.95 $\pm$ 0.4 | 0.87 $\pm$ 0.4 | 0.41 $\pm$ 0.1 | 0.30 $\pm$ 0.2   |
| <i>VviLAR2</i>  | 3.80 $\pm$ 2.2 | 3.17 $\pm$ 1.9   | 1.95 $\pm$ 0.2 | 2.48 $\pm$ 1.2 | 3.85 $\pm$ 4.2 | 0.91 $\pm$ 0.1   | 0.76 $\pm$ 0.7 | 0.64 $\pm$ 0.3   | 0.41 $\pm$ 0.1 | 0.48 $\pm$ 0.4 | 0.64 $\pm$ 0.1 | 0.70 $\pm$ 0.2   |

|                  |            |            |            |            |            |              |            |            |             |             |             |             |
|------------------|------------|------------|------------|------------|------------|--------------|------------|------------|-------------|-------------|-------------|-------------|
| <i>VviLDOX</i>   | 0.42 ± 0.1 | 0.42 ± 0.2 | 0.49 ± 0.1 | 0.57 ± 0.1 | 0.64 ± 0.3 | * 1.19 ± 0.3 | 1.21 ± 0.3 | 0.92 ± 0.2 | 2.16 ± 0.4  | 2.55 ± 0.5  | 2.86 ± 0.6  | 2.11 ± 0.8  |
| <i>VviANR</i>    | 6.64 ± 4.0 | 6.26 ± 1.5 | 1.53 ± 0.4 | 2.68 ± 2.3 | 1.90 ± 1.8 | 0.68 ± 0.1   | 0.51 ± 0.1 | 0.45 ± 0.2 | 0.33 ± 0.0  | 0.49 ± 0.2  | 0.79 ± 0.2  | 0.54 ± 0.2  |
| <i>VviUFGT</i>   | 0.15 ± 0.1 | 0.02 ± 0.0 | 0.12 ± 0.1 | 0.01 ± 0.0 | 2.97 ± 0.6 | * 0.37 ± 0.3 | 5.02 ± 1.5 | 3.45 ± 1.0 | 14.64 ± 5.0 | 14.86 ± 5.3 | 13.90 ± 3.0 | 15.79 ± 6.7 |
| <i>VviMYBPA1</i> | 2.23 ± 1.5 | 2.27 ± 1.1 | 0.49 ± 0.2 | 1.12 ± 0.5 | 2.59 ± 0.3 | * 0.95 ± 0.5 | 0.71 ± 0.1 | 0.45 ± 0.2 | 1.79 ± 2.0  | 1.16 ± 0.9  | 1.77 ± 1.0  | 0.57 ± 0.3  |
| <i>VviMYBA12</i> | 0.53 ± 0.5 | 0.02 ± 0.0 | 0.32 ± 0.4 | 0.04 ± 0.0 | 1.71 ± 0.2 | * 0.47 ± 0.2 | 2.63 ± 0.8 | 3.79 ± 0.8 | 6.03 ± 1.7  | 8.60 ± 3.7  | 8.27 ± 2.9  | 11.37 ± 3.7 |

# 22.July 2011 (BBCH 75), 29. July 2011 (BBCH 77-79), 4.August 2011 (BBCH 81), 11.August 2011 (BBCH 83), 17.August 2011 (BBCH85), 24.August 2011 (BBCH83-89)

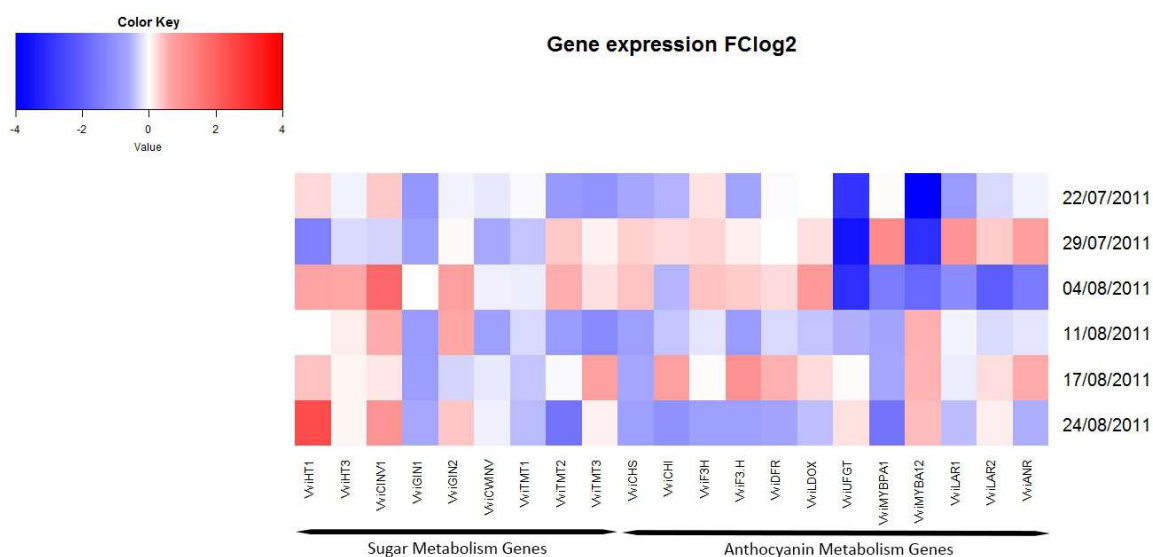


**Figure 15.** HeatMap of the gene expression of sugar related genes and anthocyanin related genes. Data are expressed as mean values of FC log<sub>2</sub> between H and BS samples.

The expression of ten key genes of the polyphenol biosynthesis pathway (*VvCHSmix*, *VvCHI*, *VvF3'H*, *VvF3Hmix*, *VvDFR*, *VvLDOX*, *VvUFGT*, *VvLAR1*, *VvLAR2*, *VvANR*) and two related MYB transcription factors (*VvMYBPA1*, *VvMYBA1A2*) were analyzed in healthy and BS berries at six different sampling dates (Table 3.2). Genes with highest expression were *VvCHSmix* and *VvCHI* from the general flavonoid biosynthesis pathway, *VvANR* from the tannin pathway and *VvUFGT* and its transcription factor *VvMYBA1A2* from the flavonoid/anthocyanin biosynthesis pathway (Bogs et al. 2007). At the first sampling dates, *VvLAR1*, *VvLAR2* and *VvANR* proanthocyanidin genes are the strongest expressed in consistence with their function in producing condensed tannins and flavan-3-ol during the pre-*véraison* growing phase of grape berry ripening. No differences were observed between healthy and BS samples during this period. In healthy grape berries the genes *VvLDOX*, *VvUFGT*, *VvMYBA1/2*, *VvMYBPA1*, *VvLAR1* and *VvLAR2* are expressed on a high level, suggesting that the biosynthesis of tannins and the anthocyanin machinery is initiated. The two peaks of tannin synthesis observed, pre-*véraison* and *véraison*, coincide with previous findings (Bogs et al. 2005). Around *véraison* the expression of some genes was significantly changed: *VvDFR* and *VvLDOX* increased and *VvLAR1*, *VvUFGT*, *VvMYBPA1* and *VvMYBA1/2* had lower expression. The reduction of the transcription factor *VvMYBPA1* could explain the reduced expression of *VvLAR1*. The same would

apply for the transcription factor *VviMYBA1/2* and *VviUFGT*. The regulation of these transcription factors would need to be addressed in future studies due to their importance for anthocyanin biosynthesis. Upstream genes *VviDFR* and *VviLDOX* are enhanced, possibly due to an accumulation of their substrates. After *véraison* the expression of *VviMYBA1/2* and *VviUFGT* is very similar in healthy and BS berries and increases in both samples continuously during the ripening period. In all samples the expression of anthocyanin related genes *VviUFGT*, *VviMYBA1/2*, but also *VviCHS* and *VviCHI*, is highest after *véraison* when anthocyanins are typically synthesized (Fournier-Level et al. 2009). Quantitatively the key anthocyanin synthesis gene *VviUFGT* reaches the highest expression values during the last two weeks of ripening and which timing coincides with the fast anthocyanin accumulation in our analysis (Fig. 11). At this time, genes like *VviCHS*, *VviCHI* and *VviF3H* reach their peak expression in healthy berries but have significantly lower expression in BS berries.

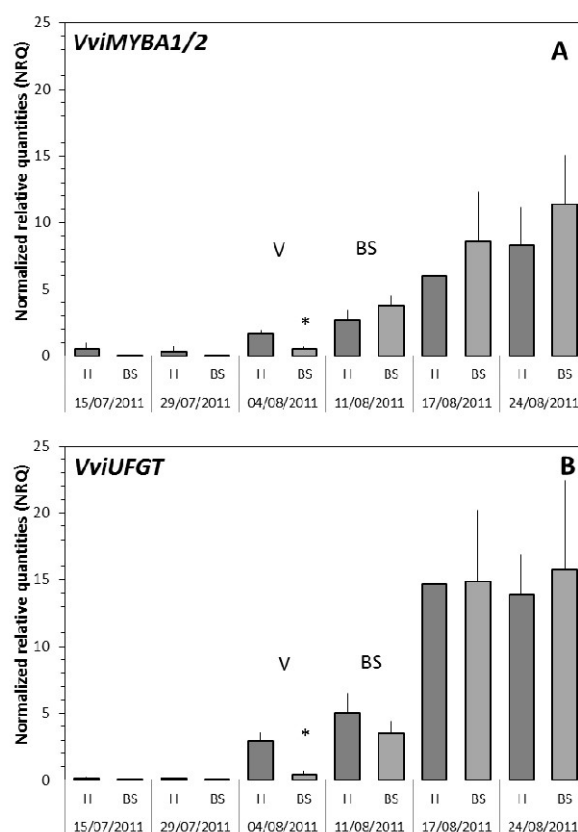


**Figure 16:** (A) Gene expression of the transcription factor MYBPA1/2 (A) and the gene UDP-glucose:flavonoid-3-O-glycosyltransferase (UFGT) (B) during berry ripening in healthy and berry shrivel grapes. Data shown represent NRQ mean values  $\pm$  standard deviation (N=4 each). Asterisks (\*) show statistical differences calculated with t-test ( $p \leq 0.05$ ). *Abbreviations:* V- *véraison*; BS- berry shrivel symptom development; H-healthy.

Pearson's correlation analyses were performed with the expression data of the 10 polyphenol genes to determine co-expression of genes (Table 4). According to these calculation, a lower correlation of *VViCHS* with *VviCHI*, *VviF3H*, *VviF3'H*, *VviDFR* and *VviLDOX* was observed in BS berries. In healthy berries *VviCHS* is highly correlated with the above mentioned genes. This would mean that when *VViCHS* has an increased expression *VviCHI*, *VviF3H*, *VviF3'H*, *VviDFR* and *VviLDOX* do not show this increase. The primer *VViCHS* is a mix of *VViCHS* gene forms (*VvCHS1*, *VvCHS2*, *VvCHS3*) being *VvCHS1* and *VvCHS2* involved in the proanthocyanin biosynthesis while *VvCHS3* is involved in coloured anthocyanin production (Goto-Yamamoto et al. 2002). The discoordination may be due to a higher expression of *VviCHS1* and *VviCHS2* in BS berries what would result in a lower induction of anthocyanin pathway genes and finally a lower production of anthocyanins. Another outstanding difference in BS berries is a higher correlation between the transcription factor *VvMYBPA1* and the related genes *VviLAR2* and *VviANR* for tannin synthesis (catechin) (Verries et al. 2008).

**Table 4.** Two tailed test Pearson’s correlation analysis of fold change (FC log2) expression levels of anthocyanin related genes in healthy and BS affected samples. Green shadings represent significant positive correlations and red shadings represent negative correlations ( $-0.7 < r_{\text{critical}} \text{ values} > 0.7$ ). Note that the Pearson’s correlation coefficient  $r$  is displayed.

| <b>A</b>         | <i>VviCHS</i> | <i>VviCHI</i> | <i>VviF3H</i> | <i>VviF3'H</i> | <i>VviDFR</i> | <i>VviLDOX</i> | <i>VviUFGT</i> | <i>VviMYBPA1</i> | <i>VviMYBA12</i> | <i>VviLAR1</i> | <i>VviLAR2</i> | <i>VviANR</i> |
|------------------|---------------|---------------|---------------|----------------|---------------|----------------|----------------|------------------|------------------|----------------|----------------|---------------|
| <i>VviCHS</i>    | 1             |               |               |                |               |                |                |                  |                  |                |                |               |
| <i>VviCHI</i>    | 0.99          | 1             |               |                |               |                |                |                  |                  |                |                |               |
| <i>VviF3H</i>    | 0.86          | 0.90          | 1             |                |               |                |                |                  |                  |                |                |               |
| <i>VviF3'H</i>   | 0.99          | 0.97          | 0.82          | 1              |               |                |                |                  |                  |                |                |               |
| <i>VviDFR</i>    | 0.77          | 0.84          | 0.91          | 0.74           | 1             |                |                |                  |                  |                |                |               |
| <i>VviLDOX</i>   | 0.91          | 0.94          | 0.99          | 0.88           | 0.90          | 1              |                |                  |                  |                |                |               |
| <i>VviUFGT</i>   | 0.78          | 0.83          | 0.98          | 0.73           | 0.87          | 0.96           | 1              |                  |                  |                |                |               |
| <i>VviMYBPA1</i> | 0.09          | 0.12          | 0.11          | 0.10           | -0.08         | 0.05           | 0.14           | 1                |                  |                |                |               |
| <i>VviMYBA12</i> | 0.91          | 0.94          | 0.99          | 0.87           | 0.89          | 0.99           | 0.97           | 0,15             | 1                |                |                |               |
| <i>VviLAR1</i>   | -0.53         | -0.52         | -0.51         | -0.46          | -0.43         | -0.61          | -0.56          | 0.46             | -0.57            | 1              |                |               |
| <i>VviLAR2</i>   | -0.58         | -0.61         | -0.76         | -0.54          | -0.81         | -0.77          | -0.75          | 0.54             | -0.71            | 0.70           | 1              |               |
| <i>VviANR</i>    | -0.35         | -0.44         | -0.54         | -0.26          | -0.68         | -0.57          | -0.60          | 0.42             | -0.55            | 0.75           | 0.76           | 1             |
| <b>B</b>         | <i>VviCHS</i> | <i>VviCHI</i> | <i>VviF3H</i> | <i>VviF3'H</i> | <i>VviDFR</i> | <i>VviLDOX</i> | <i>VviUFGT</i> | <i>VviMYBPA1</i> | <i>VviMYBA12</i> | <i>VviLAR1</i> | <i>VviLAR2</i> | <i>VviANR</i> |
| <i>VviCHS</i>    | 1             |               |               |                |               |                |                |                  |                  |                |                |               |
| <i>VviCHI</i>    | 0.63          | 1             |               |                |               |                |                |                  |                  |                |                |               |
| <i>VviF3H</i>    | 0.54          | 0.98          | 1             |                |               |                |                |                  |                  |                |                |               |
| <i>VviF3'H</i>   | 0.59          | 0.96          | 0.93          | 1              |               |                |                |                  |                  |                |                |               |
| <i>VviDFR</i>    | 0.31          | 0.90          | 0.95          | 0.82           | 1             |                |                |                  |                  |                |                |               |
| <i>VviLDOX</i>   | 0.68          | 0.96          | 0.94          | 0.95           | 0.85          | 1              |                |                  |                  |                |                |               |
| <i>VviUFGT</i>   | 0.84          | 0.95          | 0.89          | 0.91           | 0.73          | 0.93           | 1              |                  |                  |                |                |               |
| <i>VviMYBPA1</i> | -0.44         | -0.32         | -0.30         | -0.18          | -0.38         | -0.41          | -0.38          | 1                |                  |                |                |               |
| <i>VviMYBA12</i> | 0.90          | 0.89          | 0.84          | 0.82           | 0.68          | 0.89           | 0.98           | -0.49            | 1                |                |                |               |
| <i>VviLAR1</i>   | -0.67         | -0.50         | -0.39         | -0.63          | -0.24         | -0.67          | -0.63          | 0.36             | -0.60            | 1              |                |               |
| <i>VviLAR2</i>   | -0.48         | -0.69         | -0.73         | -0.56          | -0.79         | -0.76          | -0.64          | 0.81             | -0.68            | 0.37           | 1              |               |
| <i>VviANR</i>    | -0.41         | -0.56         | -0.57         | -0.46          | -0.66         | -0.66          | -0.53          | 0.91             | -0.57            | 0.47           | 0.95           | 1             |

#### 4.1.5 Invertase enzyme activity

Invertases were also examined at the enzymatic level due to their importance for sugar accumulation and sink activity. The results obtained for the enzymatic activity of the cell wall invertase (CWINV), vacuolar invertase (VINV) and neutral invertase (NINV) are shown in Fig. 17 (A-C). Comparing both treatments, healthy and BS samples show similar results of the three tested invertases, but some differences were detected. In correspondence with expression analyses of *VviGIN1*, VINV enzymatic activity (Fig. 17A) was highest in the symplastic phases before *véraison* in all the samples. Additionally the enzyme activity of VINV was lower in BS berries at the first sampling date, which was also observed for the expression of *VviGIN1*. CWINV and NINV highest activity was recorded at *véraison*. Activity of VINV and CWINV decrease strongly through ripening while NINV stays stable in healthy samples. The enzyme activity of all three tested invertases increased strongly in BS berries during the ripening phase after *véraison*.

Obvious differences between healthy and BS grapes were detected in the second part of the ripening phase when symptoms are already visible, what may indicate that enzyme activity is not involved in BS induction but rather symptom development. More interesting are the results obtained for VINV before *véraison*, as they correspond with the expression analyses and the not significant but lower sugar values observed at the same sampling dates.

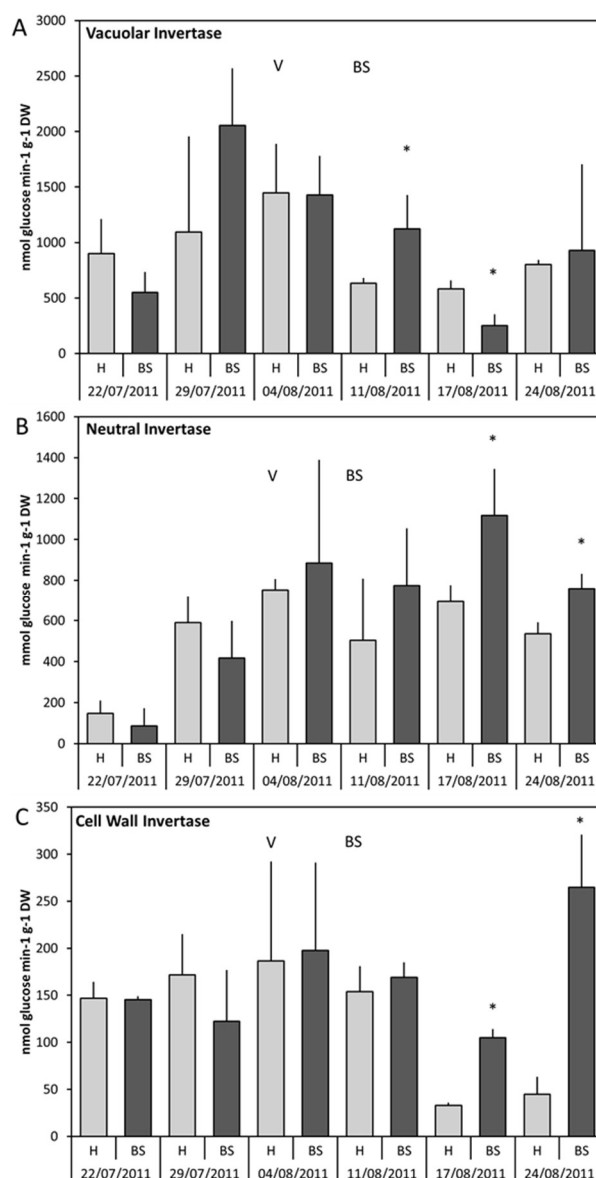


**Figure 17:** Invertase enzymatic activity of healthy and BS berries at six sampling dates throughout the berry ripening period. (A) Shows vacuolar invertase activity, (B) cytosolic invertase activity and (C) cell wall invertase activity. Data shown represent NRQ mean values  $\pm$  standard deviation (N=4 each). Asterisks (\*) show statistical differences calculated with t-test ( $p \leq 0.05$ ). *Abbreviations:* V- *véraison*; BS- berry shrivel symptom development; CWI- cell wall invertase; VINV- vacuolar invertase; NINV- cytosolic invertase.

## 4.2 Tissue anatomy analysis

In this study we try to understand the complex processes leading to BS induction and thereby we are basically following two strategies: I. Sink establishment and berry metabolism is disturbed leading to the observed symptoms (previous section) and II. Limitations in the vascular system transport of assimilates and nutrients are the cause

---

of BS symptoms (current section). Our aim through tissue anatomy analysis was to examine the general structure of the rachis and pedicel tissues in healthy and BS samples and compare them to find any abnormality that could point to a reduced assimilate conduction. Special attention was placed to the phloem due to its role in assimilate transport towards ripening grapes.

#### **4.2.1 Microscopic observation of pedicel and rachis tissues: xylem, cambium and phloem**

The general morphology of the vascular system in rachis and pedicels of healthy and BS affected grapes was analysed with light microscopy. The tissues observed in rachis and pedicel sections consisted of pith, primary and secondary xylem, cambium, secondary phloem and schlerified primary phloem (Fig. 18). Primary and secondary xylem, cambium, secondary phloem and schlerified primary phloem were organized in vascular bundles. Parenchyma rays fill the spaces between vascular bundles. Schlerified primary phloem was the most external tissue and protects the secondary phloem and other new tissues. New developing secondary phloem and xylem push schlerified primary phloem outwards and primary xylem inwards, which is located adjacent to the pith.

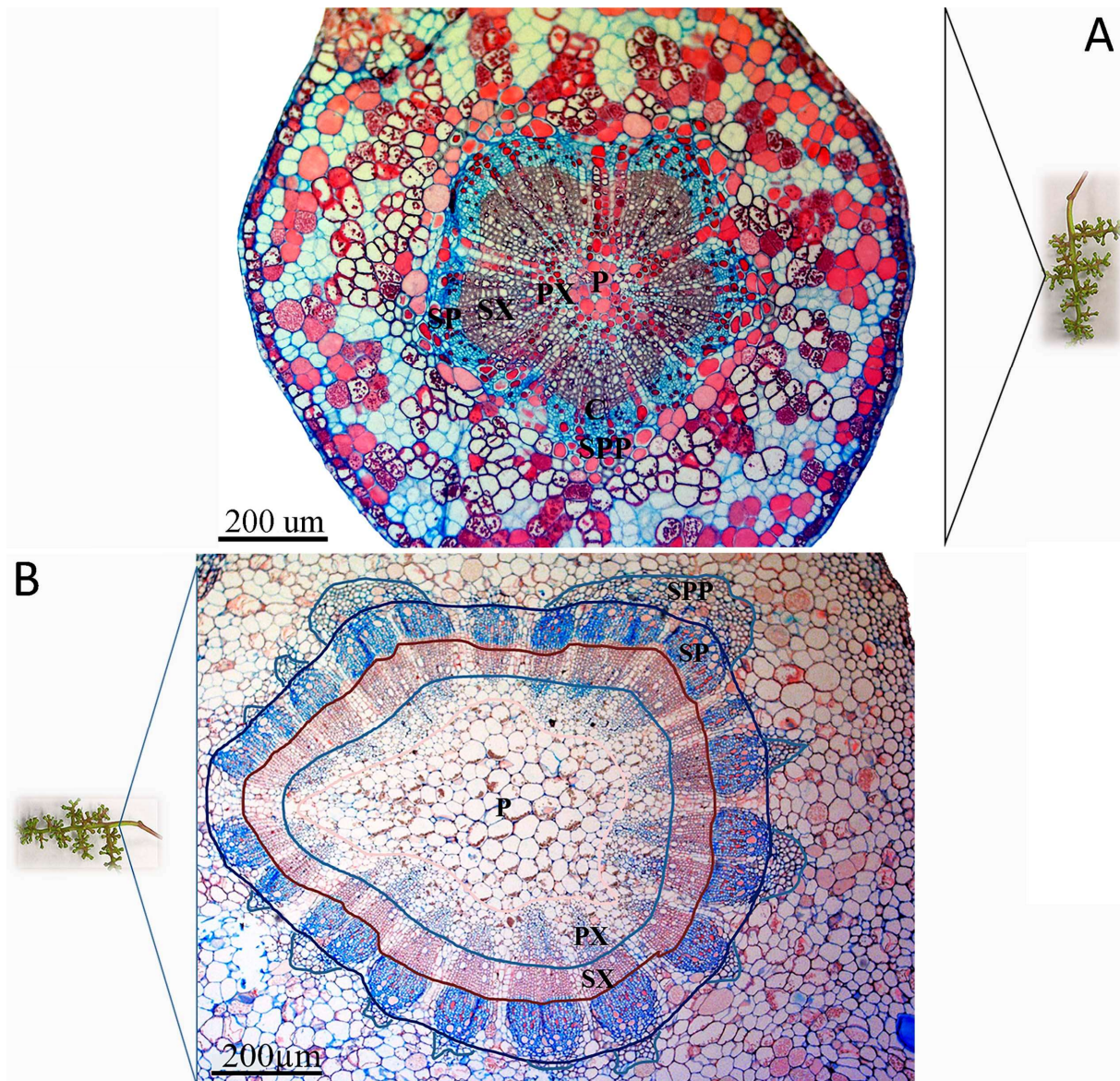


**Figure 18:** Light microscopy images of typical cross sections of rachis (A) and pedicel (B) from a BS affected cluster. Both sections are stained with the double stain safranin-astrablue, showing non-lignified tissues, as phloem, in blue and lignified tissues, as secondary xylem, in red. *Abbreviations:* SPP-sclerified primary phloem; SP- secondary phloem; PX- primary xylem; SX- secondary xylem; P- pith; Scale bars: A) 200 μm (A-B).

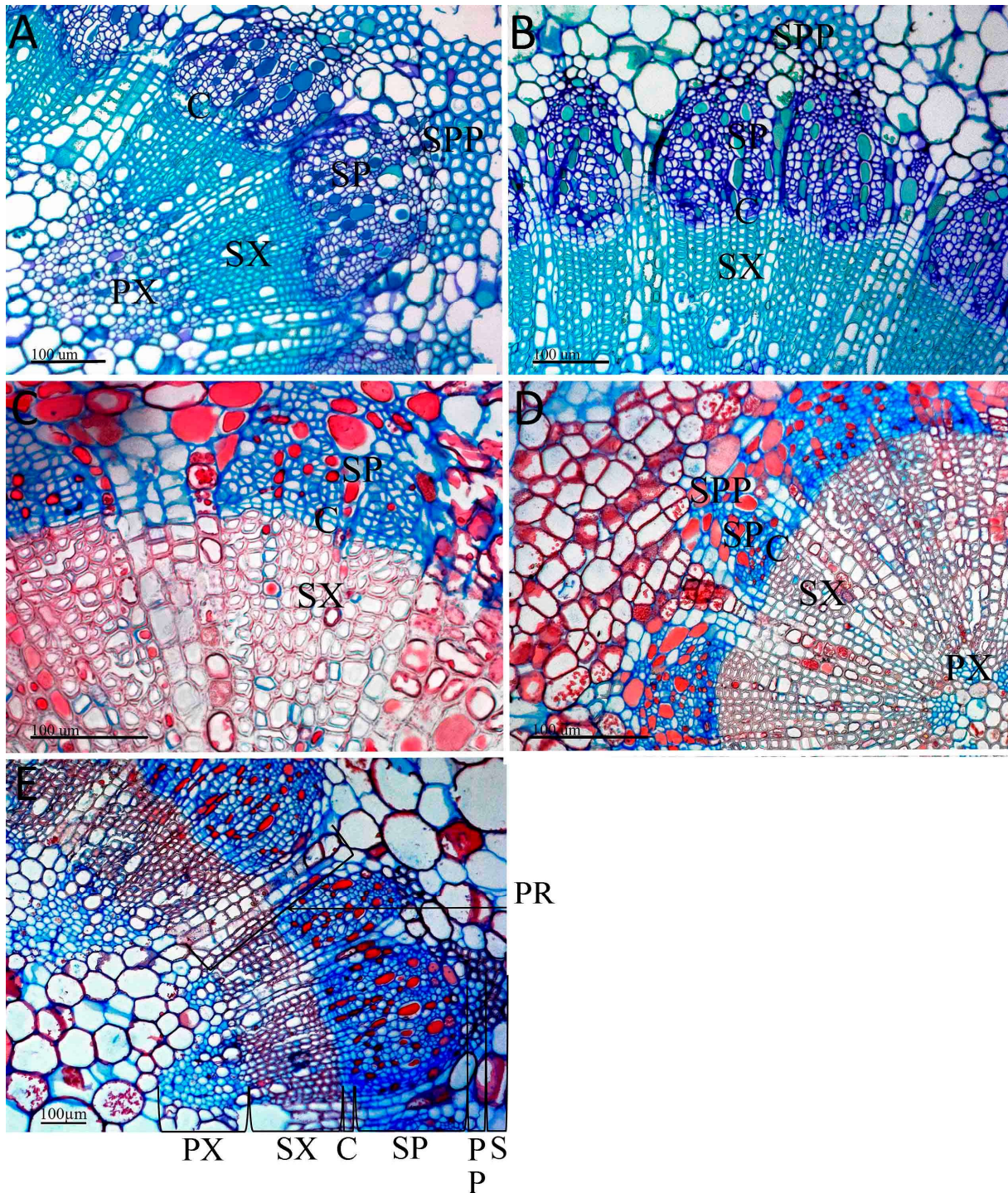


**Figure 19:** Anatomy of the vascular bundles. Light microscopy images of rachis cross sections taken through healthy cluster (A) and BS cluster (B), and pedicel cross sections of healthy cluster (C) and BS cluster (D). Cell and tissue types are pointed in a micrograph of a rachis healthy cluster (E). Sections A and B were stained with toluidine blue (stains lignin purple and polysaccharides purple). C, D and E were double-stained with safranin/astablue (stains cellulose blue and lignin red). *Abbreviations:* S- sclerenchyma; SPP- sclerified primary phloem; PR- primary ray; PP- primary phloem; SP- secondary phloem; C- cambium; PX- primary xylem; SX- secondary xylem; Scale bars: 100  $\mu\text{m}$  (A-E).

Different healthy and BS samples collected from vineyard and greenhouse plants were analysed. BS samples were further separated into early or late symptoms. No evident differences between sections of healthy and symptomatic clusters could be observed (Fig. 19). The primary phloem and xylem appear normally developed in healthy and BS grapes, indicating a normal formation of grape cluster primordia in both cases. The secondary growth of the vascular system relies on cambium activity. Light microscopic observations show secondary phloem and xylem tissue formation so it can be concluded that there is cambium activity at some extent.

TEM analyses were conducted to examine the tissues at the cellular level which are not detectable by light microscopy. These examinations revealed some differences between healthy and BS affected samples in rachis and pedicel tissues. TEM resolution revealed abnormal phloem tissue in BS affected grapes in pedicels and rachis (Fig. 20-21). Large groups of necrotised and collapsed phloem cells in rachis and pedicels of BS affected plants could be observed, indicating phloem degradation (Fig. 20B). In healthy plants necrotizing of phloem cells also occurred, but there were usually single cells adjoining to large cells with vacuoles filled with osmiophilic material (Fig. 20A). A very similar situation, necrotized phloem cells beside osmiophilic filled cells, have been described in mycoplasma infested plants as a plant defence reaction (Credi 1994). Healthy and BS samples did show a thickening of phloem cell walls. They were usually facing necrotised cells, large phloem cell containing osmiophilic material in vacuoles and most abundantly it was found at the interface between phloem cells and parenchymatic phloem ray cells (Fig. 20C-D). No traces of cell wall dissolutions were observed.

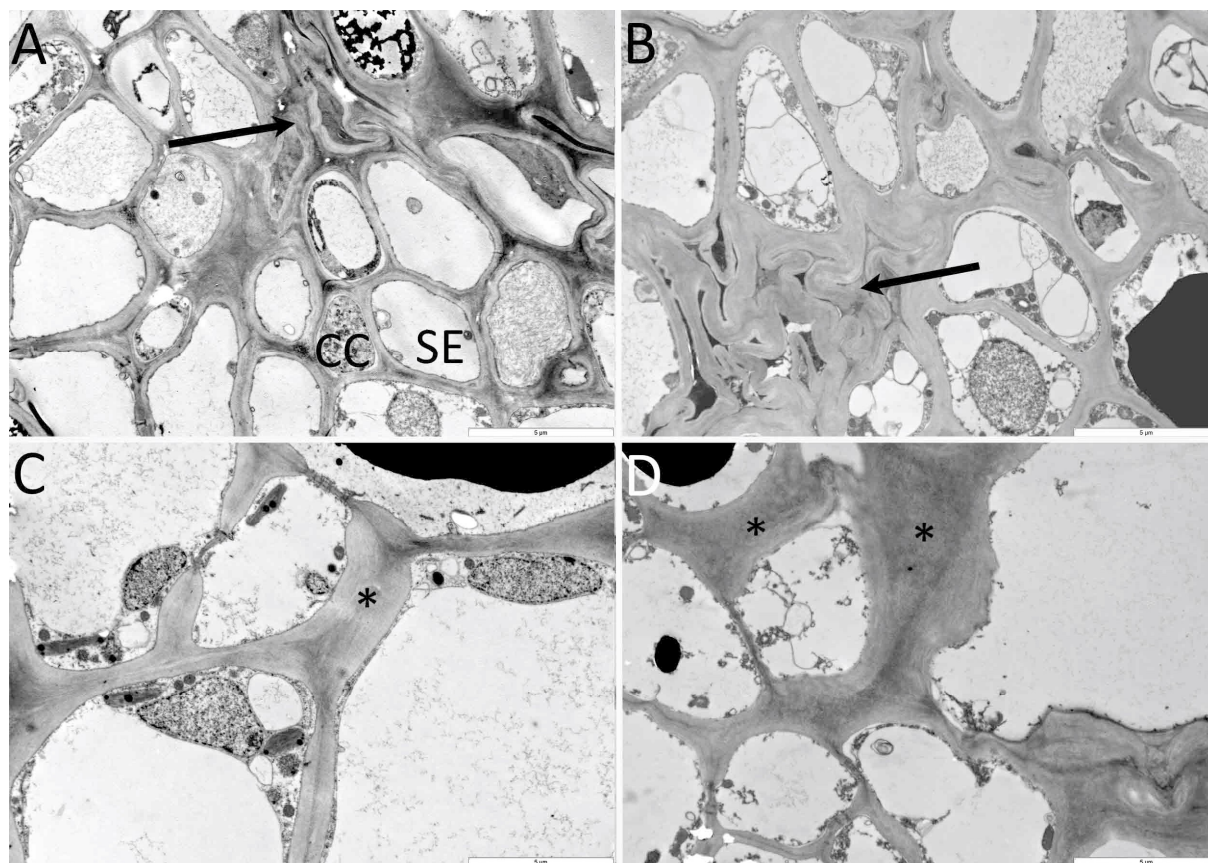


**Figure 20:** TEM micrographs showing ultrastructural details of phloem from a healthy rachis (A) and pedicel (C) and from BS affected rachis (B) and pedicel (D). Phloem showed large destructed areas in BS samples (B, D) that in healthy samples were less extended (A, C) (indicated with arrows). Thickening of cell wall was observed in both treatments, BS and healthy (C-D). *Abbreviations:* CC- companion cell, SE-sieve element, SP- sieve plate, C- callose. Scale bars: 6  $\mu\text{m}$ .

Additional to the observed effects on phloem cells, TEM analyses also revealed changes within the cambial tissue. In rachis and pedicel of healthy clusters the cambial ring consisted of 1-3 cell layers (Fig. 21A). Derivatives of cambial cells differentiated normally into elements of xylem or phloem and no cell degradation was observed in this region. In opposition, in rachis and pedicel of BS affected clusters cambium was composed of 1-2 cell layers. Reduced cell layer number in cambium has been previously related to tissue undergoing hibernation, as before winter all the cells are differentiating to phloem and xylem with exception of the so called initials (Larson 2012). Our observation could point to an inactive cambium in BS rachis and pedicels. Furthermore the youngest phloem elements located next to cambium degraded frequently and became compressed in BS affected samples (Fig. 21B), thus the development of new functional phloem elements would be strongly limited.

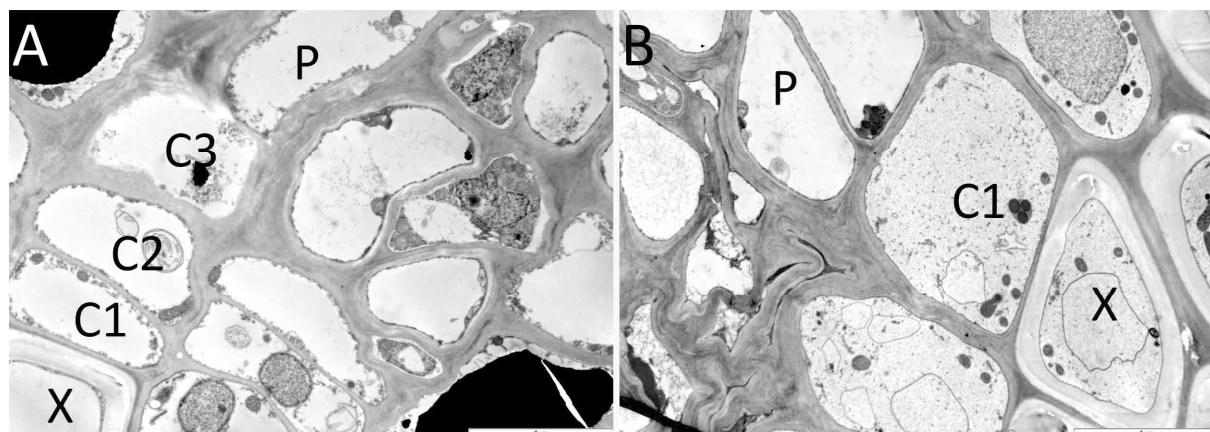


**Figure 21:** Transmission electron microscopy micrographs of cambial tissue at healthy (A) and BS pedicel (B). Abbreviations: C1, C2 and C3 – cambium layers; X – xylem; P – phloem; \*: phloem degradation. Scale bars: 5 µm.

#### 4.2.2 Measurement of xylem and phloem dimension

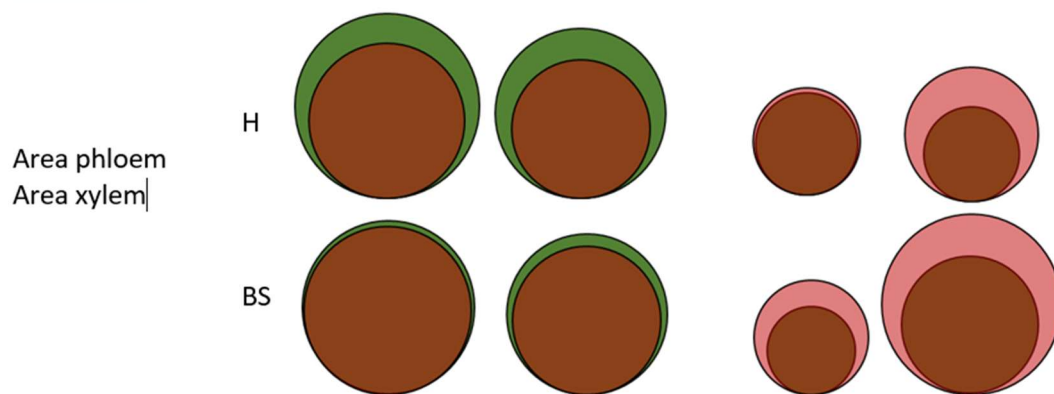
Vascular tissue architecture have a great importance for sink organs like fruits as they will partly define the transport rate towards them (Zimmermann 1969; Bustan et al. 1995). Due to the abnormal development of the phloem and the cambium detected by TEM, further analysis were conducted to detect any effects on phloem or xylem conductivity and growth. Cell and tissue sizes measurements of light microscopic cross sections taken from tangential cuttings of rachis (including cluster tip, shoulder and central part) and pedicels (distal and central part) from healthy and BS affected samples were performed (see details in Appendix B). Obtained results are shown in Table 7-8.

The size of the secondary xylem and phloem was determined in rachis and pedicels of BS grape clusters showing early and late symptoms. Using early and severe symptomatic grape clusters would allow to follow a progression of BS development. Vascular tissues enlarge usually in the early stages of fruit development but in some species with increased transport through phloem at ripening, as tomato or grape, phloem can increase its size also later on (Rančić et al. 2010). It has been demonstrated that vascular system capacity can restrict fruit growth and this restriction can be overcome by fast vascular system growth (Bustan et al. 1995). This means that if secondary enlargement would happen during ripening it may indicate an insufficient transport capacity of the vascular tissue for the grapes. The tissue size of secondary phloem and xylem in the rachis of healthy and BS grape clusters was similar (Table 7).

Contrary, in pedicel tissues the mean values of xylem size in healthy and BS samples and phloem size in BS samples is increased. The proportion of phloem to xylem tissue revealed a difference in the relative area of both tissues in pedicels and rachis.

**Table 7:** Mean values of phloem area ( $\text{mm}^2$ ), xylem area ( $\text{mm}^2$ ) and ratio phloem/xylem. Measurements were performed in samples from 2013 at different symptom progress (early, late) and different cluster tissues (rachis, pedicel). There were no statistical differences between time points. 2013 early symptoms  $H_n=4$   $BS_n=4$  and late symptoms  $H_n=4$   $BS_n=4$ ; Every sample was represented by a minimum of 3 sections. *Abbreviations:* H: healthy; BS: berry shrivel.

| Year  | Tissue | Symptoms | 2013   |      |         |      |
|---|--------|----------|--------|------|---------|------|
|   |        |          | Rachis |      | Pedicel |      |
|   |        |          | Early  | Late | Early   | Late |
| Area <sub>phloem</sub> ( $\text{mm}^2$ )            | H      | 0.45     | 0.38   | 0.14 | 0.12    |      |
|   | BS     | 0.39     | 0.34   | 0.1  | 0.26    |      |
| Area <sub>xylem</sub> ( $\text{mm}^2$ )             | H      | 0.32     | 0.25   | 0.15 | 0.24    |      |
|   | BS     | 0.37     | 0.29   | 0.17 | 0.43    |      |
| % (area <sub>phloem</sub> : area <sub>xylem</sub> ) | H      | 1.41     | 1.58   | 0.84 | 0.53    |      |
|   | BS     | 1.12     | 1.32   | 0.72 | 0.63    |      |



Another factor that regulates assimilate delivery is cell anatomy, as it may modify conductivity. Cell size measurements were conducted with all cell types of xylem and phloem tissue, regardless their morphology or function, to test the possibility of abnormal general cell growth. The phloem and xylem cell sizes were determined in healthy and BS samples and results are shown in Table 8. Phloem and xylem cell sizes

were enlarged in pedicels of BS grapes. Differences in cell enlargement may be due to differences in cell turgor, activity of cell wall loosening enzymes or cell wall composition (McQueen-Mason et al. 1992; Cosgrove 2000). On the basis of our results, we may assume that some differences in the transport capacity of phloem cells between healthy and BS grapes may arise but due to the absence of repeatability results should be verified.

**Table 8:** Mean values of secondary phloem cell size ( $\mu\text{m}^2$ ) and secondary xylem cell size ( $\mu\text{m}^2$ ). Measurements were performed in samples from two different seasons (2013, 2014), different symptom progress (early, late) and two different cluster tissues (rachis, pedicel). Statistical differences (when  $\leq 0.05$ ) between healthy and BS samples are marked with a letter (a, b). 2013 early symptoms  $H_n=4$   $BS_n=4$  and late symptoms  $H_n=4$   $BS_n=4$ ; 2014 late symptoms:  $H_n=7$   $BS_n=11$ . Every sample was represented by a minimum of 3 sections. *Abbreviations:* H: healthy; BS: berry shrivel.

| Year   | 2013   |   |   |  | 2014  |   |   |
|--|--------|---|---|--|---|---|---|
|  | Early  |   | Late  |  | Late  |   |   |
|  | Rachis | Pedicel   | Rachis  | Pedicel  | Rachis  | Pedicel   |   |
| Cell size secondary phloem ( $\mu\text{m}^2$ ) | H      | 95 <sup>a</sup>   | 60  | 109  | 62 <sup>a</sup>   | 94  | 72  |
|  | BS     | 115 <sup>b</sup>  | 69  | 140  | 141 <sup>b</sup>  | 92  | 72  |
| Cell size secondary xylem ( $\mu\text{m}^2$ )  | H      | 95  | 93  | 104  | 95  | 93  | 98 <sup>a</sup>   |
|  | BS     | 110   | 84  | 103  | 147   | 84  | 80 <sup>b</sup>   |
| Cell size secondary phloem ( $\mu\text{m}^2$ ) | H      |  |  |  |  |  |  |
|  | BS     |  |  |  |  |  |  |
| Cell size secondary xylem ( $\mu\text{m}^2$ )  | H      |  |  |  |  |  |  |
|  | BS     |  |  |  |  |  |  |

In summary, phloem and xylem morphology showed quantitative differences at vascular tissue growth and vascular tissue cell size. Significant differences appeared more frequently in pedicel tissues than in rachis. More differences were observed in grapes showing severe BS symptoms and future studies will have to reveal their contribution to BS induction and symptom development. In general, pedicel tissues

were more affected than rachis tissues and phloem cells were more affected than xylem cells.

#### **4.2.3 Sieve plate observation, characterization and conductance**

Phloem transport capacity depends on transport efficiency and not only on tissue size. Further analysis of phloem conductance capacity were carried out as observed differences in phloem cell size are supposed to influence conductance. Specialized phloem transport cells were taken into account: sieve tubes. Sieve tubes and its sieves plates were analysed with SEM (rachis) and TEM (pedicels and rachis) to detect differences that could affect assimilate translocation in BS affected rachis and pedicel tissues of healthy and BS samples. Only well-preserved sieve plates and sieve tubes were used to calculate sieve element conductance.

Different morphology of sieve plates were observed with SEM. Clean and non-occluded sieve plates were found in healthy (Fig. 22A-B) as well as BS affected samples (Fig. 23A-B). No detectable material deposited that could obstruct assimilate translocation was observed in these kind of sieve plates, which we named 'non-occluded' or 'free sieve plates'. In other sieve plates callose depositions at the border of sieve plate openings were observed in both, healthy and BS affected samples (Fig. 22C-D and 23C). Such depositions cause a substantial reduction in pore radius with possible negative effects on phloem conductivity. There was a third type of sieve plates found only in BS affected samples in which sieve pores were hardly visible as they appeared to be occluded with an unknown material that did not seem to be callose (Fig. 23D). This unknown material looked like a 'net type' structure covering not only the pores but the whole plate. The number of these sieve plates increased in BS grapes with symptoms severity. Elementary analysis performed at these occluded plates showed a carbohydrate nature of this obstructing material.

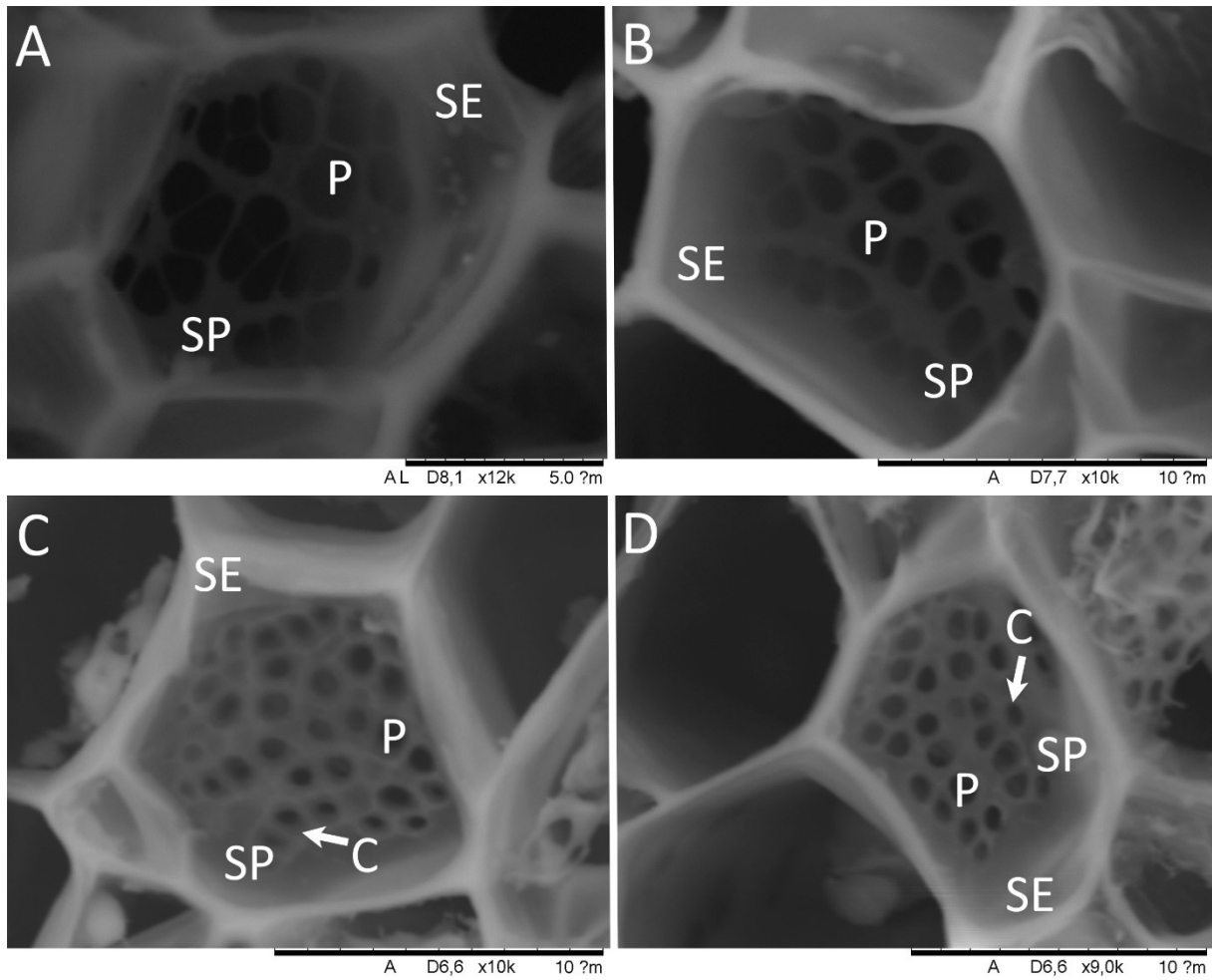


**Figure 22:** Scanning electron microscope (SEM) micrographs of sieve plates in rachis of healthy clusters without callose depositions (A and B) and occluded with callose (C and D). *Abbreviations:* SP- sieve plate; SE- sieve element; P- sieve pore; C- callose. Scale bars: A 5 μm; B, C and D 10 μm.

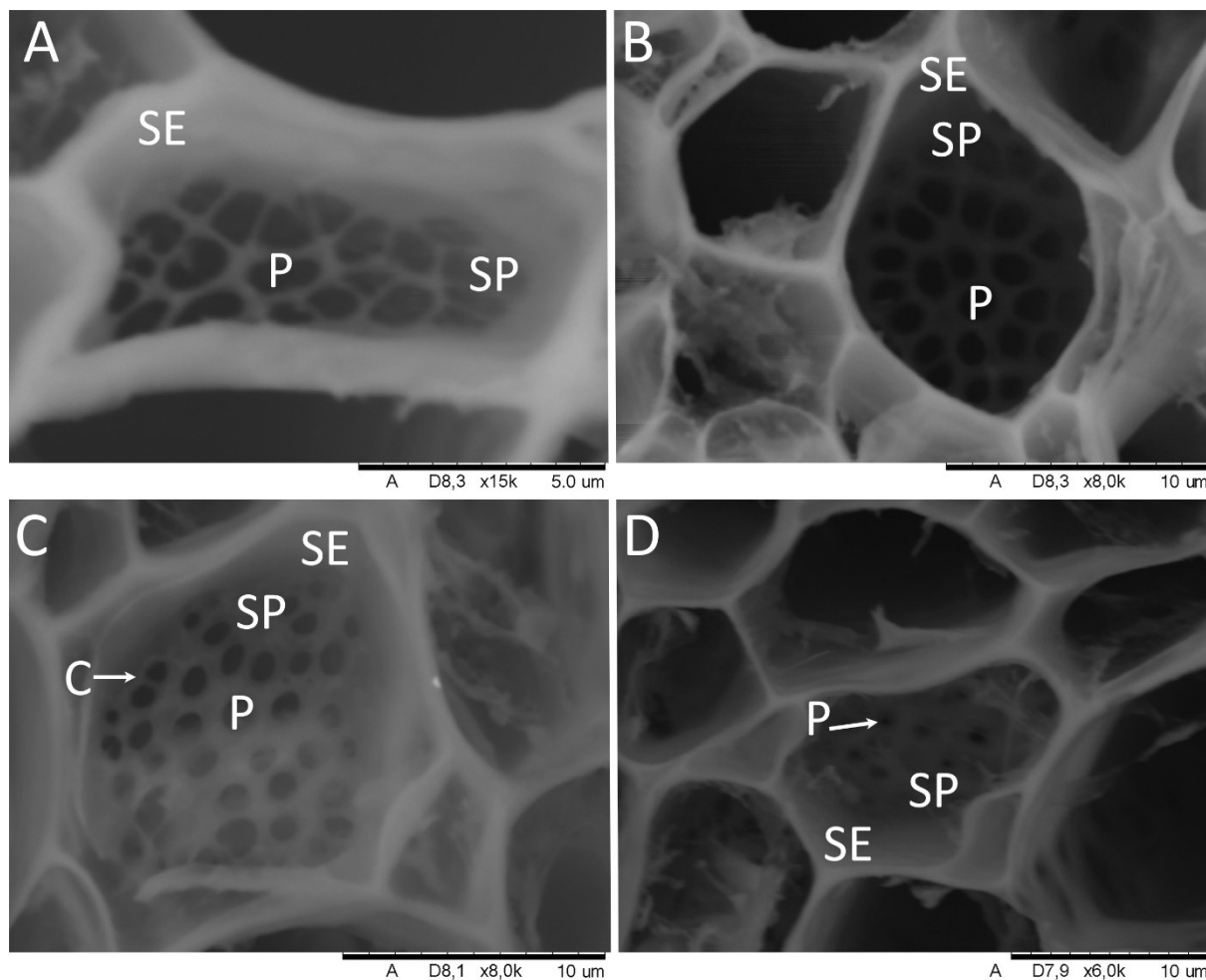


**Figure 23:** Scanning electron microscopy (SEM) micrographs of sieve plates in rachis of BS affected clusters with opened sieve pores without callose depositions (A and B), callose depositions delineating sieve pores (C) and almost completely occluded sieve pores (D) with callose or material of unknown origin. *Abbreviations:* SP- sieve plate; SE- sieve element; P- sieve pore; C- callose; Scale bars: A 5  $\mu\text{m}$ ; B, C and D 10  $\mu\text{m}$ .

Sieve plates observed are shown in Figure 24. Rachis and pedicels of healthy grape clusters usually had normal open sieve pores (Fig. 24A-C), whereas open sieve pores were rarely found in BS affected samples where most of them seemed to be occluded by abundant callose depositions (Fig. 24B-D).

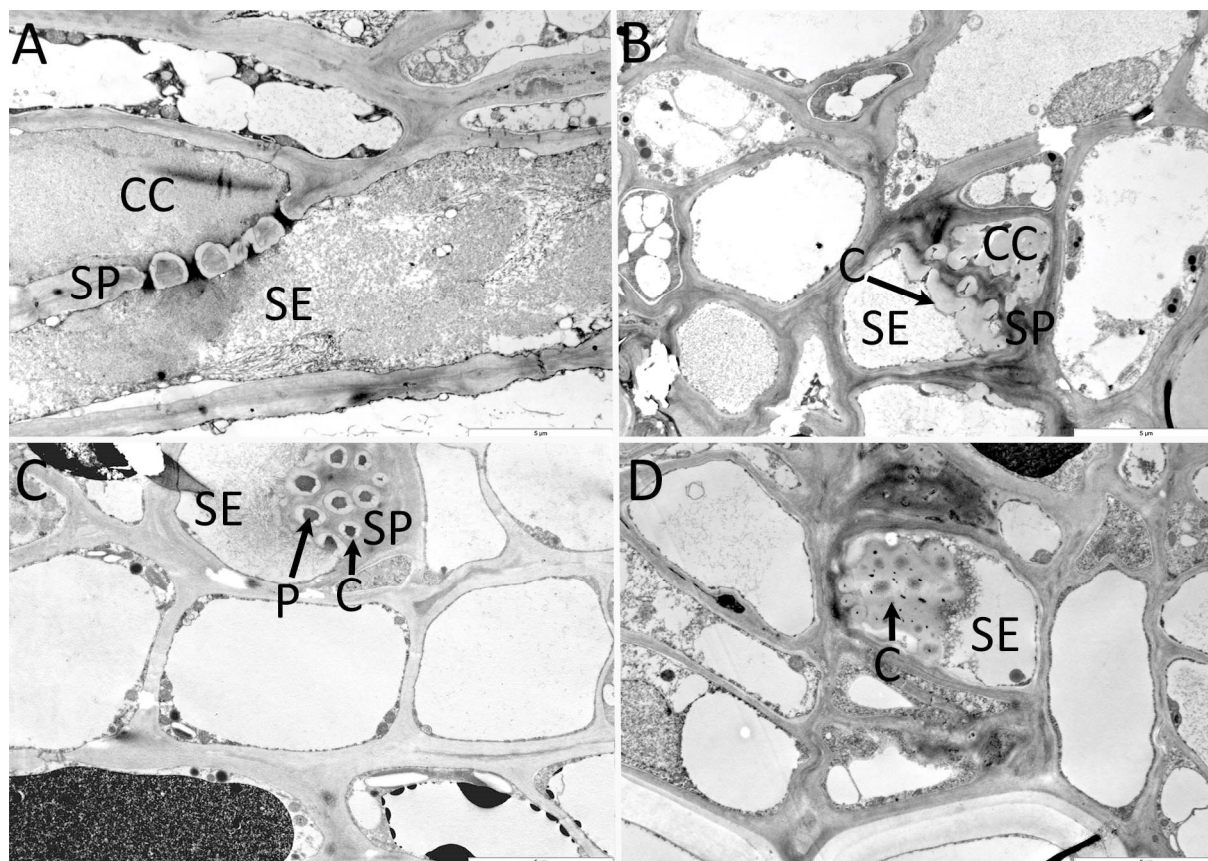


**Figure 24:** TEM micrographs showing sieve plates of pedicel (D) and rachis (A, B, C) phloem sieve elements taken from samples of healthy (A, C) and BS affected (B, D) clusters. Micrographs show longitudinal sections (A, B) and transversal (C, D). Callose in sieve elements of BS berries is extended and seem to fill the pores. *Abbreviations:* CC- companion cell, SE- sieve element, SP- sieve plate, C- callose, P- pore. Scale bars: 6  $\mu\text{m}$ .

Sections of the rachis with SEM were used to quantify sieve plate area, sieve pore area, sieve pore number and sieve tube element length (Table 9, Fig. 25). The software tool ImageJ was used to calculate sieve element conductance with obtained data sets (Table 9) (details in Appendix C). The calculation was conducted with well preserved and obviously recognisable sieve plates with a clearly visible sieve pore surface. Occluded or callose covered sieve pores were not included into phloem conductance calculations. Thus obtained measurements and values correspond to well-preserved elements only. Sieve area, sieve pore area, sieve pore number and sieve tube element length did not differ significantly between healthy and BS affected samples at early or late symptoms (Table 9). For a better visualization a scaled representation of a mean sieve tube of every treatment (healthy and BS) and time (early and late symptoms) is displayed in Figure 25.

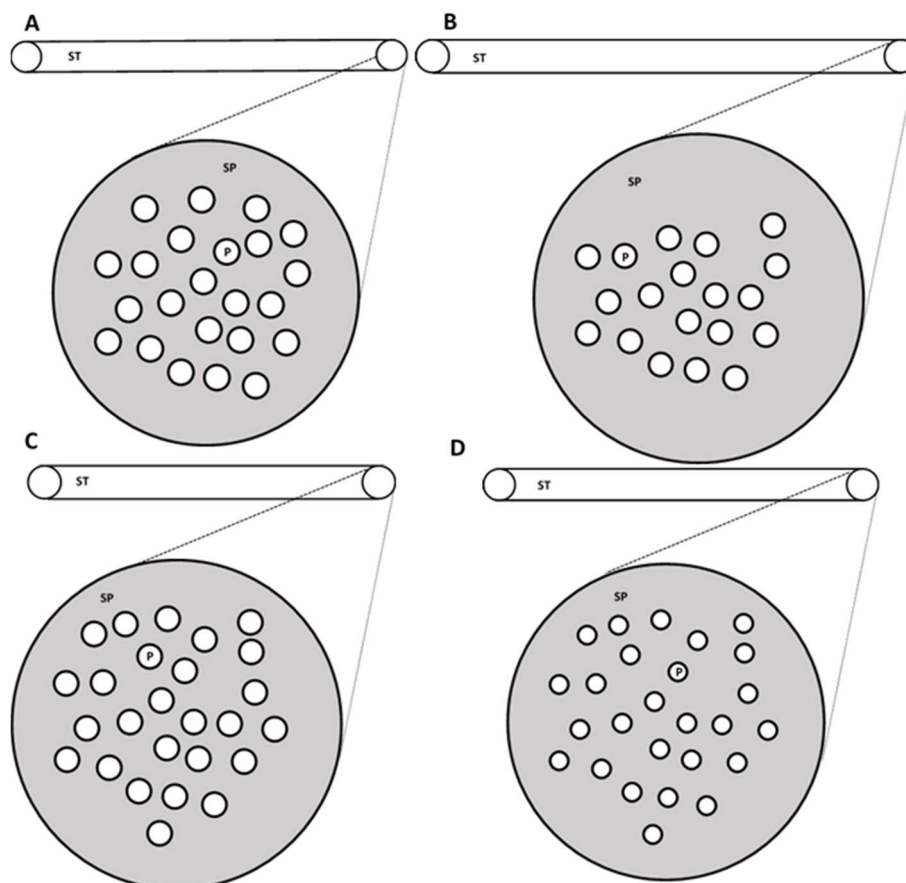


**Figure 25:** Diagram of mean sieve tubes including measurements of calculated sieve tube radius, sieve tube length, sieve pore radius and number of sieve pores from rachis phloem tissue. Mean dimensions calculated are represented in scale. A) Healthy at early symptoms; B) BS at early symptoms; C) Healthy at late symptoms; D) BS at late symptoms. *Abbreviations:* SP- sieve plate; ST- sieve tube; P- sieve pore.

Sieve plate conductance was calculated according to the equation of Thompson and Holbrook (2003). Data for sieve tube radius, sieve tube length, sieve pore radius, sieve plate thickness and number of pores per plate were used for the calculation (Table 9). Sieve element conductance was reduced in BS samples with early symptoms by 28% and by 60% in samples shown severe symptoms. The differences in the calculated sieve element conductance relied on sieve tube radius, sieve tube length, sieve pore radius, sieve plate thickness and number of pores per plate. Statistical test could not be applied to conductance as a single conductance value was calculated with the measured mean values (sieve tube radius, sieve tube length, sieve pore radius, sieve plate thickness and number of pores per plate). Sieve pores in BS samples were slightly smaller in samples with early symptoms and dropped dramatically in samples

with severe BS symptoms. Due to the higher number of not measurable sieve elements in BS affected samples (as shown in Fig. 23D) more sieve elements were excluded from the calculations comparing to samples collected from healthy plants. In general, sieve element conductance declined in all samples during the ripening phase which is in accordance with the natural degradation of sieve elements described in the previous section.

**Table 9:** Average values of sieve plate radius and thickness, sieve tube length and sieve pore radius and number. The values were collected from SEM micrographs taken from phloem rachis samples. Plants were grown under field conditions during the season 2015. The parameters were used for sieve element conductance (K) calculations. A minimum number of 130 sieve plates of every treatment and time were measured. \* Values used for sieve plate thickness are an estimation. *Abbreviations:* *r* - sieve tube radius; *l* - sieve tube length; *r<sub>p</sub>* - sieve pore radius; *l<sub>p</sub>* sieve plate thickness; *n* number of pores per plate; K: sieve element conductance; H – healthy; BS – berry shrivel .

| BS symptoms | Conductance                |  |                            |  |             | Sieve element conductance<br><i>K</i> ( $\mu\text{m}^2$ ) |               |
|-------------|----------------------------|--|----------------------------|--|-------------|---|---------------|
|             | Sieve plate                |  | Sieve tube                 | Sieve pore                             |             |   |               |
|             | <i>r</i> ( $\mu\text{m}$ ) | <i>l<sub>p</sub></i> ( $\mu\text{m}$ ) | <i>l</i> ( $\mu\text{m}$ ) | <i>r<sub>p</sub></i> ( $\mu\text{m}$ ) | <i>n</i>    |   |               |
| Early       | <i>H</i>                   | 4.49 ± 2.84                            | 1.17 ± 1.17                | 106.10 ± 16.03                         | 0.37 ± 0.29 | 22.95 ± 5.37  | 0.164 ± 0.006 |
|             | <i>BS</i>                  | 4.85 ± 2.94                            | 1.17 ± 1.17                | 138.09 ± 13.01                         | 0.34 ± 0.27 | 18.50 ± 3.59  | 0.118 ± 0.002 |
| Late        | <i>H</i>                   | 4.85 ± 2.88                            | 1.17 ± 1.17                | 97.16 ± 12.85                          | 0.35 ± 0.26 | 25.76 ± 5.90  | 0.129 ± 0.003 |
|             | <i>BS</i>                  | 4.65 ± 2.53                            | 1.17 ± 1.17                | 107.69 ± 37.95                         | 0.27 ± 0.18 | 23.20 ± 3.70  | 0.052 ± 0.002 |

As explained before, in BS affected samples non-occluded sieve plates were less abundant in special at late symptoms time. The aim was to estimate well-preserved sieve plates observed, so which may be functional. Furthermore a combination of sieve tube conductivity together with sieve plate density would give us an estimation of phloem conductivity. The area of all the visible sieve plates in a vascular bundle was combined and related to the phloem area of the vascular bundle. A detailed description of the process followed to estimate the ratio is given in Appendix D. The ratio  $\text{area}_{\text{sieve plate}} : \text{area}_{\text{phloem}}$  is used as an estimation of % of conductive area to phloem.

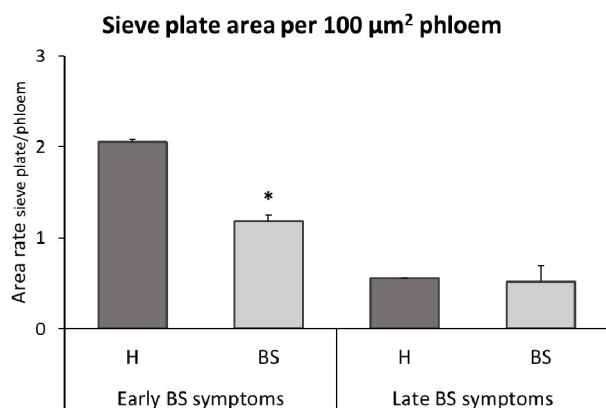


**Figure 26:** Graphic presentation of calculated total sieve plate area per 100 μm<sup>2</sup> of phloem area in samples of clusters revealing early and late BS symptoms. Represented values are mean values + standard deviation. Number of vascular bundles included in the calculations: (Early symptoms:  $N_{H\text{-vascular bundles}}=8$ ;  $N_{H\text{-plates}}=91$ ;  $N_{BS\text{-vascular bundles}}=5$ ;  $N_{BS\text{-plates}}=67$ ; Late symptoms:  $N_{H\text{-vascular bundles}}=12$ ;  $N_{H\text{-plates}}=93$ ;  $N_{BS\text{-vascular bundles}}=16$ ;  $N_{BS\text{-plates}}=38$ ). Asterisk (\*) indicates statistically significant differences.

The results show that BS samples have a lower visible sieve plate density than H samples (Figure 26): reduction of about 40% in rachis of BS samples with early symptoms and 5% with severe symptoms. In healthy as well as BS samples the visible sieve plate area is reduced between the sampling dates of early symptom and late symptom clusters. The reduction is around 70% in healthy and around 60% in BS samples. Reduced sieve plate density (Fig. 26) in combination with the reduced sieve element conductivity (table 9) may indicate a severe degradation of phloem tissue elements especially during early BS symptom development. In combination with the observed reduction of the ratio  $\text{area}_{\text{sieve plate}} : \text{area}_{\text{phloem}}$  in healthy samples towards the end of ripening, the phloem transport in BS grape clusters could be severely altered.

#### 4.2.4 Chemical tissue composition

Elementary analyses of the 'net type' residual material covering sieve plates (Fig. 23D) in BS rachis samples was conducted to give some insight of its nature. Analysis of chemical element content and distribution were performed using a table top SEM equipped with a Quantax spectrometer. The method allows a fast and easy determination of the element composition of microscopic sections, being able to

quantify and analyse separately the elementary composition of different tissues (phloem, xylem, pith, sieve plate).

**Table 10:** Percentage of chemical elements (C, O, Ca, Na, Al, Cl, N) found in sieve plates, phloem, pith and xylem cells at rachis of BS affected and healthy clusters collected from field grown 'Zweigelt' plants. Elements were quantified N = 4 samples from each treatment and every samples was characterized by N = 5 sections/sample. No statistical differences were found.

|           | Sieve plate |            | Phloem      |            | Pith       |            | Xylem      |            |
|-----------|-------------|------------|-------------|------------|------------|------------|------------|------------|
|           | H           | BS         | H           | BS         | H          | BS         | H          | BS         |
| <b>C</b>  | 66.00±1.63  | 65.86±2.63 | 57.99±1.18  | 58.51±1.71 | 56.41±1.77 | 56.32±1.37 | 59.07±1.31 | 59.04±0.25 |
| <b>O</b>  | 31.30±2.12  | 29.77±2.09 | 40.30±1.51  | 39.29±2.65 | 42.20±1.77 | 42.27±1.56 | 40.18±0.86 | 40.70±0.27 |
| <b>Ca</b> | 2.02±0.55   | 4.17±2.86  | 1.23±0.30   | 2.13±1.08  | 1.10±0.17  | 1.35±0.20  | 0.21±0.06  | 0.21±0.07  |
| <b>Na</b> | 1.18±1.05   | 0.43±0.23  | 0.51±0.23   | 0.31±0.00  | 0.34±0.08  | 0.36±0.00  | 0.29±0.12  | 0.21±0.00  |
| <b>Al</b> |             | 0.37±0.00  |             | 0.34±0.00  |            | 0.17±0.00  |            | 0.22±0.00  |
| <b>Cl</b> | 1.95±0.00   |            | 1.74 ± 1.92 |            | 0.07±0.00  |            | 0.33±0.00  |            |
| <b>N</b>  |             |            |             |            | 2.75±0.00  |            | 3.11±0.00  |            |

The elements C, O, Ca, Na, Al, Cl, and N were detected and quantified (Table 10). Spectrometric Quantax analyses allow generation of chemical elements localisation maps in the SEM micrographs (Fig. 27). Carbon and oxygen (Fig. 27C-D) were homogeneously distributed over different tissues whereas calcium (Fig. 27E) showed specific localisation in the phloem region. Healthy and BS samples did not differ significantly in any of above mentioned elements. Nevertheless some differences were found in the micronutrient analyses. Of special interest were the results of calcium localisation, which showed a very specific concentration in BS affected samples: some tissues, particularly phloem and sieve element, accumulated it in high amounts whereas other tissues in the same sample accumulated it at lower levels. Other elements were detected only in some samples at very residual concentrations, e.g. aluminium was detected only in BS affected samples whereas chlorine was only present in healthy samples and never occurred in BS affected samples.

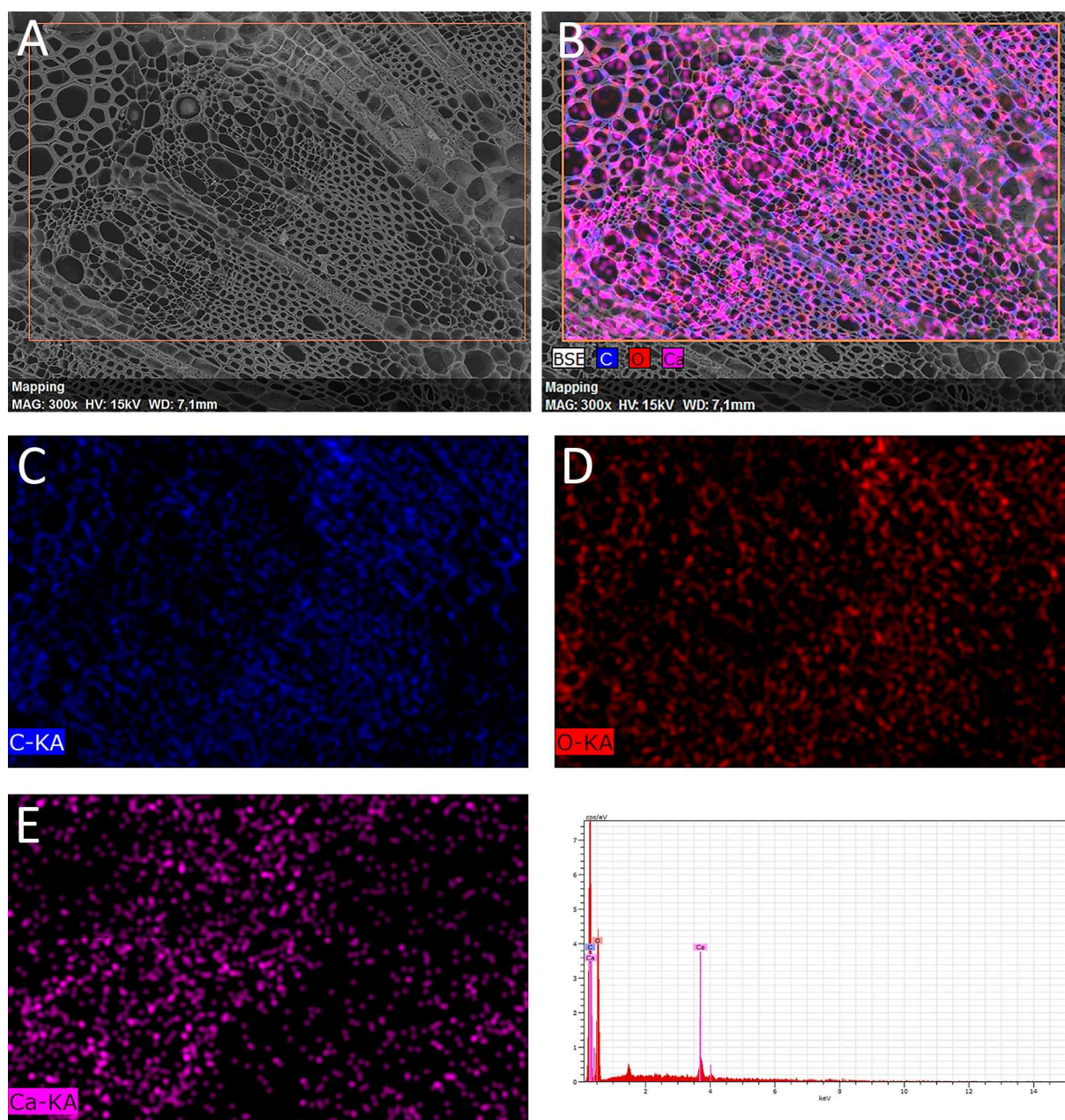


**Figure 27:** Quantax image maps showing distribution of detected chemical elements, on transversal section of a BS vascular bundle of rachis. Picture A shows the original micrograph of the vascular bundle observed with SEM; B) Combined distribution of the three elements C (blue), O (red) and Ca (pink); C) C content map through the vascular bundle; D) O content map through the vascular bundle; E) Ca content map through the vascular bundle. Abbreviations: C – carbon; O – oxygen; Ca – calcium.

#### 4.2.5 Microorganisms in BS affected samples

BS is thought to be a physiological disorder as most common virus and bacteria have been tested in dormant cane of affected clusters with negative results (Krasnow et al.

2009). In our TEM observations BS affected clusters had a higher rate of endophyte infection than healthy clusters. Based on their ultrastructure these endophytes could be recognised as bacteria (Fig. 28A). The rate of bacteria positive BS affected samples was higher in 2014, which was a year with high BS incidence in Austria. A large number of samples had epiphytes (most probably fungi as on some sections outlines of cell nuclei are visible) growing on rachis and pedicels of healthy and BS clusters (Fig. 28B). These epiphytes did not seem to induce any changes to the cuticle or epidermal cell walls, thus they were probably not harmful.

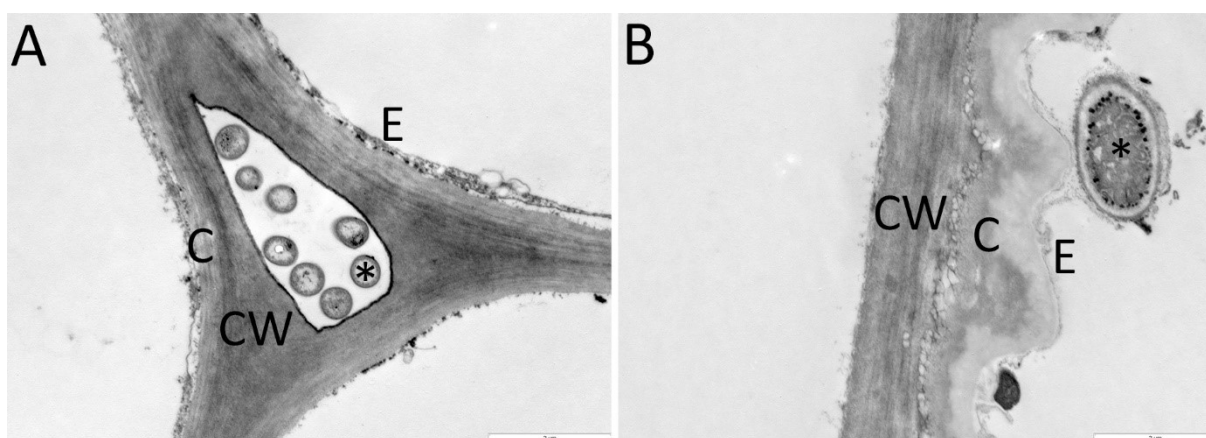


**Figure 28:** Transmission electron microscopy micrographs of BS affected cluster containing bacterial endophytes in intercellular spaces of cortical tissues at the rachis (A) and fungal epiphytes found in pedicel (B). Abbreviations: CW-cell wall, C- cuticle, E – epidermis, asterisk point the microorganism. Scale bars: 2 µm.

The cuticle of healthy samples was uniformly straight or slightly waved. On cross sections cuticle had a typical bipartite ultrastructure: an electron translucent thin outer layer and a thicker and less electron translucent inner layer that seldom contained ‘vesicles’ embedded into it (Fig. 29A-B). In contrast, cuticle of BS affected pedicels and rachis had much thickened inner layer into which numerous electron translucent ‘vesicles’ were embedded at the interface to epidermal cell wall. Thus the cuticle brought the impression of being “detached” or “detaching” from the epidermal cell walls (Fig. 29C-D). This cuticle morphology evokes to bacteria plant defence reaction, when the contact of bacteria and cell wall produces the cuticle suberization and detachment (Goodman et al. 1976). Even though these detached cuticle was not visually associated with microorganisms.

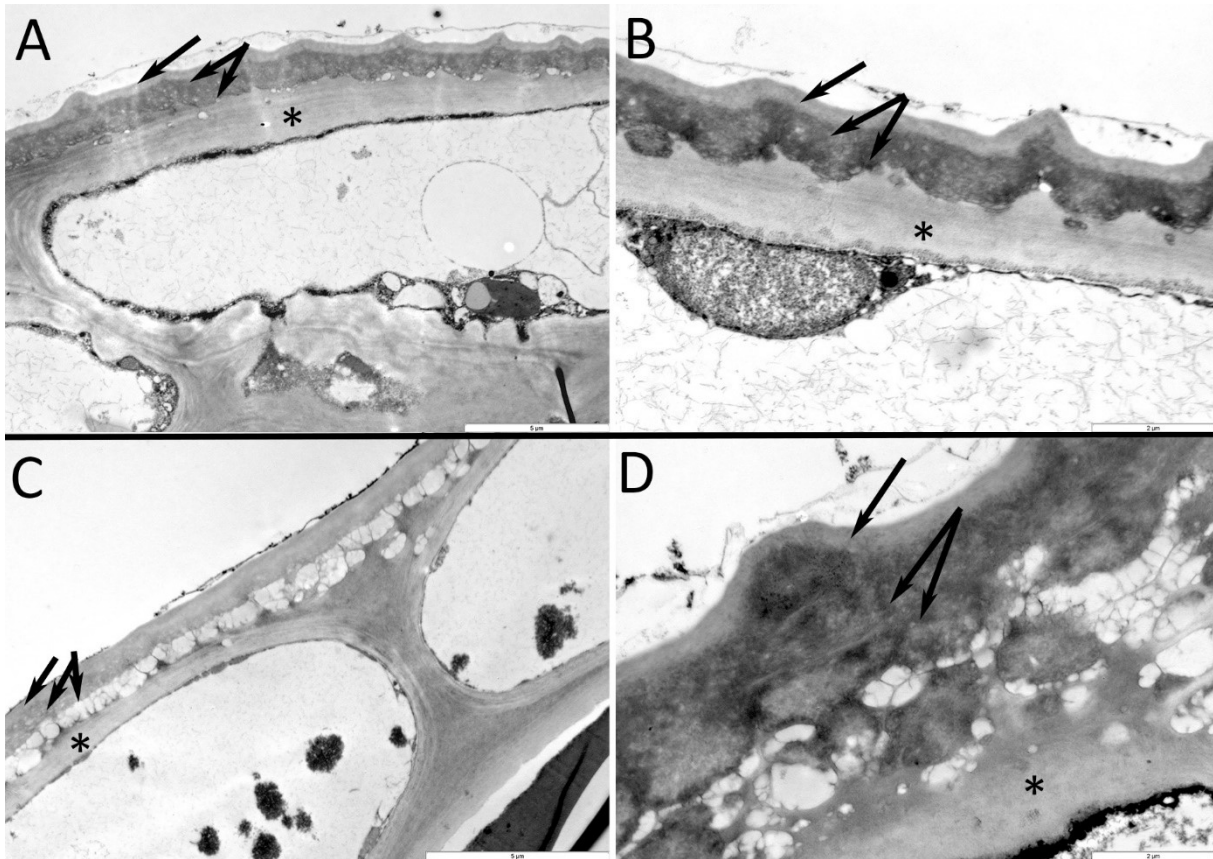


**Figure 29:** TEM micrographs showing ultrastructural details of pedicel (A) and rachis (B) cuticle from healthy cluster and pedicel cuticle from BS affected cluster (C-D). The cuticle consists of two layers: outer, more uniform and electron translucent, thus lighter on TEM images (arrow) and inner, less electron translucent, thus darker (double arrows). At pedicels of BS affected plants numerous strongly electron translucent 'vesicles' were formed at the interface to cell walls (asterisks) and regions without vesicles appear only occasionally. Scale bar: 5  $\mu\text{m}$  (A-C) and 2  $\mu\text{m}$  (B-D).

## 5 Discussion

The physiological ripening disorder berry shrivel (BS) is characterized by a stop in assimilate accumulation that becomes perceptible at the onset of ripening. Our analytical results confirm halt in accumulation of sugars and anthocyanins in BS Zweigelt berries soon after *véraison*. Through this experimental work, we pursue to understand the reasons that lead to BS berry content abnormalities that results into irregular berry ripening. We propose that a metabolic approach and/or a morphological approach may shed light over BS induction and development. The metabolic approach covers sugar metabolism, which determines the sink strength and amount of assimilates unloaded into the berry. The morphological approach covers mainly vascular system in rachis and pedicel, what would explain why usually whole clusters show BS symptoms.

### 5.1 Sugar metabolism at BS berries

Previous studies have demonstrated that sugar content in BS affected berries is strongly reduced and some indicate that cessation of sugar accumulation is happening around the start of ripening and before symptoms are visible (Krasnow et al. 2009; Knoll et al. 2010; Hall et al. 2011; Griesser et al. 2012; Keller et al. 2016). Yet no further insight has been taken in BS berry sugar metabolism. In the presented study we successfully analysed the main sugar mechanisms (invertases and transporters) that govern phloem sugar unloading and accumulation in berries through development and ripening. With a set of methods we aim to clarify some aspects concerning sugar supply of BS berries. Our results reveal that sugar metabolism is affected by BS at some time points of the ripening process but its relation with BS induction is not evident.

#### 5.1.1 Pre-ripening stage: apoplastic sink establishment

So far no information is available about sugar behaviour in BS berries before ripening starts. In this work we successfully analyzed expression of sugar related genes and enzyme activity. Our results reveal that before *véraison* BS affected berries were

showing an initial reduction in sugar content (Fig. 12). Differences were minor but may indicate an irregular grape development due to BS induction. In parallel we observed a reduced expression and activity of VINV and TMT that could explain sugar content reduction. As mentioned, grape sucrose unloading in the symplastic phase is conducted via plasmodesmata what means that unloading rate is governed by osmotic pressure concentration differences or gradients (Münch 1930). This gradient created by invertases (through sucrose hydrolysis) and transporters (through sugar compartment) will govern sugar unloading from vine phloem to grape berries and, within the grape berry, from cytosol to vacuole (Ruffner and Hawker 1977; Coombe 1988; Davies and Robinson 1996; Hayes et al. 2007).

The role that invertases would have in BS inception and development was addressed before (Keller et al. 2016). The author's prediction discarded the involvement of INV in BS as a reduced INV activity would turn into an increased sucrose content, what is not observed in BS berries. However no detailed metabolic information is available to confirm or discard this theory. Our genetic, enzymatic and analytic results confirm the prediction as the content of all sugars (hexoses and sucrose) is reduced in BS berries when VINV activity is reduced. As it has been proved in antisense vacuolar invertase tomato and carrot, when VINV activity is diminished, hexose content decreases but sucrose increases (Klann et al. 1996; Zrenner et al. 1996). In conclusion, the role of VINV in BS induction is maybe neglectable.

The fact that both sugar forms (hexoses and sucrose) are decreased in BS berries support the possibility that, from the metabolic point of view, transporters would be involved in BS development. In our results TMT (*VviTMT2*) expression is reduced in pre-*véraison* BS berries. Reduced tonoplast activity would prevent the transport of sugars to the vacuoles and sugars would accumulate in the cytosol. Further, increase sugar content in the cytosol produce higher osmotic pressure which consequently would reduce sucrose unloading. At pre-ripening most of the sugar imported is used for metabolism and sugar concentration is low (Findlay et al. 1987). TMTs are well known for the transport of hexoses through tonoplast but, it has been verified that in *Arabidopsis thaliana*, TMT1 and TMT2 are not only hexose but also sucrose antiporters at the vacuole (Schulz et al. 2011). Therefore *VviTMT2* could act as sucrose transporter before *véraison*, so its reduced expression would also contribute to the reduction of sucrose import into the vacuoles. Still further knowledge of grape berry

vacuolar functions and transporters should be acquired to clarify the role of vacuoles in BS induction (Fontes et al. 2011).

In Figure 30 is represented a grape berry cell at pre-ripening, including all representation of sugar mechanisms active at this time and the results of the metabolite analysis (including sugar contents, genetic expression and enzymatic activity) obtained in H and BS samples. In our analyses the expression of sugar metabolism genes and the enzymatic activity just before *véraison* was very similar in healthy and BS grapes, but sucrose, glucose and fructose levels remain slightly lower in BS samples. This may indicate that modulation of sugar related genes may have a limited effect in the sugar content of BS grapes. Otherwise it can be supposed that, due to the role of sugar as a signalling molecule, the initial slightly reduced sugar content has a strong impact in further grape development and BS symptom progress (Koch 2004).

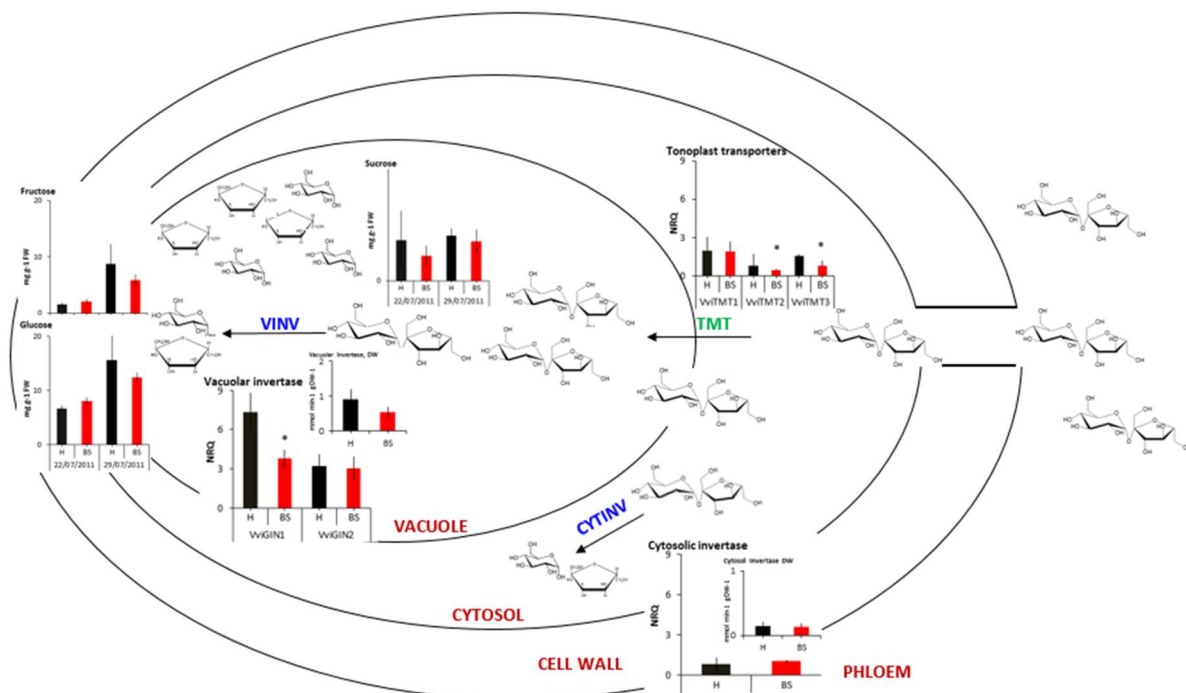


**Figure 30:** Diagram representing the sugar metabolism of a grape BS affected grape at pre-ripening. The main factors analyzed that build sink activity at the symplastic phase are here represented (sugar content (sucrose, glucose, fructose), gene expression (*VvGIN1*, *VvGIN2*, *VvCINV*), and enzyme activity (*VINV*, *CINV*)). Sugar content is expressed in mg g<sup>-1</sup> FW, gene expression in NRQ and enzyme activity in mmol min<sup>-1</sup> g<sup>-1</sup> DW. Data shown represent mean values ± standard deviation (N=4 each). Asterisks (\*) show statistical differences calculated with t-test (p≤0.05). Abbreviations: H- healthy; BS- berry shrivel symptom development; *VINV*-vacuolar invertase; *CINV*- cytosolic invertase. Invertase enzymes are marked in blue and cell compartments in red.

### 5.1.2 Sink establishment from symplast to apoplast

Grape berries undergo important metabolic changes at *véraison*. The most important is the change in sugar phloem unloading from symplastic to apoplastic what initiates massive sugar accumulation and grape ripening (Zhang et al. 2006). Sometimes BS is related to a failure in the establishment of apoplastic mechanisms as BS symptoms are typically visible after *véraison* and sugars accumulate in a very slow manner. Our transcriptomic and enzymatic analysis revealed no obvious differences between healthy and BS grape berries in the establishment of apoplastic sugar accumulation mechanisms. At *véraison* only *VviCINV* and *VviGIN2* sugar related genes were showing significant increase. *VviGIN2* has been tightly related to osmotic potential control and its up-regulation has been observed under water stress deficit (Medici et al. 2014). The enhance of *VviCINV* may be a response to increased *VviGIN2*, as cell osmotic pressure of cytosol and vacuole must be in equilibrium for a regular cell growth and development (Medici et al. 2014). Up-regulation of *VviGIN2* and *VviCINV* at *véraison* could indicate osmotic stress in BS grapes at least one week before symptoms are visible. These results may be related with previously described high osmotic potential in BS berries, due to sugars and potassium reduced content, and turgor loss observed at symptoms appearance (Bondada and Keller 2012).

### 5.1.3 Ripening: apoplastic sink strength

During early ripening and coinciding with the early appearance of BS symptoms, massive accumulation of sugars takes place in healthy berries. In our expression results and similarly as observed in *véraison*, increased expression of *VviGIN2*, *VINV* and *CINV* could indicate osmotic stress (Medici et al. 2014). Additionally, genetic expression of the three tested TMTs is reduced. Genetic expression of grape sugar transporters is strongly influenced by sugar and ABA concentration (Fillion et al. 1999; Çakir et al. 2003; Vignault et al. 2005; Conde et al. 2006; Afoufa-Bastien et al. 2010). Down-regulation of TMTs but normal expression of HTs can be an indication of cell assimilate distribution: it can be suggested that assimilates reach the cell wall space but not the cytosol. Later, from mid-ripening till the end of ripening, genetic expression and enzymatic activity in healthy grapes gradually decreases. At this time sugar content increase seem to happen due to residual activity of invertases and transporters, what implies xylem removal of water and transpiration (Rogiers et al.

2004; Rogiers 2005). Contrary BS affected grapes show an enhanced expression of some sugar metabolism related genes (strong expression of *VviHT1*, *VviCINV1* and *VviCWINV* genes and VINV, CINV and CWINV enzyme activity) (Fig. 31). It would be predictable that the activation of invertases and sugar transporters would strongly increase sink strength and massive sugar unloading is expected (Ho 1988; Herbers and Sonnewald 1998). Contrary glucose, fructose and sucrose values are significantly reduced comparing to healthy samples. Similar results were obtained before *véraison* suggesting that besides the genetic expression and enzymatic activity BS berries are unable to unload sucrose. Especially the role of *VviTMT2* seems to be important, as it is reduced in BS berries at different developmental stages. Due to its role in transport of hexoses and sugars into vacuoles, it can be assumed that assimilate distribution to different cell compartments is abnormal in BS berries.

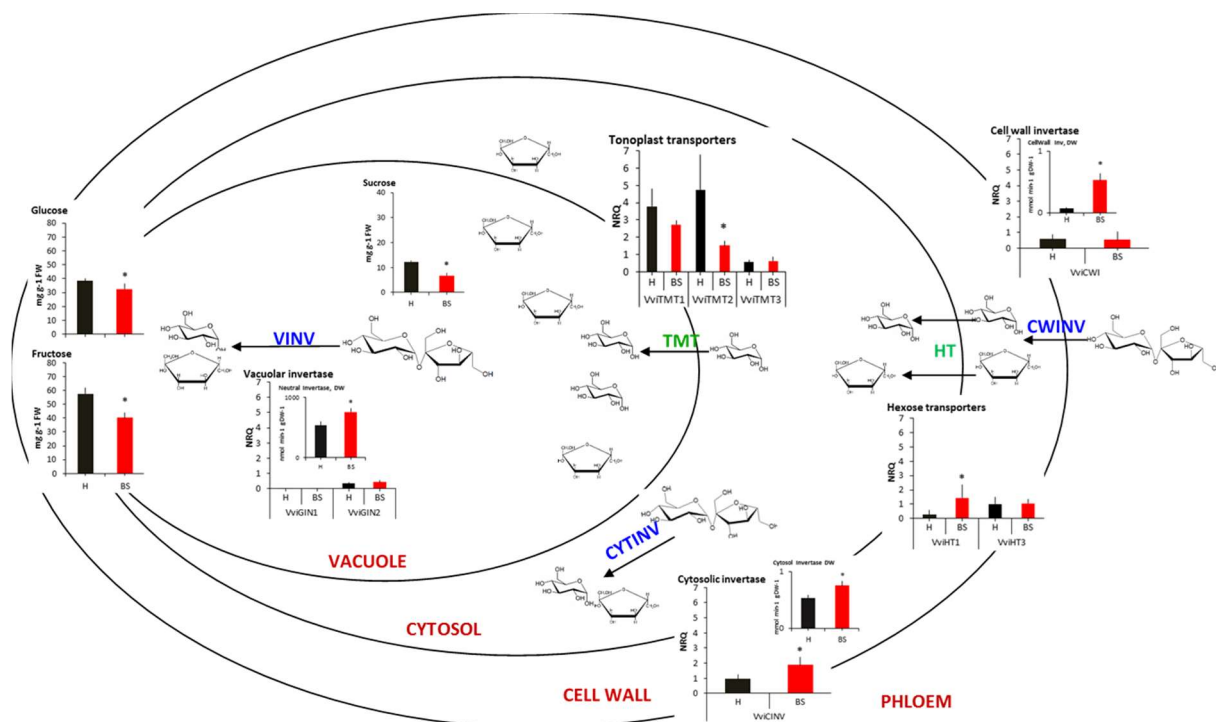


**Figure 31:** Diagram representing the sugar metabolism of a grape BS affected grape at the end of ripening (24.08.2011). All the factors analyzed are here represented: sugar content (sucrose, glucose, fructose), gene expression (*VviGIN1*, *VviGIN2*, *VviHT1*, *VviHT3*, *VvCWI*, *VvCINV*, *VvTMT1*, *VvTMT2* and *VvTMT3*), enzyme activity (VINV, CWINV, CYTINV). Sugar content is expressed in mg g<sup>-1</sup>FW, gene expression in NRQ and enzyme activity in mmol min<sup>-1</sup> g DW<sup>-1</sup>. Data shown represent mean values ± standard deviation (N=4 each). Asterisks (\*) show statistical differences calculated with t-test (p≤0.05). Abbreviations: H- healthy; BS- berry shrivel symptom development; CWI- cell wall invertase; VINV- vacuolar invertase; CINV- cytosolic invertase. Transporters are marked in green letters, invertase enzymes in blue and cell compartments in red.

## 5.2 Polyphenol metabolism

Different phenolic compounds are synthesized at different grape development and ripening stages. Flavan-3-ol and tannins are mainly synthesized from bloom until *véraison* during seed development (Boss et al. 1996). Higher concentrations of caftaric acid, flavonols and flavan-3-ols were detected at ripening in grape berries which is in accordance with other studies that also obtained higher values of simple phenols in BS samples (Krasnow et al. 2009). Expression results for flavonoid pathway genes (the transcription factor *VviMYBPA1* and the genes *VviLAR1*, *VviLAR2* and *VviANR*) responsible for tannin synthesis were similar in healthy and BS berries. Therefore differences in tannin contents in our samples cannot be explained by differences in gene expression. An overestimation due to higher representation of skin than pulp tissue in BS samples cannot be excluded for explaining these results (Ong and Nagel 1978; Teixeira et al. 2013).

*Véraison* is the starting point of anthocyanin production in red wine varieties (Pirie and Mullins 1976; Coombe and McCarthy 2000). As observed in the total anthocyanin content of healthy berries, majority of anthocyanins were synthesized in the last part of ripening. Our results confirm that delphinidin and cyanidin glycoside synthesis is reduced in BS berries (Krasnow et al. 2009). Delayed expression of genes that trigger anthocyanin biosynthesis (*VviUFGT* and its transcription factor *VviMYBPA1/2*) may not explain the shortage of anthocyanins in BS berries (Boss et al. 1996; Fournier-Level et al. 2009). The role of delayed synthesis initiation may not be critical: delayed induction of anthocyanin biosynthesis induced by auxin application results in no differences in total anthocyanin content at the end of the season in grapes (Böttcher et al. 2012). ABA and sugars, which are the main factors that regulate anthocyanin biosynthesis, may better explain the reduced content of anthocyanin in BS berries (Pirie and Mullins 1976; Hiratsuka et al. 2001; Dai et al. 2009; Castellarin et al. 2011; Dai et al. 2014). BS berries are characterized by a reduced sugar content and ABA may be limited by irregular phloem unloading (Dai et al. 2009; Dai et al. 2014). Also a tightly correlation between cell turgor pressure and anthocyanin biosynthesis has been proposed and BS cell turgor lost may also explain reduced anthocyanin biosynthesis (Knoll et al. 2010; Castellarin et al. 2011).

### **5.3 Anatomic analysis**

Through different techniques anatomical and morphological characteristics of rachis and pedicels were successfully evaluated. Special emphasis was lead on the observation of phloem tissues due to its key role in assimilate transport which defines growth and development of the fruit. Different studies have pointed towards a reduced phloem flow as a reason for BS symptoms which makes a deep study of the phloem tissue necessary (Krasnow et al. 2009; Hall et al. 2011; Bondada 2014; Zufferey et al. 2015). Due to lack of a method to forecast BS development the grapes analysed did already show BS symptoms. Microscopic methods rely on complex protocols and laborious work for material preservation which makes it extremely difficult to obtain samples before symptoms are visible. Our microscopic analysis could identify interesting differences between healthy and BS samples with early and severe symptoms.

#### **5.3.1 Anatomic abnormalities of phloem, cambium and xylem tissues**

In our analyses tissue organization of rachis and pedicels was very similar as described in previous studies (Bondada 2014). Rachis of the grape cluster is an annual structure: primary xylem and phloem develop from procambial cells which is derived from apical meristem and during the growing season secondary xylem and phloem develop from cambial cells (Schulz 1987; Esau 1953). Previous studies described hard phloem in BS berries but none of our sections were showing this unusual phenomena (Zufferey et al. 2015). The phenomenon of hard phloem regions composed of thickened cell walls of phloem fibres is programmed genetically in perennial plants to protect the cambium and it is rarely induced in growing shoots. Yet it can be induced locally and in annual organs to protect functional conducting phloem elements from mechanical compression or in regions exposed to strong tensile stress what may be the case of the analyzed samples in that work (Sobczak personal communication).

Zufferey (Zufferey et al. 2015) suggested the development of new xylem tissue formation in rachis of BS affected samples to compensate the slight reduced BS xylem conductivity in comparison to healthy samples. However no quantification of new vascular tissue development has been performed till now in BS berries. In the presented study we analysed the size of secondary xylem and phloem tissues of

grapes showing early and late BS symptoms (so at early ripening and late ripening). Main differences were detected in pedicel vascular tissues: secondary xylem enlarged in all samples being stronger pronounced in BS samples. Further only BS affected samples showed as well a growth of the secondary phloem in pedicels. Growth of secondary xylem or phloem tissue during ripening is related to a deficient conductivity of existing tissues (Bustan et al. 1995; Rančić et al. 2010). Moreover, proportional relation between pedicel diameter and transport capacity has been demonstrated (Rančić et al. 2010) and the fact that BS berries show thinner pedicels support the reduced conductance of existing vascular tissues in BS berries (Griesser et al. 2012). Growth of xylem tissues in all samples may be explained by the grape export of surplus water that takes place during ripening which could be greater in BS berries (Zhang and Keller 2017). The growth of secondary vascular tissues rely in the cambium activity. Cambium morphological alterations were observed in BS TEM micrographs: cambium was composed by only one or two rows of cells in BS rachis while in healthy samples the cambium was usually composed by three or four cell rows. Reduced number of rows in cambium tissue is related to dormant cambium (Larson 2012). Prior to dormancy cambium cells differentiate into phloem or xylem except one cell line, the so called initial cells, which undergo dormancy (Timell 1980; Larson 2012). Hence BS vascular tissue size increase may be partly due to the differentiation of cambium cells before dormancy.

Vascular tissues cell size was determined at two different BS development time points (early BS symptoms and sever BS symptoms) in rachis and pedicels and compared with control samples. Some statistical differences were observed with a tendency of higher phloem cell size in rachis and pedicel of BS berries but results were not reproducible between seasons. Cell size is regulated by water potential, which is a factor of available water plus solute concentration. In principle, phloem transported solutes are later unloaded into sink tissues, for instance berries. Due to lower analyte content in BS berries it is expected a slow phloem unloading leading to an accumulation of solutes within the cytosol and the intercellular space of the grape or the phloem cells at pedicel and rachis. Accordingly, BS phloem cells would increase solute concentration, water would flow in and increase cell size. It has been proved that low stem water potential in the phloem reduce the driving force into the fruit affecting fruit size in tomato (Johnson et al. 1992). Furthermore inverted water

potential, so lower water potential in stem phloem than in fruit, produces fruit shrinkage due to a change in the predominant direction of transport (Johnson et al. 1992). Both effects, small fruit size and high water potential, are observed in BS grapes (Krasnow et al. 2009; Griesser et al. 2012; Bondada and Keller 2012).

### **5.3.2 Reduced phloem conductivity and callosed sieve plates in BS berries**

Quantification of phloem conductance was performed to determine if the lower assimilate content observed in BS grape berries may be related to lower delivery capacity from phloem (Thompson and Holbrook 2003). Calculated sieve tube conductance based on well-conserved sieve elements showed a clear reduction in BS affected samples. When we observed early BS symptoms,  $K_{\text{phloem}}$  was 30% reduced in comparison with healthy grapes. Before harvest this reduction was even more evident reaching 60% less  $K_{\text{phloem}}$  in BS affected grape rachis.  $K_{\text{phloem}}$  was determined in rachis tissue but not in pedicel tissue. The results suggest that phloem sap delivery from the shoot to the grape may partially explain the reduction of assimilates in BS berries during ripening. Due to the lack of pre-symptomatic anatomical studies the question still remains open if an early reduction of  $K_{\text{phloem}}$  is involved in the induction of the disorder. Previous studies have related the appearance of BS with reduced  $K_{\text{phloem}}$  and our results support this theory (Hall et al. 2011; Bondada and Keller 2012; Zufferey et al. 2015). Additionally degradation of phloem tissue was also observed in TEM sections in rachis and pedicel tissues, being stronger in pedicels (Hall et al. 2011; Bondada and Keller 2012; Zufferey et al. 2015). Partially necrotised phloem was observed in healthy and BS samples what may indicate natural tissue degradation during ripening in rachis and pedicels. Nevertheless, BS samples showed larger areas of death cells, covered sieve plates and degraded sieve elements, what would further reduce the calculated  $K_{\text{phloem}}$ .

Callose deposition may also be a factor involved in reduced assimilate transport. Callose deposition is a very fast and precise response to a variety of biotic and abiotic stresses but it also has many other roles in regular developmental processes, as sieve plate formation and later determination of conductivity characteristics (Barratt et al. 2011; Xie et al. 2011). A previous study already observed callose deposition in peduncle sieve tubes of BS grape by aniline blue staining but in detail analyses are

missing (Bondada 2014). In this study, starch specific cleaning of SEM sections and high magnification of TEM allowed us to observe clean sieve plates that confirmed the presence of collapsed callose sieve pores in BS samples with both techniques. The origin that trigger this reaction in the cluster is uncertain. It is difficult to state if it has been induced prior to cluster removal and sample dissection or during sample manipulation and preparation (Knoblauch and Oparka 2012). However, as BS affected and non-affected samples were treated in the same way we attribute differences to the disorder. Callose deposition in BS rachis can be cause by increased content rachis and pedicel tissues (Kauss 1987). High  $\text{Ca}^{2+}$  concentrations were also measured in Zweigelt pedicel and rachis tissues previously (Griesser et al. 2017). Further,  $\text{Al}^{3+}$  combined with  $\text{Ca}^{2+}$  to callose deposition in different species specially at the roots (Wissemeier and Horst 1995; Bhuja et al. 2004). In our results of the Quantax analysis performed at SEM,  $\text{Al}^{3+}$  is present only in BS samples.  $\text{Al}^{3+}$  was further detected in higher amounts in ICP-MS element quantification analysis performed in rachis and berries of BS affected clusters from Mailberg 2011 (which correspond to the samples used for sugar and anthocyanin analysis in this work) what reinforce these results (Griesser et al. 2017). Non-pathogenic endophytic bacteria observed specially in BS samples may promote the synthesis of callose for preventing spreading of the microorganisms (Gindro et al. 2003). Unfortunately the question if phloem conductance and callose deposition is present before symptom development and so it is involved in BS induction remains open.

## 5.4 Outlook

Different aspects of BS induction and development have been covered in this project with a focus on grape berry sugar/anthocyanin metabolism and vascular tissue anatomy. The outlook will combine results from both approaches to draw general conclusions for BS induction and BS symptom development.

First, our results reinforce the hypothesis that berry shrivel is a physiological disorder (Krasnow et al. 2009; Keller et al. 2016). As presented, detection of non-pathogenic endophytic bacteria in TEM sections was common in BS affected samples. However these results do not mean that BS is induced by biotic factors but rather that under

specific conditions, e.g. softening, non-harmful endophytic bacteria can turn opportunistic pathogens (Nishimura et al. 2003; Gindro et al. 2003).

Many details of BS induction remain obscure but the knowledge accumulated through published studies help scientists to understand BS behaviour. From previous studies we know that seed development in BS berries is normal and symptoms appear soon after ripening starts, what promote that some authors settle BS induction on *véraison* (Hall et al. 2011). In previous investigations BS berries show evidences of reduced sugar content soon after *véraison* for hexoses as well as for sucrose (Krasnow et al. 2009; Knoll et al. 2010; Griesser et al. 2012; Keller et al. 2016). In our experiment BS Zweigelt grapes revealed visible symptoms one week after *véraison*. From the analytical results, sugar accumulation was ceased already two weeks before symptoms appearance. Significant differences were registered only at mid-late ripening while TSS changes were recorded before, one week after symptom visibility.

But rather the aim of this work was to detect induction processes and to give some light into the BS induction time-point. For that effect BS pre-symptomatic grape metabolism was analysed from green state to full-ripen. However it is difficult to comprehend the importance that pre-symptomatic metabolic abnormalities detected in BS berries have for BS induction. This is mainly due to the low sugar content of grapes during early development, so irregular metabolic behaviour may not result in perceptible irregular sugar content.

From our results and in the authors' perception, the most remarkable difference is TMTs reduced transcription in BS grapes. Some facts supporting the role of TMTs in BS development are: – *VviTMT2* and *VviTMT3* gene expression is reduced in BS grape berries in comparison with healthy samples at different times (pre-ripening and ripening). – Increase of VINV activity does no increase sugar accumulation, what indicates vacuolar isolation. – HTs gene expression is similar in healthy and BS samples what points to regular phloem unloading and hexose accumulation in the cytosol but not further transport to the vacuole (Fig. 32). As a result of prevented tonoplast transport, vacuoles would become isolated, cytosolic osmotic pressure would increase and phloem unloading would slow.

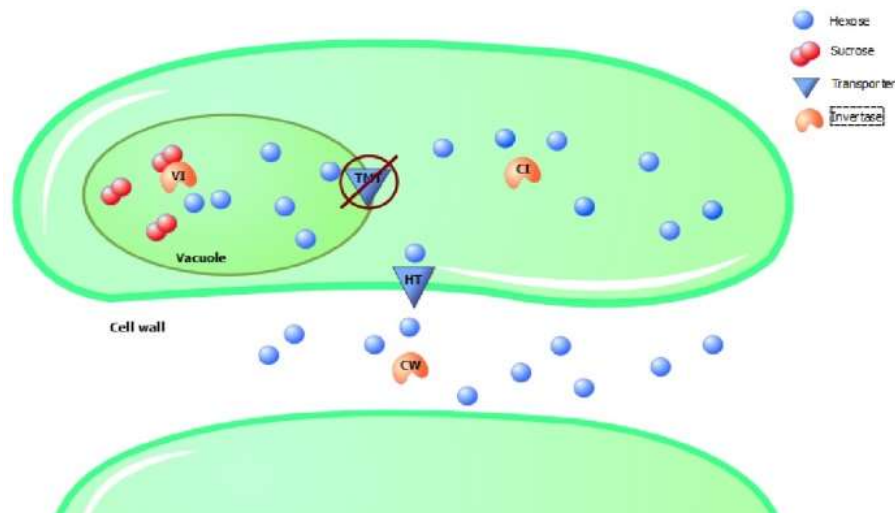


**Figure 32:** Isolation of vacuole in grape berry cell. TMT are not active and the hexoses accumulate in the cytosol and the cell wall avoiding assimilate phloem unloading. The reduction of vacuolar osmotic pressure would produce loose of turgor and cell flaccidity. Sucrose cleavage enzymes (Vacuolar invertase, VI; Cell wall invertase, CWI; Cytosolic invertase, CI) and transporters (Hexose transporters, HT; Tonoplast monosaccharide transporters, TMT). (Image designed with Tinker Cell).

Cell osmotic regulation in grape berries is under control of sugars and  $K^+$  and both contents are diminished in BS berries (Bondada and Keller 2012; Bachteler 2012; Griesser et al. 2017). Sugar and  $K^+$  keep homeostasis in vacuole and cytosol as we observed in the coupled expression of *VviGIN2* and *VviCINV* (Bondada and Keller 2012). Sugars are mainly accumulated in the vacuole while in the cytosol sugars are used in cell metabolism (Zhang et al. 2006). As for  $K^+$ , there are two main pools in plant cells which are vacuole and cytosol and, as sugars, vacuolar  $K^+$  has an osmotic function while in cytosol has osmotic and biophysical functions (Walker et al. 1996).  $K^+$  regulation within the cell takes place as well in the tonoplast: under deficit conditions  $K^+$  is exported from vacuole to cytosol to maintain  $K^+$ -related metabolism but when a minimum vacuolar  $K^+$  content is reached  $K^+$  export is ceased and cytosolic  $K^+$  decreases (Razaque Memon et al. 1985; Leigh et al. 1986; Walker et al. 1996). So  $K^+$  deficiency in BS berries may result in inverted or even prevented  $K^+$  transport through the tonoplast. Isolation of BS vacuoles, no import of sugars and/or export of  $K^+$  would explain flaccidity of BS grape berries as vacuole would lose cell turgidity (Richter 1978). Rehydration of late-season berries immersed in water support the theory of flaccidity of cells rather than shrivel or plasmolysis what would result in collapsed cell wall and cell death (Keller et al. 2016). Further genetic and enzymatic regulation till the end of

ripening suggests that cell death do not affect as massively as expected even if cell turgor is lost (Krasnow et al. 2009). Knowledge on  $K^+$  and sugar tonoplast transport as well as subcellular distribution should be acquired to better study and understand the possible effects in BS grape berries.

About polyphenol metabolism, polyphenol genetic expression did not correlate with reduced anthocyanin content registered. As has been previously suggested, more likely is that sugar content in BS ripening berries is insufficient for sugar signalling and triggering anthocyanin synthesis (Bondada and Keller 2012; Keller and Shrestha 2014; Keller et al. 2016).

The second focus was place in anatomical analysis at pedicel and rachis which raised some differences between healthy and BS grapes. Our aim was to show but also quantify differences between healthy and BS berries and so to give a specific significance to our results. It can't be neglected that microscopic quantification is a very intensive work and loads of micrographs should be measured to reliably characterize every grape berry cluster. This makes difficult to analyse a high number of clusters what would give a clearer trend in the quantitative results. TEM and SEM observations were of special importance for evaluating phloem status and our results support previous studies that related reduced  $K_{\text{phloem}}$  and phloem degradation related to BS development (Hall et al. 2011; Zufferey et al. 2015; Bondada and Keller 2012; Keller et al. 2016). Reaction of vascular tissues at BS samples (cell size,  $K_{\text{phloem}}$ , new tissue development, cell death or callose deposition) may be explained due to abnormal water relations between grape berry and stem (Figure 33) (Johnson et al. 1992; Zhang and Keller 2017). In the future, it should be clarified if BS vascular tissue abnormalities observed are due to irregular water relations, as previously stated water relations are governed by sugar and  $K^+$  content, or if  $K_{\text{phloem}}$  is the cause of BS, for which pre-symptomatic analysis of samples should be performed. What should be over-lined is the stronger abnormality incidence (phloem and xylem tissue development, cuticle detachment, phloem degradation or cambium modifications) in pedicel tissues that in rachis tissues. This may suggest that the disorder starts in the grape or the pedicel and later the illness is extended to further tissues.

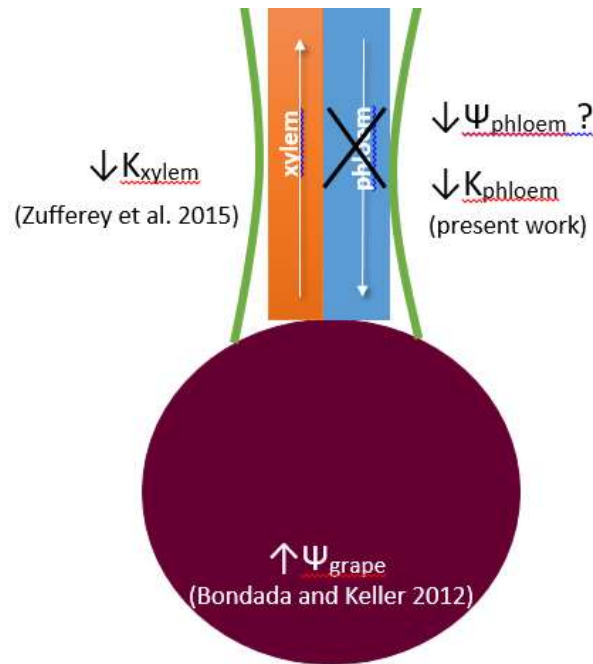


**Figure 33:** Diagram representing the water relations of a BS grape and stem. BS berries are characterized by low concentration of solutes what creates high osmotic potential and slightly reduced xylem conductivity in the stem. Furthermore reduced phloem conductivity in the stem has been largely proposed. This model agrees with the new secondary vascular tissue development and irregular cell size observed in our micrographs.

The knowledge about BS symptom development is increasing, but still it is difficult to differentiate between causal events and follow up symptoms. As in our study: reduced sugar and anthocyanin content, reduced  $K_{\text{phloem}}$ , callose deposition, vacuolar isolation or loose of cell turgidity. What becomes evident is that water relations can link many abnormalities described in BS berries and so it can play a very important role in BS induction and development. Now it is necessary to clarify the sequence of events that initiate the wilting process in BS affected berries. A method to artificially induce BS would simplify this task. Still no field treatments have been defined until now for BS prevention and our results do not provide insights for this. Further studies should be carried out with *véraison* pre-symptomatic samples to give more light into this mysterious disorder.

## 6 Summary

Berry shrivel is a physiological disorder that affects grape berries and which prevents normal grape ripening. Main symptoms of BS are related to an irregular accumulation of assimilates (sugars, anthocyanin, K and others) (Knoll et al. 2010; Krasnow et al. 2009; Griesser et al. 2012; Bondada and Keller 2012; Bachteler et al. 2015). Reduced K<sup>+</sup> and sugar content is frequently observed in different varieties, locations and years. Due to the phloem carriage of those assimilates and its relation to sugar metabolism and transportation we hypothesized that BS is due to a reduced arrival of assimilates to BS berries. To examine which may be the reason of the irregular allocation sink strength related mechanisms and vascular tissues were under study.

The sugar and anthocyanin metabolisms and accumulation mechanisms were analyzed on the analytical as well as for the first time on the transcriptional level. Metabolite levels were determined with high performance anion exchange chromatography coupled with pulsed amperometric detection (HPAEC-PAD) for sugars and liquid chromatography-tandem mass spectrometry (LC-MS/MS) for anthocyanins. At the genetic level, quantitative polymerase chain reaction (qPCR) were performed for invertases and sugar transporter genes involved in sink establishment, as well as genes of the polyphenol biosynthesis pathway for secondary metabolites production as e.g. anthocyanins. Additionally the activity of invertases was determined on the enzymatic level to possibly link analytical observations with expression data. Samples for qPCR and enzymatic assays were collected in a time scale, starting before symptoms are visible and finishing at full-ripe in approximately a weekly basis.

The phloem is a vascular tissue of main importance at ripening due to its role conducting sugars, phytohormones, K<sup>+</sup> and many other necessary molecules from the source (leaves) to the sink (grapes). The phloem transport was analyzed with different microscopic techniques (LM, SEM and TEM) to have a deep insight into the vascular tissues, as it is presumed that the assimilate transport through the phloem and towards the berry could be affected. Special attention was taken to the phloem structures related to transport as sieve elements, sieve plates, sieve pores or callose formation to evaluate if the potential amount of assimilates that anatomy would allow to deliver to BS berries is comparable to healthy grapes. Knowledge about pre-symptomatic

changes in BS affected grapes is very limiting and our approach provides us the opportunity to elucidate especially these early processes leading to BS symptom development with the focus on carbohydrates metabolism and transport.

The role of sugar metabolism at BS illness induction and development has been here evaluated in symplastic and apoplastic phases. Some irregularities were detected in both phases. Only symplastic phase or early apoplastic establishment may be related to BS induction as first symptoms appear around *véraison*. At the symplastic phase slight disturbances were observed and special role of TMT as sucrose transporters may have a role in the inception of the illness. Later on apoplastic mechanisms seem to be well established and only a delay of *véraison* seem to happen what may not explain the irregular assimilate content at BS berries. During the whole ripening enhancement of expression or enzymatic activity don't seem to correlate with sugar content that is why invertase role may be discarded. Altogether it can be concluded that BS samples seem to have irregular assimilate unloading, which origin may be placed out of the grape, and/or in an irregular tonoplast transporter regulation what may prevent that sugars enter into the vacuoles. By light microscopy it could be shown that early tissue formation is well developed in BS samples. Further secondary phloem and xylem growth and development may indicate insufficient vascular conductivity and irregular water balances between grape and stem. Additionally reduced sieve plate conductance, phloem tissue degradation and extended callose at sieve elements suggest and irregular phloem conductance of assimilates towards BS berries.

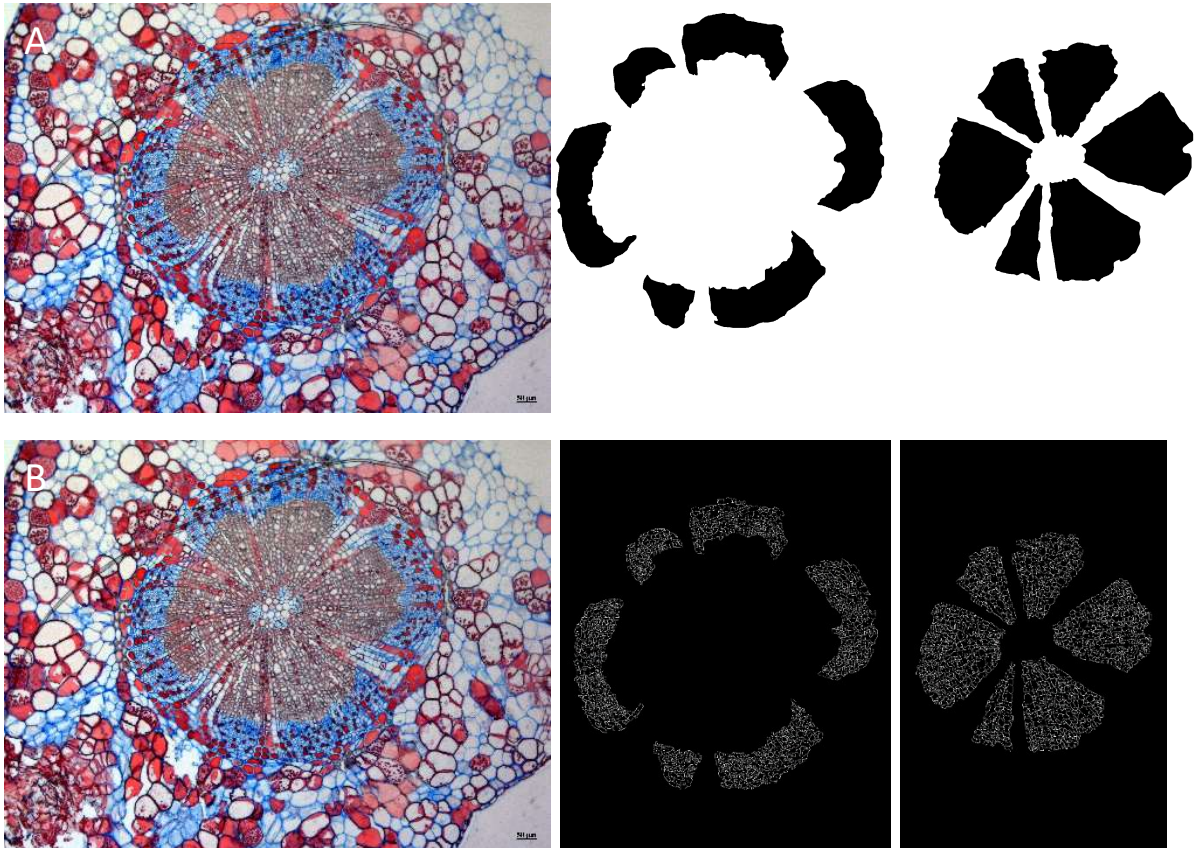
Finally for a better understanding of this complex mechanisms, modelling of the sugar metabolism would help in the interpretation and understanding of the consequences that these irregular genetic/enzymatic behaviour would have in BS development. At the microscopic studies, confirmation of these results in pre-symptomatic samples and comparison with different seasons and varieties would confirm the role that phloem conductivity may have in BS induction.

## 7 Appendix

### Appendix A

| Polyphenols analyzed with LC-MS                  | Groups of polyphenols      |
|--|----------------------------|
| caftaric acid                                    | phenolic acids             |
| 4-coumaric acid                                  | phenolic acids             |
| caffeic acid                                     | phenolic acids             |
| ferulic acid                                     | phenolic acids             |
| <i>trans</i> -resveratrol                        | stilbenes                  |
| <i>cis</i> -resveratrol                          | stilbenes                  |
| <i>trans</i> -resveratrol-3-O-glucoside          | stilbenes                  |
| <i>cis</i> -resveratrol-3-O-glucoside            | stilbenes                  |
| naringenin                                       | flavanone                  |
| eriodictyol                                      | flavanone                  |
| dihydroquercetin                                 | flavanonol                 |
| dihydrokaempferol                                | flavanonol                 |
| dihydromyricetin                                 | flavanonol                 |
| quercetin  | flavonols                  |
| quercetin-3-O-glucuronide                        | flavonols                  |
| quercetin-3-O-glucoside                          | flavonols                  |
| kaempferol-3-O-glucoside                         | flavonols                  |
| kaempferol                                       | flavonols                  |
| (+)-catechin                                     | flavan-3-ols               |
| (-)-epicatechin                                  | flavan-3-ols               |
| (-)-epicatechin gallate                          | flavan-3-ols               |
| delphinidin                                      | anthocyanin/anthocyanidins |
| DEL-3-O-glucoside                                | anthocyanin/anthocyanidins |
| DEL-3-O-(6-O-acetyl)-5-O-diglucoside             | anthocyanin/anthocyanidins |
| DEL-3-O-(6-O-p-coumaryl)-5-O-diglucoside         | anthocyanin/anthocyanidins |
| <i>cis</i> -DEL-3-O-(6-O--coumaryl)-glucoside    | anthocyanin/anthocyanidins |
| <i>trans</i> -DEL-3-O-(6-O-p-coumaryl)-glucoside | anthocyanin/anthocyanidins |
| cyanidin   | anthocyanin/anthocyanidins |
| CYA-3-O-glucoside                                | anthocyanin/anthocyanidins |
| CYA-3-O-(6-O-p-coumaryl)-5-O-(Ac)-diglucoside    | anthocyanin/anthocyanidins |
| <i>cis</i> -CYA-3-O-(6-P-p-coumaryl)-glucoside   | anthocyanin/anthocyanidins |
| <i>trans</i> -CYA-3-O-(6-O-p-coumaryl)-glucoside | anthocyanin/anthocyanidins |

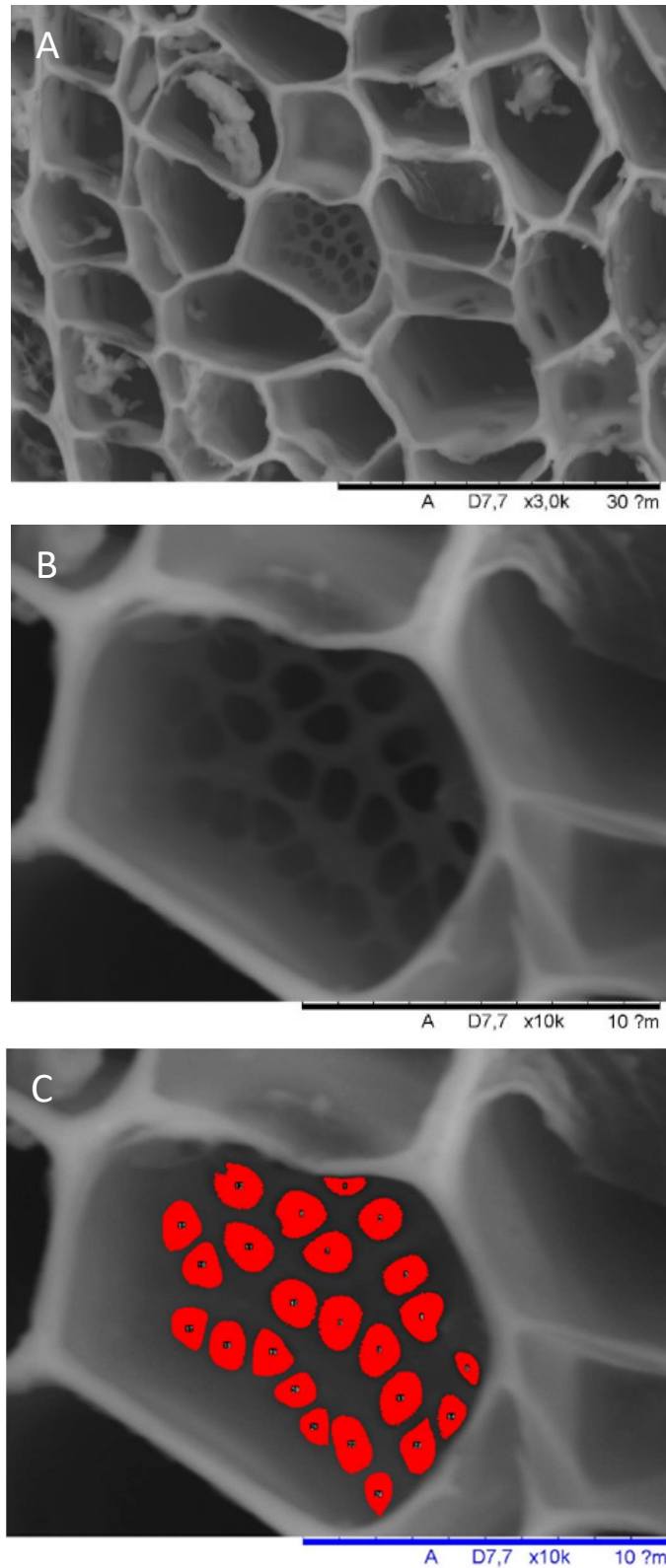
## Appendix B



**A:** Process used to measure the area of phloem and xylem tissues. Areas of phloem and xylem were delimited by hand. Then the masks were created, which contain the area selected. The first mask contains the phloem while the second mask covers the xylem. Image-J is able to measure the area of the masks created getting the area of phloem and xylem of a transversal section.

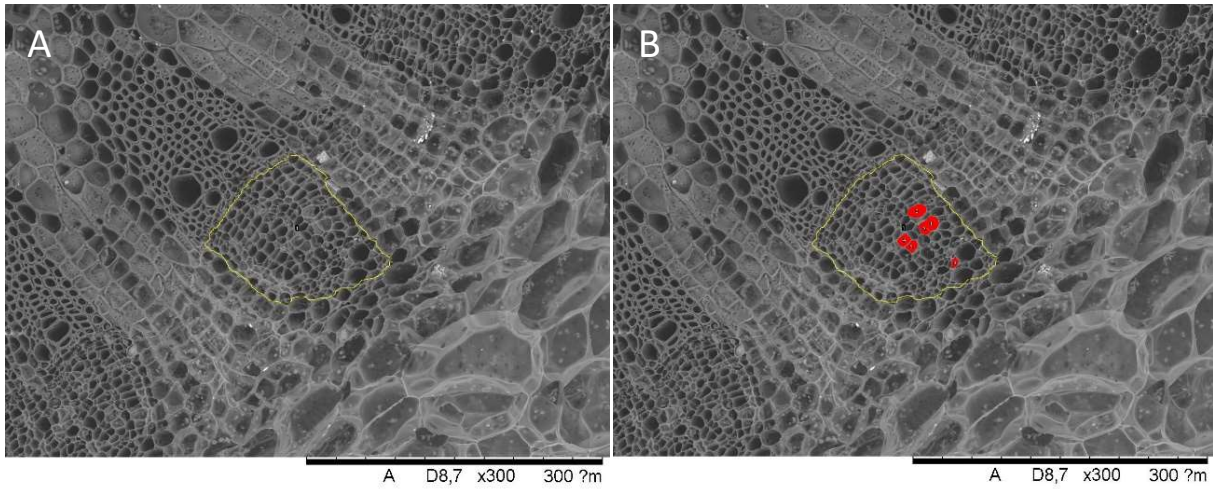
**B:** Process used to measure the area of phloem and xylem cells. No cell type was distinguished by this measurements, with the aim of determining a possible not specific but rather general abnormal cell growth. First the threshold of the image is adjusted to obtain a maximum contrast. Then Image-J detects the cell wall as edges due to the contrast created, By the function 'analyse particles' Image-J creates a new image in black and white drawing the edges of every cell (white) over a black background from which is able to measure the area and do statistics. The first image shows the original cross section. The second image (phloem) and third (xylem) show the map created by Image-J (which can be contrasted with the original).

## Appendix C



**B:** For conductivity calculation the area of all the pores of the sieve plate were measured with the program Image J. Image J detects the difference in darkness and increasing or reducing it the area of the pores is covered by a selection from which the program is able to measure the area.

## Appendix D



**C:** In the picture there is a whole vascular bundle. The micrographs show the work performed with the original pictures and Image J to determine the size total area of sieve plates per area of phloem. The yellow line delimits the area of the secondary phloem while the red spots cover all the sieve plates that have been observed in the phloem of this vascular bundle. This was used as an estimation of area of conductive tissue per area of phloem tissue.

## 8 References

- Afoufa-Bastien D, Medici A, Jeauffre J, Coutos-Thévenot P, Lemoine R, Atanassova R, Laloi M (2010) The *Vitis vinifera* sugar transporter gene family: phylogenetic overview and microarray expression profiling. *BMC plant biology* 10 (1):245
- Amor Y, Haigler CH, Johnson S, Wainscott M, Delmer DP (1995) A membrane-associated form of sucrose synthase and its potential role in synthesis of cellulose and callose in plants. *Proceedings of the National Academy of Sciences* 92 (20):9353-9357
- Andersen CL, Jensen JL, Ørntoft TF (2004) Normalization of real-time quantitative reverse transcription-PCR data: a model-based variance estimation approach to identify genes suited for normalization, applied to bladder and colon cancer data sets. *Cancer research* 64 (15):5245-5250
- Aryan A, Wilson B, Strauss C, Williams P (1987) The properties of glycosidases of *Vitis vinifera* and a comparison of their  $\beta$ -glucosidase activity with that of exogenous enzymes. An assessment of possible applications in enology. *American Journal of Enology and Viticulture* 38 (3):182-188
- Bachteler K (2012) *Nutritional and climatic effects on berry shrivel of grapevines in Southern Germany* (Doctoral dissertation). Retrieved from Universität Hohenheim (Publication No [860])
- Bachteler K, Riedel M, Merkt N, Ullrich B, Erhardt M, Wünsche J (2015) Effect of soil fertilization on the incidence of berry shrivel and the quality of resulting wine. *VITIS-Journal of Grapevine Research* 52 (1):1
- Barratt DP, Kölling K, Graf A, Pike M, Calder G, Findlay K, Zeeman SC, Smith AM (2011) Callose synthase *GSL7* is necessary for normal phloem transport and inflorescence growth in *Arabidopsis*. *Plant physiology* 155 (1):328-341
- Bhaskar Rao B, Markus K (2012) Not All Shrivels Are Created Equal—Morpho-Anatomical and Compositional Characteristics Differ among Different Shivel Types That Develop during Ripening of Grape (*Vitis vinifera* L.) Berries. *American Journal of Plant Sciences* 2012
- Bhuja P, McLachlan K, Stephens J, Taylor G (2004) Accumulation of 1, 3- $\beta$ -D-glucans, in response to aluminum and cytosolic calcium in *Triticum aestivum*. *Plant and cell physiology* 45 (5):543-549
- Biais B, Bénard C, Beauvoit B, Colombié S, Prodhomme D, Ménard G, Bernillon S, Gehl B, Gautier H, Ballias P (2014) Remarkable reproducibility of enzyme activity profiles in tomato fruits grown under contrasting environments provides a roadmap for studies of fruit metabolism. *Plant physiology* 164 (3):1204-1221
- Bogs J, Downey MO, Harvey JS, Ashton AR, Tanner GJ, Robinson SP (2005) Proanthocyanidin synthesis and expression of genes encoding leucoanthocyanidin reductase and anthocyanidin reductase in developing grape berries and grapevine leaves. *Plant Physiology* 139 (2):652-663
- Bogs J, Ebadi A, McDavid D, Robinson SP (2006) Identification of the flavonoid hydroxylases from grapevine and their regulation during fruit development. *Plant Physiology* 140 (1):279-291
- Bogs J, Jaffé FW, Takos AM, Walker AR, Robinson SP (2007) The grapevine transcription factor *VvMYBPA1* regulates proanthocyanidin synthesis during fruit development. *Plant physiology* 143 (3):1347-1361
- Bondada B (2014) Structural and compositional characterization of suppression of uniform ripening in grapevine: A paradoxical ripening disorder of grape berries with no known causative clues. *Journal of the American Society for Horticultural Science* 139 (5):567-581
- Bondada B (2016) Nutritional Aspects of Grape (*Vitis vinifera* L.) Clusters Afflicted with SOUR Shivel Is Related to Functionality of Its Vascular Tissues. *American Journal of Plant Sciences* 7 (01):194

- Bondada B, Keller M (2012) Morphoanatomical Symptomatology and Osmotic Behavior of Grape Berry Shriveling. *Journal of the American Society for Horticultural Science* 137 (1):20-30
- Bondada B, Keller M Structural and fruit compositional anomalies related to various shrivel types developing during ripening of grape berries. In: IX International Symposium on Grapevine Physiology and Biotechnology 1157, 2013. pp 49-54
- Boss PK, Davies C, Robinson SP (1996) Analysis of the expression of anthocyanin pathway genes in developing *Vitis vinifera* L. cv Shiraz grape berries and the implications for pathway regulation. *Plant Physiology* 111 (4):1059-1066
- Böttcher C, Boss PK, Davies C (2012) Delaying Riesling grape berry ripening with a synthetic auxin affects malic acid metabolism and sugar accumulation, and alters wine sensory characters. *Functional Plant Biology* 39 (9):745-753. doi:<http://dx.doi.org/10.1071/FP12132>
- Bustan A, Erner Y, Goldschmidt E (1995) Interactions between developing citrus fruits and their supportive vascular system. *Annals of Botany* 76 (6):657-666
- Cabello Campos S (2013) *Sugar Processing in Nematode Infected Plants* (Doctoral dissertation). Retrieved from Österreichischer Bibliothekenverbund (Accession No [AC10775541])
- Çakir B, Agasse A, Gaillard C, Saumonneau A, Delrot S, Atanassova R (2003) A grape ASR protein involved in sugar and abscisic acid signaling. *The Plant Cell* 15 (9):2165-2180
- Çakir B, Giachino RR (2012) VvTMT2 encodes a putative tonoplast monosaccharide transporter expressed during grape berry (*Vitis vinifera* cv. Sultanine) ripening. *Plant Omics* 5 (6):576
- Carbonell-Bejerano P, Diago M-P, Martínez-Abaigar J, Martínez-Zapater JM, Tardáguila J, Núñez-Olivera E (2014) Solar ultraviolet radiation is necessary to enhance grapevine fruit ripening transcriptional and phenolic responses. *BMC Plant Biology* 14 (1):183. doi:10.1186/1471-2229-14-183
- Castellarin SD, Di Gaspero G, Marconi R, Nonis A, Peterlunger E, Paillard S, Adam-Blondon A-F, Testolin R (2006) Colour variation in red grapevines (*Vitis vinifera* L.): genomic organisation, expression of flavonoid 3'-hydroxylase, flavonoid 3', 5'-hydroxylase genes and related metabolite profiling of red cyanidin/blue delphinidin-based anthocyanins in berry skin. *BMC Genomics* 7 (1):12
- Castellarin SD, Gambetta GA, Wada H, Shackel KA, Matthews MA (2011) Fruit ripening in *Vitis vinifera*: spatiotemporal relationships among turgor, sugar accumulation, and anthocyanin biosynthesis. *Journal of Experimental Botany* 62 (12):4345-4354
- Conde C, Agasse A, Glissant D, Tavares R, Gerós H, Delrot S (2006) Pathways of glucose regulation of monosaccharide transport in grape cells. *Plant Physiology* 141 (4):1563-1577
- Conde C, Silva P, Fontes N, Dias ACP, Tavares RM, Sousa MJ, Agasse A, Delrot S, Gerós H (2007) Biochemical changes throughout grape berry development and fruit and wine quality.
- Coombe B The grape berry as a sink. In: Sixth International Symposium on Growth Regulators in Fruit Production., In *International Symposium on Growth Regulators in Fruit Production 1988: Penticton, BC*. 1988. International Society for Horticultural Science., pp 149-158
- Coombe B (1992) Research on development and ripening of the grape berry. *American Journal of Enology and Viticulture* 43 (1):101-110
- Coombe BG (1960) Relationship of growth and development to changes in sugars, auxins, and gibberellins in fruit of seeded and seedless varieties of *Vitis vinifera*. *Plant physiology* 35 (2):241
- Coombe BG, Hale C (1973) The hormone content of ripening grape berries and the effects of growth substance treatments. *Plant physiology* 51 (4):629-634
- Coombe BG, McCarthy M (2000) Dynamics of grape berry growth and physiology of ripening. *Australian Journal of Grape and Wine Research* 6 (2):131-135
- Cosgrove DJ (2000) Loosening of plant cell walls by expansins. *Nature* 407 (6802):321-326

- Credi R (1994) Occurrence of Anomalous Mycoplasma-like Organisms in Grapevine Yellow-diseased Phloem. *Journal of Phytopathology* 142 (4):310-316
- Cronshaw J, Esau K (1967) Tubular and fibrillar components of mature and differentiating sieve elements. *The Journal of cell biology* 34 (3):801-815
- Cuellar T, Azeem F, Andrianteranagna M, Pascaud F, Verdeil JL, Sentenac H, Zimmermann S, Gaillard I (2013) Potassium transport in developing fleshy fruits: the grapevine inward K<sup>+</sup> channel VvK1. 2 is activated by CIPK–CBL complexes and induced in ripening berry flesh cells. *The Plant Journal* 73 (6):1006-1018
- Currier H (1957) Callose substance in plant cells. *American Journal of Botany*:478-488
- Czemmel S, Stracke R, Weisshaar B, Cordon N, Harris NN, Walker AR, Robinson SP, Bogs J (2009) The grapevine R2R3-MYB transcription factor VvMYB1 regulates flavonol synthesis in developing grape berries. *Plant physiology* 151 (3):1513-1530
- Chervin C, El-Kereamy A, Roustan J-P, Latché A, Lamon J, Bouzayen M (2004) Ethylene seems required for the berry development and ripening in grape, a non-climacteric fruit. *Plant Science* 167 (6):1301-1305
- Chervin C, Terrier N, Ageorges A, Ribes F, Kuapunyakoon T (2006) Influence of ethylene on sucrose accumulation in grape berry. *American journal of enology and viticulture* 57 (4):511-513
- Dai J, Gupte A, Gates L, Mumper R (2009) A comprehensive study of anthocyanin-containing extracts from selected blackberry cultivars: extraction methods, stability, anticancer properties and mechanisms. *Food and chemical toxicology* 47 (4):837-847
- Dai ZW, Meddar M, Renaud C, Merlin I, Hilbert G, Delrot S, Gomès E (2014) Long-term in vitro culture of grape berries and its application to assess the effects of sugar supply on anthocyanin accumulation. *Journal of experimental botany* 65 (16):4665-4677
- Dai ZW, Ollat N, Gomès E, Decroocq S, Tandonnet J-P, Bordenave L, Pieri P, Hilbert G, Kappel C, van Leeuwen C (2011) Ecophysiological, genetic, and molecular causes of variation in grape berry weight and composition: a review. *American Journal of Enology and Viticulture* 62 (4):413-425
- Darriet P, Thibon C, Dubourdiou D, Gerós H, Chaves M, Delrot S (2012) Aroma and aroma precursors in grape berry. *The biochemistry of the grape berry*:111-136
- Davies C, Boss PK, Robinson SP (1997) Treatment of grape berries, a nonclimacteric fruit with a synthetic auxin, retards ripening and alters the expression of developmentally regulated genes. *Plant physiology* 115 (3):1155-1161
- Davies C, Robinson SP (1996) Sugar accumulation in grape berries (cloning of two putative vacuolar invertase cDNAs and their expression in grapevine tissues). *Plant Physiology* 111 (1):275-283
- Davies C, Robinson SP (2000) Differential screening indicates a dramatic change in mRNA profiles during grape berry ripening. Cloning and characterization of cDNAs encoding putative cell wall and stress response proteins. *Plant physiology* 122 (3):803-812
- Davies C, Shin R, Liu W, Thomas MR, Schachtman DP (2006) Transporters expressed during grape berry (*Vitis vinifera* L.) development are associated with an increase in berry size and berry potassium accumulation. *Journal of Experimental Botany* 57 (12):3209-3216
- Davies C, Wolf T, Robinson SP (1999) Three putative sucrose transporters are differentially expressed in grapevine tissues. *Plant Science* 147 (2):93-100
- De Beer D, Harbertson JF, Kilmartin PA, Roginsky V, Barsukova T, Adams DO, Waterhouse AL (2004) Phenolics: A comparison of diverse analytical methods. *American Journal of Enology and Viticulture* 55 (4):389-400
- De Jong M, Mariani C, Vriezen WH (2009) The role of auxin and gibberellin in tomato fruit set. *Journal of experimental botany* 60 (5):1523-1532
- Deluc L, Gimplet J, Wheatley M, Tillett R, Quilici D, Osborne C, Schooley D, Schlauch K, Cushman J, Cramer G (2007) Transcriptomic and metabolite analyses of Cabernet Sauvignon grape berry development. *BMC genomics* 8 (1):429
- Dokoozlian N, Kliewer W (1996) Influence of light on grape berry growth and composition varies during fruit development. *Journal of the American Society for Horticultural Science* 121 (5):869-874

- Dokoozlian NK (2000) Grape berry growth and development. *Raisin production manual* 3393:30
- Downey MO, Harvey JS, Robinson SP (2004) The effect of bunch shading on berry development and flavonoid accumulation in Shiraz grapes. *Australian Journal of Grape and Wine Research* 10 (1):55-73
- El-Kereamy A, Chervin C, Roustan JP, Cheynier V, Souquet JM, Moutounet M, Raynal J, Ford C, Latché A, Pech JC (2003) Exogenous ethylene stimulates the long-term expression of genes related to anthocyanin biosynthesis in grape berries. *Physiologia plantarum* 119 (2):175-182
- Esau K (1953) Plant anatomy. *Soil Science* 75 (5):407
- Esau K, Cheadle VI, Risley E (1962) Development of sieve-plate pores. *Botanical Gazette*:233-243
- Esau K, Gill RH (1971) Aggregation of endoplasmic reticulum and its relation to the nucleus in a differentiating sieve element. *Journal of ultrastructure research* 34 (1-2):144-158
- Etzold H (2002) Simultanfärbung von Pflanzenschnitten mit Fuchsin, Chrysoidin und Astrablau. *Mikrokosmos* 91 (5):316
- Evert RF (1982) Sieve-tube structure in relation to function. *Bioscience* 32 (10):789-795
- Falcone Ferreyra ML, Rius S, Casati P (2012) Flavonoids: biosynthesis, biological functions, and biotechnological applications. *Frontiers in Plant Science* 3 (222). doi:10.3389/fpls.2012.00222
- Fang Z, Bhandari B (2011) Effect of spray drying and storage on the stability of bayberry polyphenols. *Food Chemistry* 129 (3):1139-1147
- Fernandez L, Romieu C, Moing A, Bouquet A, Maucourt M, Thomas MR, Torregrosa L (2006) The Grapevine fleshless berry Mutation. A Unique Genotype to Investigate Differences between Fleshy and Nonfleshy Fruit. *Plant Physiology* 140 (2):537-547. doi:10.1104/pp.105.067488
- Fillion L, Ageorges A, Picaud S, Coutos-Thévenot P, Lemoine R, Romieu C, Delrot S (1999) Cloning and expression of a hexose transporter gene expressed during the ripening of grape berry. *Plant Physiology* 120 (4):1083-1094
- Findlay N, Oliver K, Nil N, Coombe B (1987) Solute accumulation by grape pericarp cells: IV. Perfusion of pericarp apoplast via the pedicel and evidence for xylem malfunction in ripening berries. *Journal of Experimental Botany* 38 (4):668-679
- Finkelstein RR, Gibson SI (2002) ABA and sugar interactions regulating development: cross-talk or voices in a crowd? *Current opinion in plant biology* 5 (1):26-32
- Fontes N, Gerós H, Delrot S (2011) Grape berry vacuole: a complex and heterogeneous membrane system specialized in the accumulation of solutes. *American Journal of Enology and Viticulture:ajev*. 2011.10125
- Fournier-Level A, Le Cunff L, Gomez C, Doligez A, Ageorges A, Roux C, Bertrand Y, Souquet J-M, Cheynier V, This P (2009) Quantitative genetic bases of anthocyanin variation in grape (*Vitis vinifera* L. ssp. *sativa*) berry: a quantitative trait locus to quantitative trait nucleotide integrated study. *Genetics* 183 (3):1127-1139
- Francis D (2001) *The plant cell cycle and its interfaces*. CRC Press,
- Froelich DR, Mullendore DL, Jensen KH, Ross-Elliott TJ, Anstead JA, Thompson GA, Pélissier HC, Knoblauch M (2011) Phloem ultrastructure and pressure flow: sieve-element-occlusion-related agglomerations do not affect translocation. *The Plant Cell* 23 (12):4428-4445
- Fuentes S, Sullivan W, Tilbrook J, Tyerman S (2010) A novel analysis of grapevine berry tissue demonstrates a variety-dependent correlation between tissue vitality and berry shrivel. *Australian Journal of Grape and Wine Research* 16 (2):327-336
- Furch AC, Hafke JB, Schulz A, van Bel AJ (2007) Ca<sup>2+</sup>-mediated remote control of reversible sieve tube occlusion in *Vicia faba*. *Journal of Experimental Botany* 58 (11):2827-2838
- Gerlach D (1984) *Botanische Mikrotechnik*. Georg Thieme Verlag New York:311
- Gholami M (1996) *Biosynthesis and translocation of secondary metabolite glycosides in the grapevine Vitis vinifera L./by Mansour Gholami (Doctoral dissertation)*.

- Gibon Y, Blaesing OE, Hannemann J, Carillo P, Höhne M, Hendriks JH, Palacios N, Cross J, Selbig J, Stitt M (2004) A robot-based platform to measure multiple enzyme activities in *Arabidopsis* using a set of cycling assays: comparison of changes of enzyme activities and transcript levels during diurnal cycles and in prolonged darkness. *The Plant Cell* 16 (12):3304-3325
- Gibson SI (2005) Control of plant development and gene expression by sugar signaling. *Current opinion in plant biology* 8 (1):93-102
- Gindro K, Pezet R, Viret O (2003) Histological study of the responses of two *Vitis vinifera* cultivars (resistant and susceptible) to *Plasmopara viticola* infections. *Plant Physiology and Biochemistry* 41 (9):846-853
- Gindro K, Spring J-L, Pezet R, Richter H, Viret O (2015) Histological and biochemical criteria for objective and early selection of grapevine cultivars resistant to *Plasmopara viticola*. *VITIS-Journal of Grapevine Research* 45 (4):191
- Giovannoni J (2001) Molecular biology of fruit maturation and ripening. *Annual review of plant biology* 52 (1):725-749
- Giribaldi M, Gény L, Delrot S, Schubert A (2010) Proteomic analysis of the effects of ABA treatments on ripening *Vitis vinifera* berries. *Journal of Experimental Botany* 61 (9):2447-2458
- Glad C, Regnard J, Querou Y, Brun O, Morot-Gaudry J (1992) Phloem sap exudates as a criterion for sink strength appreciation in *Vitis vinifera* cv. Pinot noir grapevines. *Vitis* 31 (3):131-138
- Glories Y (1988) Anthocyanins and tannins from wine: organoleptic properties. *Plant flavonoids in biology and medicine II: biochemical, cellular, and medicinal properties.* ( ):123-134
- Golinowski W, Grundler F, Sobczak M (1996) Changes in the structure of *Arabidopsis thaliana* during female development of the plant-parasitic nematode *Heterodera schachtii*. *Protoplasma* 194 (1-2):103-116
- Goodman R, Huang P-Y, White J (1976) Ultrastructural evidence for immobilization of an incompatible bacterium, *Pseudomonas pisi*, in tobacco leaf tissue. *Phytopathology* 66:754-764
- Goto-Yamamoto N, Wan G, Masaki K, Kobayashi S (2002) Structure and transcription of three chalcone synthase genes of grapevine (*Vitis vinifera*). *Plant Science* 162 (6):867-872
- Greenspan MD, Shackel K, Matthews M (1994) Developmental changes in the diurnal water budget of the grape berry exposed to water deficits. *Plant, Cell & Environment* 17 (7):811-820
- Gregory R, Warnes BB, Lodewijk Bonebakker, Robert Gentleman, Wolfgang Huber Andy Liaw, Thomas Lumley, Martin Maechler, Arni Magnusson, Steffen Moeller, Marc Schwartz and Bill Venables (2016) *gplots: Various R Programming Tools for Plotting Data.*
- Griesser M, Crespo Martinez S, Weidinger ML, Kandler W, Forneck A (2017) Challenging the potassium deficiency hypothesis for induction of the ripening disorder berry shrivel in grapevine. *Scientia Horticulturae* 216:141-147
- Griesser M, Eder R, Besser S, Forneck A (2012) Berry shrivel of grapes in Austria—Aspects of the physiological disorder with cultivar Zweigelt (*Vitis vinifera* L.). *Scientia Horticulturae* 145:87-93
- Guignard C, Jouve L, Bogéat-Triboulot MB, Dreyer E, Hausman J-F, Hoffmann L (2005) Analysis of carbohydrates in plants by high-performance anion-exchange chromatography coupled with electrospray mass spectrometry. *Journal of Chromatography A* 1085 (1):137-142
- Hall GE, Bondada BR, Keller M (2011) Loss of rachis cell viability is associated with ripening disorders in grapes. *Journal of experimental botany* 62 (3):1145-1153
- Harrell D, Williams L (1987) The influence of girdling and gibberellic acid application at fruitset on Ruby Seedless and Thompson Seedless grapes. *American journal of enology and viticulture* 38 (2):83-88
- Harris J, Kriedemann P, Possingham J (1968) Anatomical aspects of grape berry development. *Vitis* 7 (2):106-119

- Harris N, Luczo J, Robinson S, Walker A (2013) Transcriptional regulation of the three grapevine chalcone synthase genes and their role in flavonoid synthesis in Shiraz. *Australian Journal of Grape and Wine Research* 19 (2):221-229
- Hayes MA, Davies C, Dry IB (2007) Isolation, functional characterization, and expression analysis of grapevine (*Vitis vinifera* L.) hexose transporters: differential roles in sink and source tissues. *Journal of experimental botany* 58 (8):1985-1997
- Hedrich R (2012) Ion channels in plants. *Physiological reviews* 92 (4):1777-1811
- Herbers K, Sonnewald U (1998) Molecular determinants of sink strength. *Current opinion in plant biology* 1 (3):207-216
- Hiratsuka S, Onodera H, Kawai Y, Kubo T, Itoh H, Wada R (2001) ABA and sugar effects on anthocyanin formation in grape berry cultured in vitro. *Scientia Horticulturae* 90 (1):121-130
- Ho LC (1988) Metabolism and compartmentation of imported sugars in sink organs in relation to sink strength. *Annual Review of Plant Physiology and Plant Molecular Biology* 39 (1):355-378
- Hoshino T, Matsumoto U, Goto T (1980) The stabilizing effect of the acyl group on the copigmentation of acylated anthocyanins with C-glucosylflavones. *Phytochemistry* 19 (4):663-667
- Jackson D, Lombard P (1993) Environmental and management practices affecting grape composition and wine quality—a review. *American Journal of Enology and Viticulture* 44 (4):409-430
- Jeong ST, Goto-Yamamoto N, Kobayashi S, Esaka M (2004) Effects of plant hormones and shading on the accumulation of anthocyanins and the expression of anthocyanin biosynthetic genes in grape berry skins. *Plant Science* 167 (2):247-252
- Johnson R, Dixon M, Lee D (1992) Water relations of the tomato during fruit growth. *Plant, Cell & Environment* 15 (8):947-953
- Kalua CM, Boss PK (2009) Evolution of volatile compounds during the development of Cabernet Sauvignon grapes (*Vitis vinifera* L.). *Journal of Agricultural and Food Chemistry* 57 (9):3818-3830
- Kauss H (1987) Some aspects of calcium-dependent regulation in plant metabolism. *Annual Review of Plant Physiology* 38 (1):47-71
- Keller M (2010) *The Science of Grapevines: Anatomy and Physiology*.
- Keller M, Hrazdina G (1998) Interaction of nitrogen availability during bloom and light intensity during veraison. II. Effects on anthocyanin and phenolic development during grape ripening. *American Journal of Enology and Viticulture* 49 (3):341-349
- Keller M, Shrestha PM (2014) Solute accumulation differs in the vacuoles and apoplast of ripening grape berries. *Planta* 239 (3):633-642. doi:10.1007/s00425-013-2004-z
- Keller M, Shrestha PM, Hall GE, Bondada BR, Davenport JR (2016) Arrested Sugar Accumulation and Altered Organic Acid Metabolism in Grape Berries Affected by the Berry Shivel Syndrome. *American Journal of Enology and Viticulture*. doi:10.5344/ajev.2016.16048
- Keller M, Smith JP, Bondada BR (2006) Ripening grape berries remain hydraulically connected to the shoot. *Journal of Experimental Botany* 57 (11):2577-2587
- Klann EM, Hall B, Bennett AB (1996) Antisense acid invertase (TIV1) gene alters soluble sugar composition and size in transgenic tomato fruit. *Plant Physiology* 112 (3):1321-1330
- Kliwer W (1970) Effect of day temperature and light intensity on coloration of *Vitis vinifera* L. grapes. *Journal of the American Society of Horticultural Science* 95:693-697
- Knight H, Trewavas AJ, Knight MR (1997) Calcium signalling in *Arabidopsis thaliana* responding to drought and salinity. *The Plant Journal* 12 (5):1067-1078
- Knoblauch M, Oparka K (2012) The structure of the phloem—still more questions than answers. *The Plant Journal* 70 (1):147-156
- Knoblauch M, Peters WS, Ehlers K, van Bel AJ (2001) Reversible calcium-regulated stopcocks in legume sieve tubes. *The Plant Cell* 13 (5):1221-1230

- Knoll M, Achleitner D, Redl H (2006) Response of Zweigelt grapevine to foliar application of potassium fertilizer: Effects on gas exchange, leaf potassium content and incidence of Traubenwelke. *Journal of plant nutrition* 29 (10):1805-1817
- Knoll M, Achleitner D, Redl H (2010) Sugar accumulation in 'Zweigelt' grapes as affected by 'Traubenwelke'. *Vitis* 49 (3):101-106
- Kobayashi S, Yamamoto, N.G. and Hirochika, H. (2005) Association of VvmybA1 gene expression with anthocyanin production in grape (*Vitis vinifera*) skin – color mutants. *Journal of the Japanese Society for Horticultural Science* 74:196–203
- Koch K (2004) Sucrose metabolism: regulatory mechanisms and pivotal roles in sugar sensing and plant development. *Current opinion in plant biology* 7 (3):235-246
- Koes RE, Quattrocchio F, Mol JN (1994) The flavonoid biosynthetic pathway in plants: function and evolution. *BioEssays* 16 (2):123-132
- Kortekamp A, Wind R, Zyprian E (2015) The role of callose deposits during infection of two downy mildew-tolerant and two-susceptible *Vitis* cultivars. *VITIS-Journal of Grapevine Research* 36 (2):103
- Krasnow M, Matthews M, Shackel K (2008) Evidence for substantial maintenance of membrane integrity and cell viability in normally developing grape (*Vitis vinifera* L.) berries throughout development. *Journal of experimental botany* 59 (4):849-859
- Krasnow M, Weis N, Smith RJ, Benz MJ, Matthews M, Shackel K (2009) Inception, progression, and compositional consequences of a berry shrivel disorder. *American journal of enology and viticulture* 60 (1):24-34
- Lakso AN, Kliewer WM (1975) The influence of temperature on malic acid metabolism in grape berries I. Enzyme responses. *Plant Physiology* 56 (3):370-372
- Lalonde S, Tegeder M, Throne-Holst M, Frommer W, Patrick J (2003) Phloem loading and unloading of sugars and amino acids. *Plant, Cell & Environment* 26 (1):37-56
- Larson PR (2012) *The vascular cambium: development and structure*. Springer Science & Business Media,
- Lebon G, Wojnarowicz G, Holzapfel B, Fontaine F, Vaillant-Gaveau N, Clément C (2008) Sugars and flowering in the grapevine (*Vitis vinifera* L.). *Journal of Experimental Botany* 59 (10):2565-2578
- Lecourieux F, Kappel C, Lecourieux D, Serrano A, Torres E, Arce-Johnson P, Delrot S (2013) An update on sugar transport and signalling in grapevine. *Journal of experimental botany*:ert394
- Lee J, Durst RW, Wrolstad RE (2005) Determination of total monomeric anthocyanin pigment content of fruit juices, beverages, natural colorants, and wines by the pH differential method: collaborative study. *Journal of AOAC international* 88 (5):1269-1278
- Leigh R, Chater M, Storey R, Johnston A (1986) Accumulation and subcellular distribution of cations in relation to the growth of potassium-deficient barley. *Plant, Cell & Environment* 9 (7):595-604
- Loewus FA (1999) Biosynthesis and metabolism of ascorbic acid in plants and of analogs of ascorbic acid in fungi. *Phytochemistry* 52 (2):193-210
- Mann HB, Whitney DR (1947) On a test of whether one of two random variables is stochastically larger than the other. *The annals of mathematical statistics*:50-60
- Mazza G, Miniati E (1993) Anthocyanins in fruits, vegetables, and grains.
- McCarthy MG, Coombe B (1999) Is weight loss in ripening grape berries cv. Shiraz caused by impeded phloem transport? *Australian Journal of Grape and Wine Research* 5 (1):17-21
- McNairn R, Currier H (1968) Translocation blockage by sieve plate callose. *Planta* 82 (4):369-380
- McQueen-Mason S, Durachko DM, Cosgrove DJ (1992) Two endogenous proteins that induce cell wall extension in plants. *The Plant Cell* 4 (11):1425-1433
- Medici A, Laloi M, Atanassova R (2014) Profiling of sugar transporter genes in grapevine coping with water deficit. *FEBS letters* 588 (21):3989-3997
- Mori K, Goto-Yamamoto N, Kitayama M, Hashizume K (2007) Loss of anthocyanins in red-wine grape under high temperature. *Journal of Experimental Botany* 58 (8):1935-1945

- Mpelasoka BS, Schachtman DP, Treeby MT, Thomas MR (2003) A review of potassium nutrition in grapevines with special emphasis on berry accumulation. *Australian Journal of Grape and Wine Research* 9 (3):154-168
- Mullendore DL, Windt CW, Van As H, Knoblauch M (2010) Sieve tube geometry in relation to phloem flow. *The Plant Cell* 22 (3):579-593
- Münch E (1930) *Die Stoffbewegungen in der Pflanze*. Verlag Gustav Fischer, vol 234.
- Nishimura MT, Stein M, Hou B-H, Vogel JP, Edwards H, Somerville SC (2003) Loss of a callose synthase results in salicylic acid-dependent disease resistance. *Science* 301 (5635):969-972
- Nonis A, Ruperti B, Pierasco A, Canaguier A, Adam-Blondon A-F, Di Gaspero G, Vizzotto G (2008) Neutral invertases in grapevine and comparative analysis with *Arabidopsis*, poplar and rice. *Planta* 229 (1):129-142
- Nunan KJ, Sims IM, Bacic A, Robinson SP, Fincher GB (1998) Changes in cell wall composition during ripening of grape berries. *Plant Physiology* 118 (3):783-792
- O'Brien TP, McCully ME (1981) *The study of plant structure: principles and selected methods*. Melbourne, Termarcarphi Pty Ltd
- Ong B, Nagel C (1978) Hydroxycinnamic acid-tartaric acid ester content in mature grapes and during the maturation of White Riesling grapes. *American journal of enology and viticulture* 29 (4):277-281
- Ozga JA, Yu J, Reinecke DM (2003) Pollination-, development-, and auxin-specific regulation of gibberellin 3 $\beta$ -hydroxylase gene expression in pea fruit and seeds. *Plant Physiology* 131 (3):1137-1146
- Pan QH, Li MJ, Peng CC, Zhang N, Zou X, Zou KQ, Wang XL, Yu XC, Wang XF, Zhang DP (2005) Abscisic acid activates acid invertases in developing grape berry. *Physiologia Plantarum* 125 (2):157-170
- Pape S (2012) EasyqpcR: EasyqpcR for Easy Analysis of Real-Time PCR Data at IRTOMIT-INSERM U1082. English R package IRTOMIT-INSERM U 1082
- Pirie A, Mullins MG (1976) Changes in anthocyanin and phenolics content of grapevine leaf and fruit tissues treated with sucrose, nitrate, and abscisic acid. *Plant physiology* 58 (4):468-472
- Raifer B, Haas F, Cassar A (2014) Influence of leaf canopy height on the occurrence of berry shrivel. *Vitis* 53 (3):117-123
- Raifer B, Roschatt C (2001) Welkekrankheit bei Weintrauben. *Das Deutsche Weinmagazin* 38:143-145
- Rančić D, Quarrie SP, Pečinar I (2010) Anatomy of tomato fruit and fruit pedicel during fruit development. *Microscopy: Science, Technology, Applications and Education*:851-861
- Razaque Memon A, Saccomani M, Glass AD (1985) Efficiency of potassium utilization by barley varieties: the role of subcellular compartmentation. *Journal of Experimental Botany* 36 (12):1860-1876
- Reddy AS (2001) Calcium: silver bullet in signaling. *Plant Science* 160 (3):381-404
- Reid KE, Olsson N, Schlosser J, Peng F, Lund ST (2006) An optimized grapevine RNA isolation procedure and statistical determination of reference genes for real-time RT-PCR during berry development. *BMC plant biology* 6 (1):27
- Richter H (1978) A diagram for the description of water relations in plant cells and organs. *Journal of Experimental Botany* 29 (5):1197-1203
- Robinson SP, Davies C (2000) Molecular biology of grape berry ripening. *Australian Journal of Grape and Wine Research* 6 (2):175-188
- Roby G, Harbertson JF, Adams DA, Matthews MA (2004) Berry size and vine water deficits as factors in winegrape composition: anthocyanins and tannins. *Australian Journal of Grape and Wine Research* 10 (2):100-107
- Rogiers SY (2005) Understanding Shiraz berry shrivel. *The Australian & New Zealand Grapegrower and Winemaker* (501):28
- Rogiers SY, Hatfield JM, Jaudzems VG, White RG, Keller M (2004) Grape berry cv. Shiraz epicuticular wax and transpiration during ripening and preharvest weight loss. *American Journal of Enology and Viticulture* 55 (2):121-127

- Rogiers SY, Keller M, Holzzapfel BP, Virgona JM (2000) Accumulation of potassium and calcium by ripening berries on field vines of *Vitis vinifera* (L) cv. Shiraz. *Australian Journal of Grape and Wine Research* 6 (3):240-243
- Roitsch T, Balibrea ME, Hofmann M, Proels R, Sinha AK (2003) Extracellular invertase: key metabolic enzyme and PR protein. *J Exp Bot* 54 (382):513-524
- Roitsch T, Ehneß R (2000) Regulation of source/sink relations by cytokinins. *Plant Growth Regulation* 32 (2-3):359-367
- Roitsch T, González M-C (2004) Function and regulation of plant invertases: sweet sensations. *Trends in plant science* 9 (12):606-613
- Ruan Y-L, Xu S-M, White R, Furbank RT (2004) Genotypic and developmental evidence for the role of plasmodesmatal regulation in cotton fiber elongation mediated by callose turnover. *Plant Physiology* 136 (4):4104-4113
- Ruffner H, Hawker J (1977) Control of glycolysis in ripening berries of *Vitis vinifera*. *Phytochemistry* 16 (8):1171-1175
- Sapozhnikova Y (2014) Development of liquid chromatography–tandem mass spectrometry method for analysis of polyphenolic compounds in liquid samples of grape juice, green tea and coffee. *Food chemistry* 150:87-93
- Schindelin J, Rueden CT, Hiner MC, Eliceiri KW (2015) The ImageJ ecosystem: An open platform for biomedical image analysis. *Molecular reproduction and development* 82 (7-8):518-529
- Schneider CA, Rasband WS, Eliceiri KW (2012) NIH Image to ImageJ: 25 years of image analysis. *Nat methods* 9 (7):671-675
- Schoedl K, Forneck A, Sulyok M, Schuhmacher R (2011) Optimization, in-house validation, and application of a liquid chromatography–tandem mass spectrometry (LC–MS/MS)-based method for the quantification of selected polyphenolic compounds in leaves of grapevine (*Vitis vinifera* L.). *Journal of agricultural and food chemistry* 59 (20):10787-10794
- Schulz A (1987) Sieve-element differentiation and fluoresceine translocation in wound-phloem of pea roots after complete severance of the stele. *Planta* 170 (3):289-299
- Schulz A, Beyhl D, Marten I, Wormit A, Neuhaus E, Poschet G, Büttner M, Schneider S, Sauer N, Hedrich R (2011) Proton-driven sucrose symport and antiport are provided by the vacuolar transporters SUC4 and TMT1/2. *The Plant Journal* 68 (1):129-136
- Seidelmann K, Melzer B, Speck T (2012) The complex leaves of the monkey's comb (*Amphilophium crucigerum*, Bignoniaceae): A climbing strategy without glue. *American journal of botany* 99 (11):1737-1744
- Shapiro SS, Wilk MB (1965) An analysis of variance test for normality (complete samples). *Biometrika* 52 (3/4):591-611
- Smith GJ, Markham KR (1998) Tautomerism of flavonol glucosides: relevance to plant UV protection and flower colour. *Journal of Photochemistry and Photobiology A: Chemistry* 118 (2):99-105
- Spanswick RM (1981) Electrogenic ion pumps. *Annual Review of Plant Physiology* 32 (1):267-289
- Sparvoli F, Martin C, Scienza A, Gavazzi G, Tonelli C (1994) Cloning and molecular analysis of structural genes involved in flavonoid and stilbene biosynthesis in grape (*Vitis vinifera* L.). *Plant molecular biology* 24 (5):743-755
- Sturm A (1999) Invertases. Primary structures, functions, and roles in plant development and sucrose partitioning. *Plant physiology* 121 (1):1-8
- Sullivan-Brown J, Bisher ME, Burdine RD (2011) Embedding, serial sectioning and staining of zebrafish embryos using JB-4 resin. *Nature protocols* 6 (1):46-55
- Swanson C, El-Shishiny E (1958) Translocation of Sugars in the Concord Grape. *Plant Physiology* 33 (1):33
- Sweetman C, Deluc LG, Cramer GR, Ford CM, Soole KL (2009) Regulation of malate metabolism in grape berry and other developing fruits. *Phytochemistry* 70 (11):1329-1344

- Symons G, Davies, C., Shavrukov, Y., Dry, I., Reid, J. and Thomas, M. (2006) Grapes on steroids. Brassinosteroids are involved in grape berry ripening. *Plant Physiology* 140:150-158
- Team RC (2016) R: A Language and Environment for Statistical Computing.
- Teixeira A, Eiras-Dias J, Castellarin SD, Gerós H (2013) Berry phenolics of grapevine under challenging environments. *International journal of molecular sciences* 14 (9):18711-18739
- Terrier N, Glissant D, Grimplet J, Barrieu F, Abbal P, Couture C, Ageorges A, Atanassova R, Léon C, Renaudin J-P (2005) Isogene specific oligo arrays reveal multifaceted changes in gene expression during grape berry (*Vitis vinifera* L.) development. *Planta* 222 (5):832-847
- Terrier N, Torregrosa L, Ageorges A, Violet S, Verriès C, Cheynier V, Romieu C (2009) Ectopic expression of VvMybPA2 promotes proanthocyanidin biosynthesis in grapevine and suggests additional targets in the pathway. *Plant Physiology* 149 (2):1028-1041
- Thompson MV (2006) Phloem: the long and the short of it. *Trends in plant science* 11 (1):26-32
- Thompson MV, Holbrook NM (2003) Application of a single-solute non-steady-state phloem model to the study of long-distance assimilate transport. *Journal of Theoretical Biology* 220 (4):419-455
- Timell T (1980) Organization and ultrastructure of the dormant cambial zone in compression wood of *Picea abies*. *Wood Science and Technology* 14 (3):161-179
- Turgeon R (1996) Phloem loading and plasmodesmata. *Trends in Plant Science* 1 (12):418-423
- Tuteja N, Sopory SK (2008) Chemical signaling under abiotic stress environment in plants. *Plant signaling & behavior* 3 (8):525-536
- van Bel AJ (2003) The phloem, a miracle of ingenuity. *Plant, Cell & Environment* 26 (1):125-149
- Verriès C, Guiraud J-L, Souquet J-M, Violet S, Terrier N, Ollé D (2008) Validation of an extraction method on whole pericarp of grape berry (*Vitis vinifera* L. cv. Shiraz) to study biochemical and molecular aspects of flavan-3-ol synthesis during berry development. *Journal of agricultural and food chemistry* 56 (14):5896-5904
- Vignault C, Vachaud M, Cakir B, Glissant D, Dédaldéchamp F, Büttner M, Atanassova R, Fleurat-Lessard P, Lemoine R, Delrot S (2005) VvHT1 encodes a monosaccharide transporter expressed in the conducting complex of the grape berry phloem. *Journal of experimental botany* 56 (415):1409-1418
- Walker AR, Lee E, Bogs J, McDavid DA, Thomas MR, Robinson SP (2007) White grapes arose through the mutation of two similar and adjacent regulatory genes. *The Plant Journal* 49 (5):772-785
- Walker DJ, Leigh RA, Miller AJ (1996) Potassium homeostasis in vacuolate plant cells. *Proceedings of the National Academy of Sciences* 93 (19):10510-10514
- Wardlaw IF (1990) Tansley Review No. 27 The control of carbon partitioning in plants. *New phytologist* 116 (3):341-381
- Welch BL (1947) The generalization of student's' problem when several different population variances are involved. *Biometrika* 34 (1/2):28-35
- Wen Y-Q, Zhong G-Y, Gao Y, Lan Y-B, Duan C-Q, Pan Q-H (2015) Using the combined analysis of transcripts and metabolites to propose key genes for differential terpene accumulation across two regions. *BMC plant biology* 15 (1):240
- Wheeler S, Loveys B, Ford C, Davies C (2009) The relationship between the expression of abscisic acid biosynthesis genes, accumulation of abscisic acid and the promotion of *Vitis vinifera* L. berry ripening by abscisic acid. *Australian Journal of Grape and Wine Research* 15 (3):195-204
- Wissemeier A, Horst W (1995) Effect of calcium supply on aluminium-induced callose formation, its distribution and persistence in roots of soybean (*Glycine max* (L.) Merr.). *Journal of Plant Physiology* 145 (4):470-476

- Wormit A, Trentmann O, Feifer I, Lohr C, Tjaden J, Meyer S, Schmidt U, Martinoia E, Neuhaus HE (2006) Molecular identification and physiological characterization of a novel monosaccharide transporter from Arabidopsis involved in vacuolar sugar transport. *The Plant Cell Online* 18 (12):3476-3490
- Xie B, Wang X, Zhu M, Zhang Z, Hong Z (2011) CalS7 encodes a callose synthase responsible for callose deposition in the phloem. *The Plant Journal* 65 (1):1-14
- Xu F, Xi Z-m, Zhang H, Zhang C-j, Zhang Z-w (2015) Brassinosteroids are involved in controlling sugar unloading in *Vitis vinifera* 'Cabernet Sauvignon' berries during *véraison*. *Plant Physiology and Biochemistry* 94:197-208
- Zeng L, Wang Z, Vainstein A, Chen S, Ma H (2011) Cloning, Localization, and Expression Analysis of a New Tonoplast Monosaccharide Transporter from *Vitis vinifera* L. *Journal of Plant Growth Regulation* 30 (2):199-212
- Zhang X-Y, Wang X-L, Wang X-F, Xia G-H, Pan Q-H, Fan R-C, Wu F-Q, Yu X-C, Zhang D-P (2006) A shift of phloem unloading from symplasmic to apoplasmic pathway is involved in developmental onset of ripening in grape berry. *Plant Physiology* 142 (1):220-232
- Zhang Y, Keller M (2017) Discharge of surplus phloem water may be required for normal grape ripening. *Journal of experimental botany* 68 (3):585-595
- Zimmermann MH (1969) Translocation velocity and specific mass transfer in the sieve tubes of *Fraxinus americana* L. *Planta* 84 (3):272-278
- Zrenner R, Schüler K, Sonnewald U (1996) Soluble acid invertase determines the hexose-to-sucrose ratio in cold-stored potato tubers. *Planta* 198 (2):246-252
- Zufferey V, Spring J-L, Voinesco F, Viret O, Gindro K (2015) Physiological and histological approaches to study berry shrivel in grapes. *J Int Sci Vigne Vin* 4:113-125

## 9 Abbreviations

- ABA: Abscisic acid
- Al: Aluminium
- ANOVA: Analysis of variance
- BS : Berry shrivel
- BSN: Bunch stem necrosis
- Ca<sup>2+</sup>: Calcium
- CINV: Cytosolic invertase
- Cl: Chlorine
- CWINV: Cell wall invertase
- CYA: Cyanidin
- DEL: Delphinidin
- DEPC: Diethylpyrocarbonate
- DNA: Deoxyribonucleic acid
- dNTP: Nucleoside triphosphate
- DTT: Dithiothreitol
- DW: Dry weight
- EDTA: Ethylenediaminetetraacetic acid
- EGTA: ethylene glycol tetraacetic acid
- ESI: Electrospray ionization
- EtOH: Ethanol
- GA: Giberellins
- HEPES: 4-(2-hydroxyethyl)-1-piperazineethanesulfonic acid
- HT: Hexose transporter
- IAA: Indole acetic acid
- K: Conductance
- K<sup>+</sup>: Potassium
- L: Sieve plate length
- LC-MS/MS: Liquid chromatography tandem mass spectrometry
- Lp: Sieve plate thickness
- Normalized relative quantities

- Np: Number of sieve pores/sieve plate
- NRQ: PEP: Phosphoenolpyruvate
- PMSF: phenylmethane sulfonyl fluoride
- P-protein: Phloem protein
- PVP: Polyvinylpyrrolidone
- PVPP: Polyvinylpolypyrrolidone
- qPCR: Quantitative polymerase chain reaction
- R: Radius sieve element
- RNA: Ribonucleic acid
- Rp: Radius sieve plate
- SRM: Selected reaction monitoring
- TE: Tris – EDTA
- TMT: Tonoplast monosaccharide transporter
- v/v: volume per volume
- VIN: Vacuolar invertase
- vol: Volume

## 10 Declaration

I hereby declare that I have written this thesis independently. All the results presented in the results section have been obtained by my own work except mentioned below. All the intellectual property used for the preparation of this work has been cited properly.

Contribution of the others:

Markus Eitle has performed the qPCR with anthocyanin genes; Anthocyanin analysis with LC-MS/MS were made by Rainer Schuhmacher; Glucose, fructose and sucrose content was analysed by Christelle Andre; Sample embedding, sectioning, observation and image for TEM was developed by Miroslaw Sobczak.

---

## 11 Curriculum vitae

### Personal data

**Name:** Sara Crespo Martínez  
**Personal address:** Plz/ Fuente de la Salud nº 25 2ºA, CP 31200 Estella, Navarra  
**Institute address:** Division of Viticulture and Pomology, Department of Crop Sciences, BOKU, UFT, Konard-Lorenz-Strasse 24, 3430 Tulln, Austria  
**Date of birth** 11<sup>th</sup> June 1985  
**Place of birth** Estella, Navarra, Spain  
**Nationality** Spanish  
**Email** [saraolexa@hotmail.com](mailto:saraolexa@hotmail.com)

### Education

2012 – present **Doctorate in Agricultural Sciences**, *University of Natural Resources and Life Sciences, Vienna*  
'Analysing changes in assimilate transport and grapevine ripening metabolism induced by the ripening disorder Berry Shrivel.' Berry shrivel (BS) is a physiological disorder that appears in berries after *véraison* but is still difficult to determine yet the time point when this illness is initiated. The symptoms of BS are manifested in the berries but pedicel and rachis appear to be healthy and berries show disturbed sugar accumulation, pH, elasticity and anthocyanin production between others. In the presented work we try to understand the role of sugar and anthocyanin metabolism and the implication of phloem tissue in the illness development.

2010 – 2012 **International Horticulture Master**, joined program from *University of Bologna, University of Budapest and University of Natural Resources and Life Sciences, Vienna*

2003 – 2009 **Agronomic Engineering**, *Public University of Navarra*

2001 – 2003 **High school in Life Sciences**, *IES Tierra Estella*